24TH INTERNATIONAL WORKSHOP ON OPTICAL WAVE & WAVEGUIDE THEORY AND NUMERICAL MODELLING

OWTNM2016

20–21 MAY | WARSAW | POLAND

OWTNM

The University of Nottingham
UNITED KINGDOM · CHINA · MALAYSIA

SUPPORTED BY

CZIiTT Centre for Innovation and Technology Transfer Management WUT

SKKP POLISH CONFERENCE & CONGRESS ASSOCIATION

CEZAMAT

EPIC European Photonics Industry Consortium

OWTNM2016

24TH INTERNATIONAL WORKSHOP ON OPTICAL WAVE & WAVEGUIDE THEORY AND NUMERICAL MODELLING

20–21 MAY | WARSAW | POLAND

THURSDAY, 19.05.2016

19.00–22.00	Welcome reception

FRIDAY, 20.05.2016

08.00–09.00	Coffee	
09.00–10.30	**ECIO+OWTNM PLENARY JOINT SESSION 1.01 + 2.01** **CHAIR: Trevor M. BENSON,** University of Nottingham, UK	
	09.00–09.30	**ECIO|I-25**| INVITED TALK | Andrea Melloni, **Tunable integrated photonics toolbox: from realistic models to control algorithms**
	09.30–10.00	**ECIO|I-26**| INVITED TALK | Philippe Lalanne, **Light interaction with resonance**
	10.00–10.30	**OWTNM|I-01**| INVITED TALK | Wim Bogaerts, **Challenges for Designing Large-scale Integrated Photonics**
10.30–11.00	Coffee break	
11.00–13.00	**ECIO+OWTNM SESSION | SIMULATIONS/MODELLING 4.04 + 4.05** **CHAIR: Andrea MELLONI,** Politecnico di Milano, Italy	
11.00–11.15	**ECIO|O-43**| Mariangela Gioannini, **Analysis of Quantum Dot Single Section FP Lasers for Comb spectra generation**	
11.15–11.30	**ECIO|O-44**| Daan Lenstra, **Rate-Equation Analysis for an Integrated Coupled- Cavity Laser with MMI Anti-Phase Coupler**	
11.30–11.45	**ECIO|O-45**| Giannis Poulopoulos, **Angled 3D Glass-to-SiPh adiabatic coupler**	
11.45–12.00	**ECIO|O-46**| Wim Bogaerts, **Optimization of Silicon Photonic Components using Multi-Fidelity Simulations and Co-Kriging**	
12.00–12.15	**ECIO|O-47**| Perry van Schaijk, **Feedback-Insensitive Integrated Laser**	
12.15–12.30	**OWTNM|O-01**| Alonso Millan Mejia, **Design of an Optical Nanoantenna with Focusing Sub-wavelength Grating Couplers and Metallic Reflector**	
12.30–12.45	**OWTNM|O-02**| Vipul Rastogi, **Effect of Dielectric Nanoparticles on Efficiency of Organic Solar Cell**	
12.45–13.00	**OWTNM|O-03**| Gregory V. Morozov, **Band Structure Analysis of a 1D Photonic Crystal with a Sawtooth Refractive Index**	
13.00–14.30	Lunch	
14.30–16.00	**OWTNM SESSION #1 | OPTICAL ARRAYS, GRATINGS AND VIAS 4.04 + 4.05** **CHAIR: Gregory MOROZOV,** University of the West of Scotland, UK	
14.30–15.00	**OWTNM|I-02**| INVITED TALK | Anatole Lupu, **Local Parity-Time-symmetry Grating Devices for Integrated Optics**	
15.00–15.15	**OWTNM|O-04**| Trevor M. Benson, **Time-Modulated Gain and Loss Parity-Time Symmetric Resonators**	
15.15–15.30	**OWTNM|O-05**| Ya Yan Lu, **Plane Wave Diffraction by Periodic Arrays of Nonlinear Cylinders**	
15.30–15.45	**OWTNM|O-06**| Nadège Rassem, **On the Thin Spectral Width of Cavity-resonator-integrated grating filters**	
15.45–16.00	**OWTNM|O-07**| Ripalta Stabile, **Design of an Optical Via for Large Scale Monolithic Multilayer PICs**	

16.00–16.45	**POSTER SESSION 4th floor, hall**
	OWTNM|p-01| Anna Piotrowska, **Strain Detection in Two- and Three-Dimensional Periodic Structures with the Low Index Contrast by Monitoring their Optical Response**
	OWTNM|p-02| Anne-Laure Fehrembach, **Electromagnetic modelling of large subwavelength-patterned highly resonant structures**
	OWTNM|p-03| Jan Fiala, **On the Origin of the Wood's anomalies in the Extraordinary Transmission through One-dimensional Sub-wavelength Periodic Arrays**
	OWTNM|p-04| Olga Kuryzheva, **Resonances Excited by an Airy Pulse in a Dielectric Laye**
	OWTNM|p-05| Nadiia Stognii, **Transient Plasmons Dynamics in Metallic Structures**
	OWTNM|p-06| Tomek Kaczmarek, **Dispersion and loss managed soliton communication system with use of new type of step-index optical fiber**
	OWTNM|p-07| Beata Derkowska-Zielińska, **Third Order Nonlinear Optical Properties of DCM**
	OWTNM|p-08| Hanna Stawska, **The Numerical Prediction of the Characteristics of Directional Multimodal Couplers for Two-Photon Endoscopy**
	OWTNM|p-09| Lukasz Pajewski, **Ray Tracing Methods in Numerical Analysis of Double-clad Microstructured Optical Fibre Coupler**
	OWTNM|p-10| Eliza Miśkiewicz, **Analysis of the Absorption and Refraction Spectra of Photorefractive GaAs – AlGaAs Heterostructures for Dynamic Diffractive Elements**
	OWTNM|p-11| Vladimir Burdin, **Model for a Few-Mode Nonlinear Propagation of Optical Pulse in Multimode Optical Fiber**
16.45–18.15	**OWTNM SESSION #2 | PLASMONICS 4.04 + 4.05** **CHAIR: Manfred HAMMER,** University of Paderborn, Germany
16.45–17.00	**OWTNM|O-08|** Pavel Kwiecien, **Simulations of sensing capabilities of propagating modes supported by a sparse array of metal nanoparticles**
17.00–17.15	**OWTNM|O-09|** Gilles Rosolen, **Doping and connecting graphene dimers for a tunable absorption spectrum**
17.15–17.30	**OWTNM|O-10|** Thomas Christopoulos, **Optical Bistability and Self-Pulsation with Long-Range Hybrid Plasmonic Disk Resonators**
17.30–17.45	**OWTNM|O-11|** Gilles Renversez, **Improved nonlinear plasmonic waveguides: modal spatial transitions and loss reduction**
17.45–18.00	**OWTNM|O-12|** Hung-chun Chang, **Leaky and Bound Modes on Stripe Plasmonic Waveguide Related Structures**
18.00–18.15	**OWTNM|O-13|** T. V. Raziman, **Detecting weak modes in plasmonic systems using complex polarisation charge**
19.30–24.00	Grill dinner **LOLEK PUB (Pole Mokotowskie), ul. Rokitnicka 20**

SATURDAY, 21.05.2016

08.00–09.00	Coffee
09.00–10.30	**SESSION #3 | WAVEGUIDE BASED DESIGN 4.04 + 4.05** **CHAIR: Anne-Laure FEHREMBACH,** Aix-Marseille Université, CNRS, France
09.00–09.15	**OWTNM|O-14|** Manfred Hammer, **Hybrid Coupled Mode Modelling**
09.15–09.30	**OWTNM|O-15|** Hannes Lüder, **Coupled-Mode Theory for Complex-Index, Corrugated Multilayer Stacks**
09.30–09.45	**OWTNM|O-16|** Igor Lyubchanskii, **Optical Properties of a Four-Layer Waveguiding Nanocomposite Structure in the Near-IR Regime**
09.45–10.00	**OWTNM|O-17|** Christoph Wächter, **Low Loss Estimation in Thin Film Configurations by Means of Leaky Wave Resonances**
10.00–10.15	**OWTNM|O-18|** Yufei Xing, **Backscatter Model for Nanoscale Silicon Waveguides**
10.15–10.30	**OWTNM|O-19|** Jon Ø. Kjellman, **Design of Dual Layer, Dual Width Waveguides for Giant Group Velocity Dispersion**

10.30–11.00	Coffee break
11.00–13.00	**SESSION #4 | PHOTONIC DESIGN 4.04 + 4.05** **CHAIR: Christoph WÄCHTER,** Fraunhofer Institute for Applied Optics and Precision Engineering, Jena, Germany
11.00–11.15	**OWTNM|O-20** | Lukasz Sójka, **Numerical Investigation of Mid-infrared Laser Action in Pr^{3+} Doped Chalcogenide Fibre Laser**
11.15–11.30	**OWTNM|O-21** | Ľ. Scholtz, **Numerical Investigation of All-Optical Switching in Nonlinear Chalcogenide Fibre Bragg Gratings due to Cross-Phase and Self-Phase Modulation**
11.30–11.45	**OWTNM|O-22** | Marian Marciniak, **Analysis of Single-Frequency Radiation from Fiber Laser with Bragg Reflectors: Numerical Simulation by the Method of Single Expression**
11.45–12.00	**OWTNM|O-23** | Anton Bourdine, **Design of Silica Few-Mode Optical Fibers with Enlarged Core Diameter**
12.00–12.15	**OWTNM|O-24** | Vipul Rastogi, **Six-mode-group Fiber Amplifier for SDM System**
12.15–12.30	**OWTNM|O-25** | Libor Ladányi, **Numerical Simulation of the Dispersion-Managed Soliton Pulse Propagation**
12.30–12.45	**OWTNM|O-26** | Siergei Mingaleev, **VPImodeDesigner: An Integrated Framework for Modeling Optical Waveguides and Fibers**
12.45–13.00	**OWTNM|O-27** | Alberto Parini, **Design Space Exploration of Functional Blocks for On-chip Mode Division Multiplexing**
13.00–14.00	Lunch **gound floor, hall**
14.00–15.30	**SESSION #5 | ANALYSIS, THEORY AND MODELLING 4.04 + 4.05** **CHAIR: Marian MARCINIAK,** National Institute of Telecommunications, Poland
14.00–14.30	**OWTNM|I-03** | INVITED TALK | Daryl Beggs, **Polarisation singularities in disordered photonic crystal waveguides for on-chip spin-photon entanglement**
14.30–14.45	**OWTNM|O-28** | Alberto Parini, **Two-mode Waveguide with Nonlinear Ring Resonator**
14.45–15.00	**OWTNM|O-29** | Martina Gerken, **Simulation Methods for Multiperiodic and Aperiodic Nanostructured Dielectric Waveguides**
15.00–15.15	**OWTNM|O-30** | Eugene Sokolov, **High-Order Split-Step Time-Domain Modelling of Optoelectronic Devices with Distributed Feedback**
15.15–15.30	**OWTNM|O-31** | Hendrik Kleene, **An Assessment of Polynomial Approximations for the Time-Domain Beam Propagator**
15.30–16.00	**Closing remarks 4.04 + 4.05**

24TH INTERNATIONAL WORKSHOP ON OPTICAL WAVE & WAVEGUIDE THEORY AND NUMERICAL MODELLING

OWTNM2016

20–21 MAY | WARSAW | POLAND

FRIDAY 20TH MAY 2016

09:00-10:30

OWTNM + ECIO PLENARY JOINT SESSION

CHAIR: **TREVOR M. BENSON,**
UNIVERSITY OF NOTTINGHAM, UK

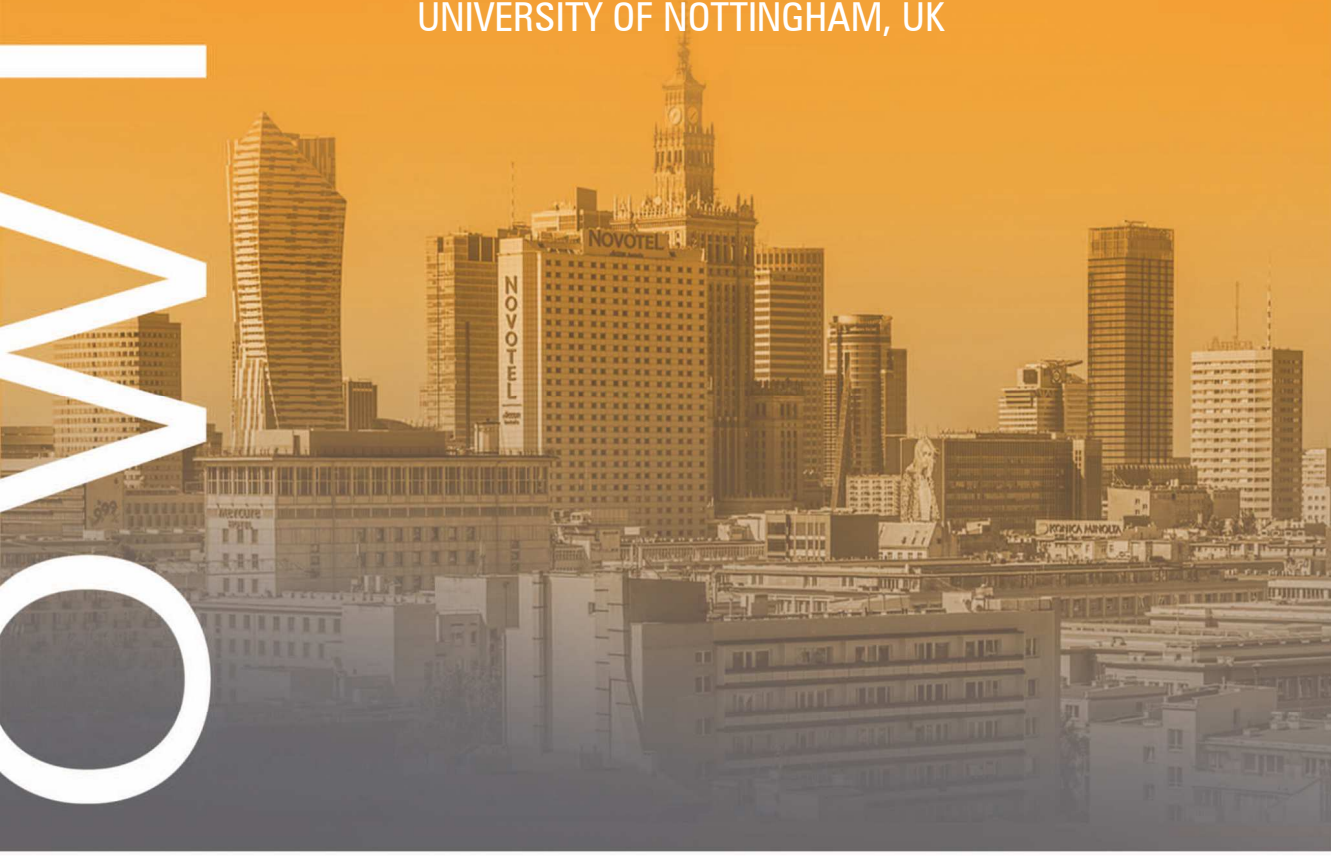

The University of Nottingham
UNITED KINGDOM · CHINA · MALAYSIA

SUPPORTED BY

CZIiTT Centre for Innovation and Technology Transfer Management WUT

SKKP POLISH CONFERENCE & CONGRESS ASSOCIATION

CEZAMAT

EPIC European Photonics Industry Consortium

OWTNM 2016 | 24TH INTERNATIONAL WORKSHOP ON OPTICAL WAVE & WAVEGUIDE THEORY AND NUMERICAL MODELLING

Tunable photonic integrated toolbox: from realistic models to control algorithm

Andrea MELLONI*, Daniele MELATI, Stefano GRILLANDA, Andrea ANNONI, Nicola PESERICO[1] and Francesco MORICHETTI

Dipartimento di Elettronics, Informazione e Bioingegneria, Politecnico di Milano, via Ponzio 34/5, 20133 Milano, Italy

* andrea.melloni@polimi.it

The evolution towards complex photonic circuits integrating many building blocks and functionalities poses major issues on the design as well as on the control of the functionality in real operation conditions. Optical and thermal interactions between single devices, spurious effects, drifts, non-idealities and fabrication uncertainties can prevent the realized circuits to work as expected. As a consequence, advanced photonic devices must be considered as a system to control with feedback loops and algorithms, and the above non-idealities must be taken into account also during the early design stages to evaluate their impact on the circuit behavior and perform robust optimizations towards the parameters of interest.

Here, the estimation of the impact of the tolerances on a tunable delay line and a robust optimization of a filter, are reported. Further, the tools needed to monitor and control a complex circuit are described and an example discussed.

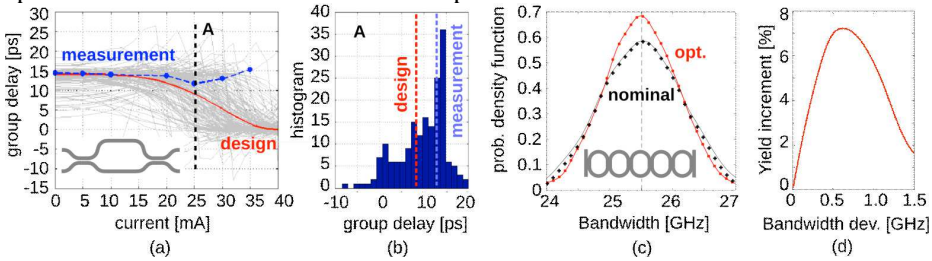

Fig. 1. (a) Group delay of a Mach-Zehnder filter as function of the current fed into the controller of the tunable couplers and (b) histogram at 25 mA. (c) Probability density function of the 3-dB bandwidth of a five-ring-resonator filter for nominal (black curve) and optimized design (red curve). (d) Circuit yield increment for the optimized design.

Circuit simulators enriched by advanced Process Design Kits and complex models are emerging as the right tools to perform this kind of analyses [1,2]. As an example, Fig.1 (a) shows the Monte-Carlo analysis of the group delay of a tunable delay line based on unbalanced Mach-Zehnder Interferometer (MZI) with tunable couplers (realized with two balanced MMI-based MZIs) when exposed to fabrication uncertainties. Group delay is reported as function of the current fed to the thermal actuators used to change the splitting ratio of the two couplers. Simulations were performed with the commercial circuit simulator Aspic [3]. Red curve shows the designed group delay that is expected to drop of about 15 ps applying a current of 40 mA. In order to describe realistic "grand challenge" and a major obstacle to the advent of large-scale photonic integrated systems. The possibility to control the PIC is a key requirement for different reasons and in many applications: i) reconfigurability of circuits to provide the required functionality such as in routers, cross-connects, tunable bandwidth filters, reconfigurable add-drop multiplexers, etc.; ii) adaptive circuits that modify their behavior depending on the state of the system such as signal polarization

state, signal to noise ratio, crosstalk, eye aperture, BER, etc.; iii) locking or stabilization of the circuit in a well-defined state independently of the temperature, electrical fluctuations, drifts, stress, aging, etc; iv) compensation of fabrication tolerances and technological non-uniformities. All these requirements become even more critical when dealing with wavelength selective devices, such as microrings resonators, high bit rate signals operating in coherent domain, dense WDM systems and densely integrated PICs realised on semiconductor platforms, such as silicon and indium phosphide InP. Local and global feedback control tools and strategies will soon become the ordinary way to operate even for simple circuits.

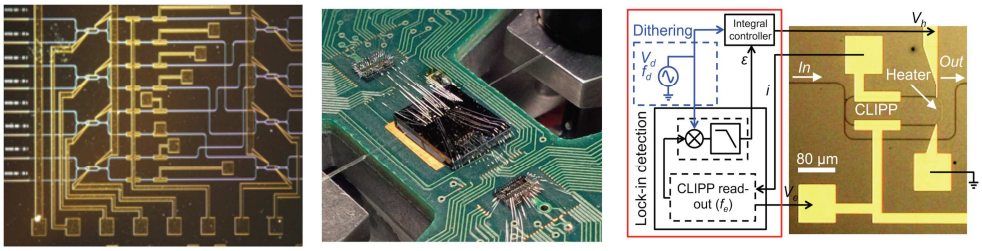

Fig. 2. (from left to right) An 8x8 Silicon Photonic Router with heathers and CLIPPs, mounted on a PCB with two CMOS ASICs for the control and readout and a detail of a ring resonator with feedback control loop.

In order to realize a feedback control loop, light monitors and actuators are required, in addition to an electronic control unit and control strategies. Monitoring approaches based on conventional photodetectors are not effectively scalable to large-scale PICs due to the need for multi-point light tapping. In this work, we report on our recent achievements on the development of an in-line transparent integrated detector, named ContactLess Integrated Photonic Probe (CLIPP) [5,6,7], that can monitor the light intensity in semiconductor waveguides without introducing any photon absorption in excess to the waveguide propagation loss and on the control strategies for PICs. Results shown in this work demonstrate the effectiveness of the non-invasive CLIPP technology for the feedback-control tuning, switching, and locking of silicon PICs. As an example, Fig. 2 shows an 8x8 Silicon Photonic Router with heathers and CLIPPs, mounted on a PCB with two CMOS ASICs for the control and readout and a detail of a ring resonator with feedback control loop. The CLIPPs permits to monitor the circuit in every desired point and control the working points of the various elements individually.

Also, when multiple optical signals are simultaneously injected at different input ports of a circuit, like a switch fabric, CLIPP detectors can be used to identify channels coming from specific input ports regardless of the presence of other concurrent channels injected at the other input ports if these are labelled with a tone with an intensity modulation

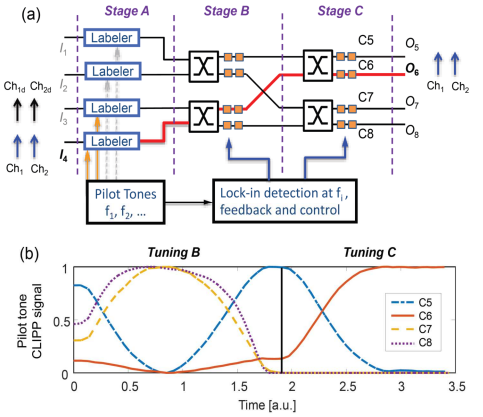

Fig. 3. CLIPP assisted lightpath tracking using on-chip labelling with pilot tones: scheme and CLIPPs signal after the stage B and stage C.

amplitude of a few percent and a frequency in the order of some kilohertz. Fig. 3 shows the CLIPP assisted lightpath tracking of concurrent signals distinguished by using on-chip labelling through pilot tones.

In conclusion, we have shown the software tools for the design and analysis of circuits in presence of tolerances, non-perturbative probes for monitoring and feedback algorithms and for locking and control of complex PIC. This toolbox is strategic for a fully exploitation of the capabilities of photonic circuits.

References

[1] D. Melati,et al., *Statistical Process Design Kits: analysis of fabrication tolerances in integrated photonic circuits,* Proceedings IPR, IT4A–5, OSA, 2015

[2] T. Weng, et al., *Uncertainty quantification of silicon photonic devices with correlated and non-Gaussian random parameters*, Optics express 23, 4242–4254 (2015)

[3] Aspic, http://www.aspicdesign.com, Phoenix bv, http://www.phoenixbv.com

[4] T. Weng, et al., *Stochastic Simulation and Robust Design Optimization of Integrated Photonic Filters*, submitted to Nanophotonics

[5] F. Morichetti et al., "Non-invasive on-chip light observation by contactless waveguide conductivity monitoring," IEEE J. Sel. Top. Quantum Electron. 20, 1–10, 2014

[6] S. Grillanda *et al.*, "Non-invasive monitoring and control in silicon photonics using CMOS integrated electronics," Optica 1, 129-136, 2014

[7] D. Melati et al., "Contactless integrated photonic probe for light monitoring in InP-based devices. IET Opt. 9, 2015

OWTNM 2016 | 24TH INTERNATIONAL WORKSHOP ON OPTICAL WAVE & WAVEGUIDE THEORY AND NUMERICAL MODELLING

Light interaction with resonance

Philippe LALANNE, Rémi FAGGIANI and Jianji YANG
LP2N, CNRS, Institut d'Optique, IOGS - Univ. Bordeaux, 33400 Talence, France
* philippe.lalanne@institutoptique.fr

Thanks to an efficient and intuitive quasi-normal mode formalism valid for micro and nanoresonators made of dielectric as well as lossy and dispersive materials, we shine new light on the physics and modelling of light interaction with electromagnetic resonances [1]. In particular in the present context, we will discuss the role of quenching for light emission in metallic nanogap devices and will revisit the perturbation theory of electromagnetic resonance.

Simply because they enhance the electromagnetic field, micro/nano resonators play an important role in modern photonics. Perhaps they are as important as waveguides. A resonance mode is a solution of Maxwell's equations without source with a complex frequency, and the resonance quality factor Q equals the ratio between the real and imaginary parts of the frequency.

However, the maturity level of the theory and computation of resonances is ridiculously small compared to that reached for waveguides (see, e.g., the books by Marcuse, Snyder and Love, Vassalo …). As a matter of fact, very few scientists in nanophotonics and optics would be able to calculate and properly normalize the resonance modes with a complex frequencies.

As the frequency is complex, the resonance field exponentially diverges as the distance r to the resonator increases, $\exp(ikr) \rightarrow \infty$ since $k=w/c$ is complex, making a mode normalization difficult. We have recently challenged the longstanding normalization issue of resonance modes, and have been able to define (properly?) the "famous" mode volume [1].

Thanks to this theoretical upstream work, we explain why an emitter placed in a metallic nanogap (thickness < 10 nm) does not quench much despite the small distance to the metal, and the consequences for nanogap antenna [2] and revisit perturbation theory of resonator [3].

References

[1] C. Sauvan, J. P. Hugonin, I. S. Maksymov, and P. Lalanne, *Theory of the Spontaneous Optical Emission of Nanosize Photonic and Plasmon Resonators*, Phys. Rev. Lett. 110, pp. 237401, 2013
[2] R. Faggiani, J. Yang, P. Lalanne, *Quenching, Plasmonic, and Radiative Decays in Nanogap Emitting Devices*, *ACS Photonics 2* (12), pp 1739-1744, 2015
[3] J. Yang, H. Giessen, P. Lalanne, *Simple Analytical Expression for the Peak-Frequency Shifts of Plasmonic Resonances for Sensing*, Nano Lett. 15 (5), pp 3439-3444, 2015

OWTNM 2016 | 24TH INTERNATIONAL WORKSHOP ON OPTICAL WAVE & WAVEGUIDE THEORY AND NUMERICAL MODELLING

Challenges for Designing Large-scale Integrated Photonics

Wim BOGAERTS[1,2*]
[1]Ghent University – IMEC, 9000 Ghent, Belgium
[2]Luceda Photonics, 9200 Dendermonde, Belgium
* wim.bogaerts@ugent.be

With the growing adoption of silicon photonics in data- and telecommunication as well as sensing and spectroscopy, the difficulties of designing larger circuits in this technology have become more prominent. Silicon photonic waveguides have submicron dimensions, and can therefore be integrated in large numbers on a chip. But these same submicron dimensions give rise to extreme sensitivity of the waveguide response to small variations in geometry, temperature, stress etc. Multiply this with thousands of functional building blocks and even more interconnects, and it is clear that it becomes very challenging to guarantee the correct functionality of a photonic integrated circuit. Even if the circuit is nominally correct, compound variability can still dramatically lower the yield.

When designing silicon photonic chips, it is important to start from a workflow which has the largest chance of transferring the intent of the designer to a working chip layout for fabrication. Such a workflow is known in electronic design automation (EDA). It makes sense to reuse this model from electronics because photonic circuits are ever more tightly integrated with electronics, both technologies make use of similar planar manufacturing processes, design frameworks exist and there is a large community of expertise. An EDA workflow starts from a schematic circuit that can be optimized for the desired functionality. As electronics and photonics use different physics, it is challenge is to combine the two circuit models into a single design flow. The circuit description can then be implemented in a chip layout manually or with assistance of a *schematic driven layout* tool. Again, photonics imposes different constraints on layout than electronics. The resulting layout should then be verified against design rules (*design rule check*) and the functionality is checked against the original specifications (*layout-vs-schematic*). Here as well, photonics imposes challenges in extracting the connectivity and verifying the curved geometries.

While the similarities in design flows already enable photonic designers to a large extent, the challenges in each step, combined with the inherent variability of the process and operational conditions, make it very hard to accurately predict the yield of larger circuits. *Design-for-Manufacturability* (DfM) techniques that are used for electronics cannot necessarily be applied for photonics. We will discuss the different challenges in detail and also present some of the solutions that are emerging.

References

[1] W. Bogaerts, M. Fiers, P. Dumon,, *Design Challenges in Silicon Photonics*, J. Sel. Top. Quantum Electron., vol. 20, no. 4, 1-8, 2014
[2] L. Alloatti, M. Wade, V. Stojanovic, M. Popovic and R. J. Ram, *Photonics design tool for advanced CMOS nodes,* in IET Optoelectronics, vol. 9, no. 4, pp. 163-167, 8 2015.
[3] M. Heins, et al. *Design Flow Automation for Silicon Photonics: Challenges, Collaboration, and Standardization,* Silicon Photonics III. Springer Berlin Heidelberg, 2016. 99-156.

24TH INTERNATIONAL WORKSHOP ON OPTICAL WAVE & WAVEGUIDE THEORY AND NUMERICAL MODELLING

OWTNM2016

20–21 MAY | WARSAW | POLAND

FRIDAY 20TH MAY 2016

11:00-13:00

OWTNM+ECIO JOINT SESSION

SIMULATIONS/MODELLING

CHAIR: **ANDREA MELLONI,**
POLITECNICO DI MILANO, ITALY

OWTNM 2016 | 24TH INTERNATIONAL WORKSHOP ON OPTICAL WAVE & WAVEGUIDE THEORY AND NUMERICAL MODELLING

Analysis of Quantum Dot Single Section FP Lasers for Comb Spectra Generation

Mariangela GIOANNINI*, Paolo BARDELLA, Ivo MONTOSSET
Dipartimento di Elettronica e Telecomunicazioni, Politecnico di Torino, Torino, Italy
*mariangela.gioannini@polito.it

There is an increasing interest on Quantum Dot lasers as light source in silicon photonic integrated circuit; one promising application is the use of a QD comb laser as compact WDM source that could replace a DFB array more difficult to integrate with the Si PIC[1]. Many experiments on single section Fabry Perot QD lasers have demonstrated the possibility of generating wide optical comb spectra at telecom wavelengths but there is still a lack of modelling work for providing physical explanations on the capability of the QD lasers of generating phase locked optical modes. We present a Time Domain Travelling Wave model we have recently developed to move the first step in this direction [2]. We discuss here the role of some key QD material parameters such as the large gain compression factor (ε-parameter), the inhomogeneous gain broadening due to QD self-assembled growth process, the homogeneous gain broadening due to polarization dephasing time and the carrier relaxation time.

Numerical Model The spatio-temporal evolution of the optical electric field is described by the slowly varying forward/backward components of the electric field coupled with the slowly varying components of the macroscopic polarization which is the sum of the polarizations of each QD sub-group (ie: QDs with almost the same size) of the inhomogeneous ensemble. The polarization equations are coupled with electron and hole multi-population rate equations and the whole system is then solved with a finite difference scheme [2].

Simulation results and discussion We consider a 500 μm FP laser with 10 QD layers. We analyse the role of the QD material parameters on the phase locking of the longitudinal modes and on the stability of the intensity of the optical lines. The phase locking is evaluated by the possibility of generating narrow pulses after including the numerical group delay dispersion (GDD) compensation of the FP laser output field. If the modes are in a stable phase relation one respect to the other, the GDD compensation corrects the non-linear phase variation and allows the pulse formation . The intensity stability of each longitudinal mode is analysed by calculating the RIN of each single line compared to the RIN of the total power [3]. The numerical results are summarized in the following figures. Fig. 1(a) plots the output power vs time after a current step of 500mA at *t=0s* and Fig. 1(b) is the optical spectrum showing a -10dB bandwidth of 10nm. Fig. 1(c) reports the intensity vs time of each optical line showing that only few modes initially turns on at *t=0s.* These seed modes start transferring the power to the other adjacent modes thanks to the quite large gain compression of the QDs (ε=1.5 10^{-16} cm^3) . This transient concludes at about 250ns with a rather broad optical spectrum. From this time instant, applying the GDD compensation we can obtain pulses as depicted in Fig. 1(d) and (e).

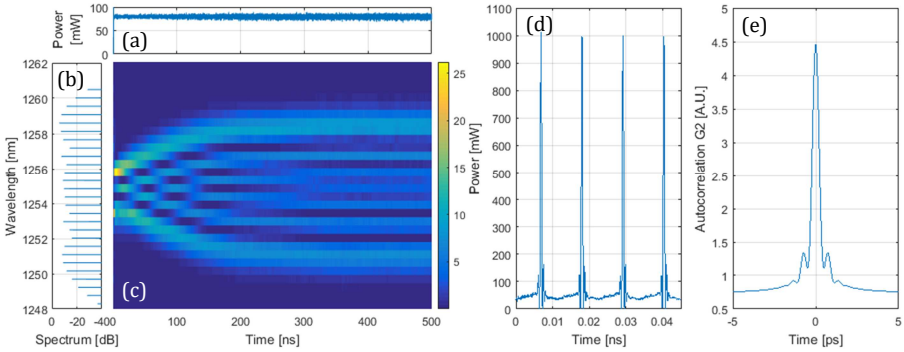

Fig. 1. (a) Power versus time, (b) optical spectrum, (c) mode intensity versus time, (d) pulses after GDD compensation and (e) corresponding autocorrelation.

Fig. 2 reports the calculated RIN of the output power and of the individual spectral lines. In good agreement with the experiments [3] the total RIN is much smaller than the RIN of each single line indicating that the intensity fluctuations of the optical lines are coupled and compensate each other. The comparison of Fig. 2a and 2b evidences that a large ε-parameter increases the RIN because of the stronger coupling among the modes. In Fig. 3 we compare the role of the homogeneous broadening (Fig. 3a), of the inhomogeneous broadening (Fig. 3b) and of the carrier relaxation time from the QD excited state to the ground state (Fig. 3c) on the pulse formation and therefore on the number of phase locked modes of the spectrum. From the comparison we conclude that a very homogeneous material (large homogeneous broadening and small inhomogeneous broadening) is the best case for narrow pulses and therefore for increasing the number of locked modes in the spectrum. A slower relaxation time and a slower gain recovery (respect to the cavity round trip) also inhibit multiple pulse formation and improve pulse stability.

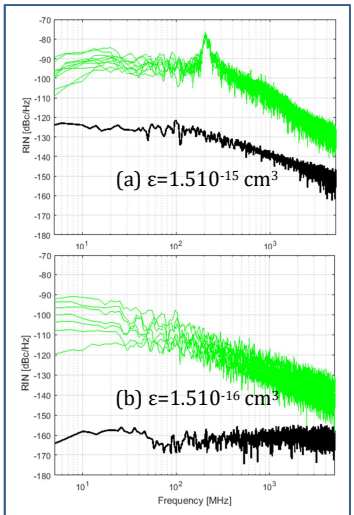

Fig. 2 Calculated RIN of each optical line (green) and total power (black).

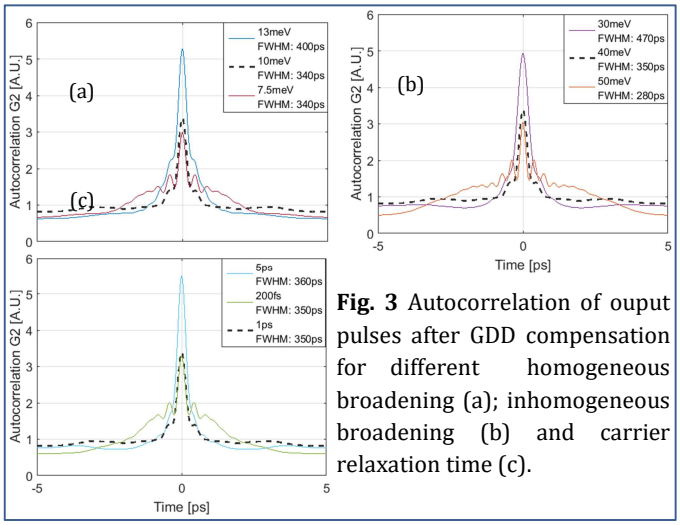

Fig. 3 Autocorrelation of ouput pulses after GDD compensation for different homogeneous broadening (a); inhomogeneous broadening (b) and carrier relaxation time (c).

References

[1] C. Schulien , PIC International Conf., Brussels, 1-2 March 2016
[2] M. Gioannini et al. IEEE J. Select. Top. Quantum Electron., vol. 21, no. 6, 2015
[3] Y .M'Sallem et al. Phot. Tech. Lett., vol. 23, no. 7, 2011

OWTNM 2016 | 24TH INTERNATIONAL WORKSHOP ON OPTICAL WAVE & WAVEGUIDE THEORY AND NUMERICAL MODELLING

Rate-Equation Analysis for an Integrated Coupled-Cavity Laser with MMI Anti-Phase Coupler

Daan LENSTRA
Eindhoven University of Technology, P.O.Box 513, 5600MB , The Netherlands
* d.lenstra@tue.nl

In this paper a dynamical theory is reported for the coupled-cavity laser (CCL) with a multi-mode interference (MMI) coupler, which provides an excellent description of the locking and other operational aspects of the laser realized by D'Agostino et al. in 2015 [1]. The revived interest in CCLs as widely tuneable lasers for sensing and other applications is due to the specially designed MMI anti-phase coupler as described in [1]. The theory explains if, why and how the two individual isolated constituent modes combine to one single "super mode", a situation referred to as locked state. A comprehensive formulation of the model and derivation of the rate equations for the CCL with quantum-well active material can be found in [2].

We consider two Fabry-Pérot (FP) lasers that are very similar except they differ 5–10 % in length and couple by a reflective MMI coupler. The amplitudes indicated (Fig.1) are evaluated at the point where each laser touches the MMI-coupler. Note that the coupling parameters have been designed in such a way that C_{bar} and C_x are 180 degrees out of phase and the sum of their absolute values equals unity. This is a property of the 3x3 reflective coupler in which only the two outer ports are used [1,2]. The ideal theoretical values for the coupling coefficients are C_{bar}=0.79 and C_x=-0.21 [1,2]. This implies that if the amplitudes E_1 and E_2 are equal and opposite, the coupler behaves as a 100% reflector for both lasers. Due to small deviations from growth specifications the ideal values for the coupling coefficients can very well be somewhat different. In fact, we found that best agreement with experimental data was achieved by taking smaller values for C_{bar}, i.e. 0.75 instead of 0.79, and for $|C_x|$, i.e. 0.18 instead of 0.21.

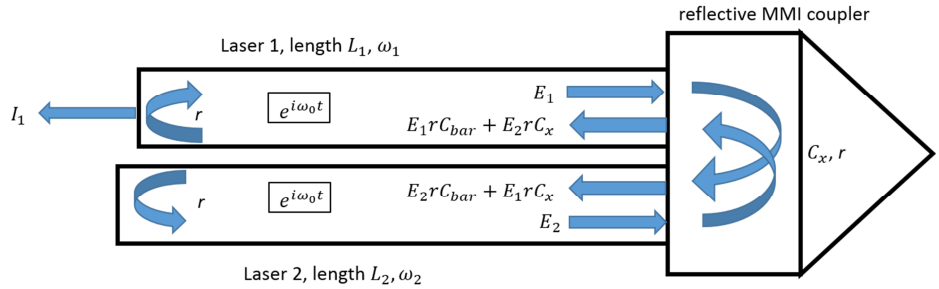

Fig. 1. Sketch of two FP-lasers coupled by a reflective MMI coupler with designed coupling parameters C_{bar} and C_x. The slowly-varying amplitudes are relative to the exponential time factor as indicated, where ω_0 is the locked frequency. ω_1 , ω_2 are the frequencies of the isolated lasers, i.e. when C_x=0.

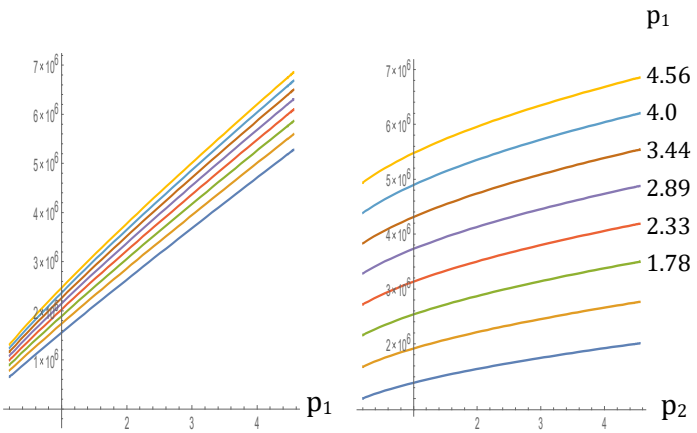

Fig. 2. Left: Intensity I_1 versus p_1, at fixed p_2 = {0.67, 1.22, 1.78, 2.33, 2.89, 3.44, 4., 4.65}. Right: intensity I_1 versus p_2, with fixed p_1 = {same values}; optimized detuning assumed. The shapes of the curves hardly depend on the precise value of α . The values for C_{bar} and C_x as in table 1 were taken so as to optimize the qualitative and quantitative proportionality agreement with the measured curves in [1].

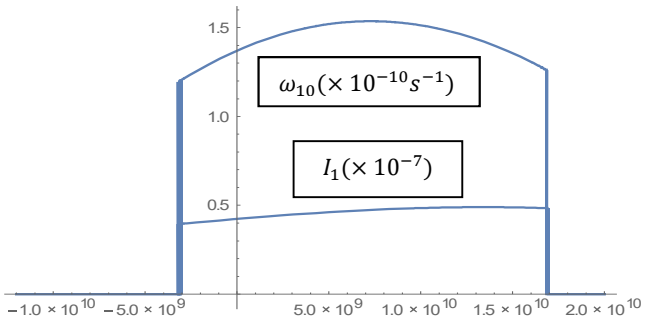

Fig. 3. Intensity $I_1(\times 10^{-7})$ and operation frequency shift $\omega_{10}(\times 10^{-10})$ versus detuning $\omega_{21} \equiv \omega_2 - \omega_1$ within the locking range. The pump strengths are $p1$=4, $p2$=2.

Fig. 2 left shows the output-intensity curves of laser 1 versus its pump strength for various values of the pump strength of laser 2; Fig. 2 right shows the output intensities versus the pump strength of laser 2 with the pump strength of laser 1 as parameter. Here we define for j=1,2 the pump strengths as $p_j \equiv \Delta J_j / J_{thr,j}$ where ΔJ_j is the injection current w.r.t. the threshold current $J_{thr,j}$ (i.e. when each laser stands on its own, that is, without any coupling. The shapes of the curves agree well with the measured curves in [1]. Fig. 3 shows numerical results for the output intensity of laser 1 and the operation frequency within the locking range.

References

[1] D. D'Agostino, D. Lenstra, H. P. M. M. Ambrosius, and M. K. Smit, *Coupled cavity laser based on anti-resonant imaging via multimode interference*, OPTICS LETTERS, vol. 40, pp. 653-656, 2015

[2] D.Lenstra, *Rate-equation analysis for the coupled-cavity laser with MMI anti-phase coupler*, **DOI:** 10.13140/RG.2.1.2747.6245, 2016

OWTNM 2016 | 24TH INTERNATIONAL WORKSHOP ON OPTICAL WAVE & WAVEGUIDE THEORY AND NUMERICAL MODELLING

Angled 3D Glass-to-SiPh adiabatic coupler

Giannis POULOPOULOS[1*], Dimitrios KALAVROUZIOTIS[1], John R. MACDONALD[2], Paul MITCHELL[2], Nicholas PSAILA[2], Joek TUIN[3], Rutger SMINK[3], Sander DORRESTEIN[3], Michiel VAN RIJNBACH[3], Jeroen DUIS[3], Hercules AVRAMOPOULOS[1]

[1]National Technical University of Athens, Patission 42, Athens, 10682, Greece
[2]Optoscribe Ltd, 5 Bain Square, Kirkton Campus, Livingston, EH54 7DQ. UK
[3]TE Connectivity, Rietveldenweg 32, 5222 AR 's-Hertogenbosch, The Netherlands
[*] jpoul@mail.ntua.gr

Concept Despite the promise of Silicon Photonics (SiPh) towards next-generation deployments seamlessly combining the on-chip advanced optical functionality with efficient E/O and O/E conversion, their wide penetration across all communication layers is currently hindered by the lack of efficient and scalable optical input-outputs (I/O) that can be realized using standard low-cost assembly equipment. To this end, diffraction-based structures, such as grating couplers, have been lately superseded by in-place coupling solutions employing inverse tapers [1] or metamaterial waveguides [2] in order to achieve coupling to SMFs through spot-size conversion. Nevertheless, those structures suffer from either increased fabrication complexity, including material engineering and undercut waveguide sections, or considerable losses due to poor mode matching. Recently, a very interesting concept was presented by Soganci et al. [3], proposing a compliant polymer interface between SMFs and nanophotonic waveguides, relying on adiabatic coupling. The first experimental demonstration of the interface [4] revealed the necessity of a well-defined, angled adhesive gap so as contain the scattering loss at the chip edge that is degrading the performance. However, considering the coefficient of thermal expansion (CTE) mismatch between the polymer and the SiPh chip, such an accurate control over the adhesive gap will significantly increase the intricacy of the assembly process.

In the current manuscript we propose and simulate, an adiabatic coupling scheme between a 2 degrees angled 3D glass waveguide and a SiPh platform, as shown in Fig. 1. The concept relies on the simultaneous and reverse tapering of the two waveguide cores, that increases the coupling performance and reduces the coupling length, while it alleviates the edge chip scattering loss thanks to the angled approach. The 3D glass waveguide exhibits a mode diameter of about 7um and it relies on the 3D waveguide inscription technology developed by Optoscribe.

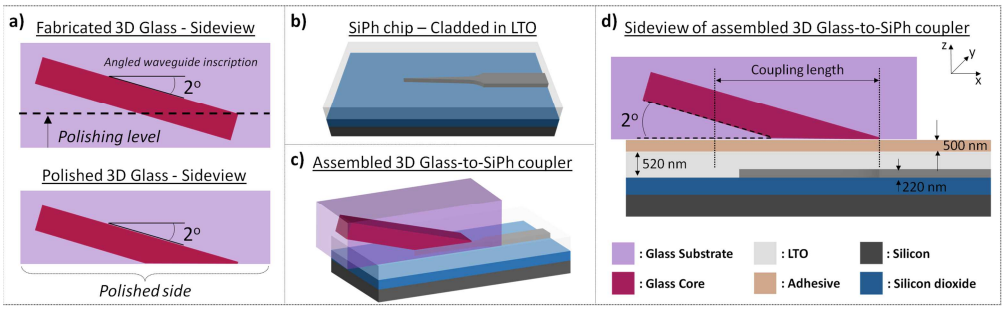

Fig. 1. (a) Angled 3D glass waveguide, (b) SiPh chip, (c) 3D sketch and (d) Sideview of the assembled 3D Glass-to-SiPh coupler.

Access to the glass waveguide, prior the assembly, can be achieved by regular polishing (Fig. 1a). The SiPh chip employs 220nm top-Si strip waveguide configuration, with 450nm nominal waveguide width and 520nm LTO cladding (Fig. 1b), whereas a 500nm-thick adhesive gap, separating the two platforms, is also considered. A 3D sketch and a sideview of the assembled structure are shown in Figs. 1c and 1d.

Simulations Coupler's design relies on the calculation of the optimum taper shape that will allow for maximum power coupling within the coupling length that is firmly specified by the angle of the glass waveguide. The ends of the tapering sections of both waveguides are aligned (marker A, Fig 1d) and the assembled structure is backwards divided into fixed-length segments. For each segment, the width of the silicon waveguide is varied and the excited supermodes are calculated, employing Lumerical's Finite Difference Eigenmode solver (FDE). The optimum silicon width is chosen based on the simultaneous fulfillment of the two following criteria: (i) the overlap integral between the fundamental TE supermode of the current and the previous segment should lay within 0.9975 and 0.9999, (ii) the supermode's effective index should be equal or higher than the effective index of the glass mode so to avoid leaky mode excitation. The resulting taper shape is shown in Fig.2a revealing a rather slow slope from 170nm to 240nm and fast transitions before and after that. The minimum silicon width was 150nm so as to enable standard photolithography and avoid e-beam.

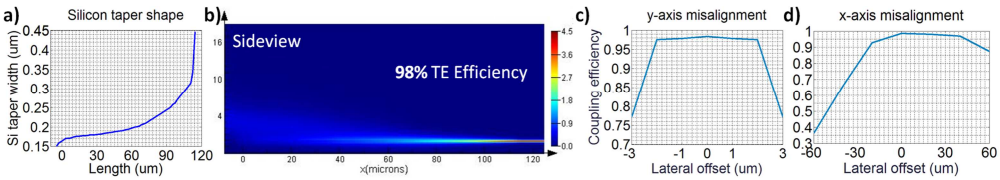

Fig. 2. (a) Silicon taper shape, (b), Sideview of the EME TE propagating field, and effect of the (c) y-axis and (d) x-axis lateral assembly misalignments on the coupling efficiency.

The coupler design was then imported into a 3D Eigenmode Expansion (EME) propagation simulation environment under the assumption the 2 degrees angle of the propagating field can be ignored. The overall TE glass-to-silicon coupling efficiency was found to be 98% while the coupling length was as low as 120um. A sideview impression of the TE propagating field is shown in Fig. 2b. The effect of the lateral assembly misalignments on the coupling efficiency was also briefly investigated using the EME solver. The results shown in Fig. 2c and 2d indicate adequate tolerance to lateral misalignments both along the y- and the x-axis, enabling the use of low-cost passive alignment assembly equipment.

Acknowledgments This work was supported by European Commission under FP7 projects PHOXTROT (318240) and MIRAGE (318228).

References

[1] X. Tu *et al.*, *Low polarization-dependent-loss silicon photonic trident edge coupler fabricated by 248 nm optical lithography*, Proceedings of the Conference ACP 2015, AS4B.3

[2] T. Barwicz *et al. An O-band Metamaterial Converter Interfacing Standard Optical Fibers to Silicon Nanophotonic Waveguides,* Proceedings of the Conference OFC 2015, Th3F.3

[3] I. M. Soganci *et al.*, *Flip-chip optical couplers with scalable I/O count for silicon photonics*, Optics Express, vol. 21, no. 13, pp. 16075-16085, 2013

[4] T. Barwicz *et al.*, *Optical Demonstration of a Compliant Polymer Interface between Standard Fibers and Nanophotonic Waveguides,* in Proceedings of the Conference OFC 2015, Th3F.5

OWTNM 2016 | 24TH INTERNATIONAL WORKSHOP ON OPTICAL WAVE & WAVEGUIDE THEORY AND NUMERICAL MODELLING

Optimization of Silicon Photonic Components using Multi-Fidelity Simulations and Co-Kriging

Pierre WAHL[1,6], Ivo COUCKUYT[2], Christian KREMERS[3], Frank DEMMING[3]
Tom DHAENE[2], Wim BOGAERTS[1,4,5*]
[1]Luceda Photonics, Dendermonde, Belgium
[2]Surrogate Modelling Group, Ghent University-iMinds, Dept. of Information Technology, G. Crommenlaan 8 Blok C0 bus 201, 9050 Ghent, Belgium
[3]CST-Computer Simulation Technology AG, Bad Nauheimer Strasse 19, 64289 Darmstadt, Germany.
[4]Photonics Research Group, Ghent University-Imec, Technologiepark 15, 9052 Ghent, Belgium
[5]Center for Nano- and Biophotonics, Ghent University, Belgium
[6]Brussels Photonics Team B-PHOT, Department of Applied Physics and Photonics, Vrije Universiteit Brussel, Brussels, Belgium
[*] Wim.Bogaerts@ugent.be

Silicon photonic devices can be very compact because of the high refractive index contrast. But this also makes them very sensitive to geometry variations, and hard to model [1]. Typically, a fully vectorial, 3D solution of Maxwell's equations is the only reliable simulation technique, be it with *eigenmode expansion* (EME) or *finite-difference-time-domain* (FDTD). Finding an optimum geometry of a parametric component is therefore computationally very expensive, and it is important to keep the number of these 'expensive' simulation as small as possible. *Efficient global optimization* (EGO) uses *Kriging* to reduce the number of simulations by adaptively selecting the simulation point with the largest likelyhood of producing a better component. However, individual simulations are still expensive.

In this work, we combine expensive, high-precision 3D-FDTD simulations with much cheaper, lower-precision 2D EME simulations to accelerate the optimization. This *Co-Kriging* technique uses the cheap simulations to learn the trends of the component behavior, which are calibrated with the expensive simulations [2]. The cheap simulations allow a quick building of the landscape of multi-dimensional parameter space, which minimized the use of the expensive simulations.

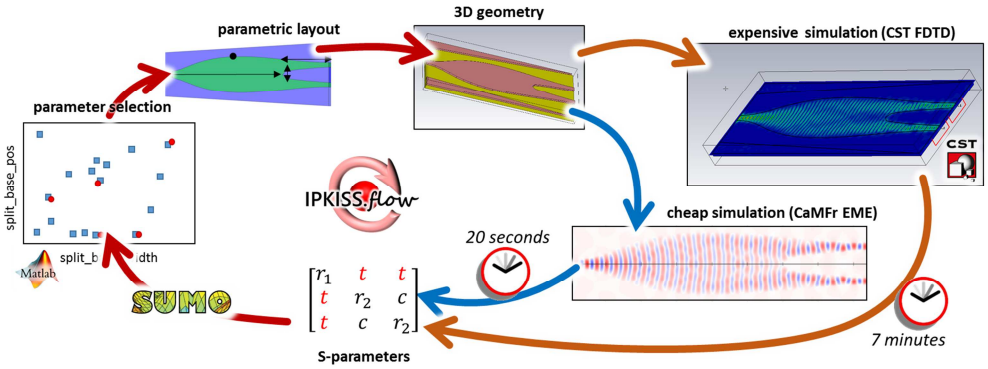

Fig. 2. Optimization of a photonic component using cheap and expensive simulations.

We have optimized the geometry of a silicon 1×2 splitter for maximum transmission over the entire wavelength range 1.5-1.6µm. The splitter is a parametric component in the IPKISS design framework, and has 5 parameters for the smooth shape shown in Fig. 2. We defined 2 simulation strategies: a fast 2D EME simulation in CaMFr, and an accurate 3D-FDTD simulation in CST Studio Suite. Both simulations are launched from the IPKISS python interface [3]. The CoKriging optimization is controlled by the *SUMO* and *ooDACE* toolboxes for Matlab [4,5].

The results of this optimization are shown in Fig. 2. The exploration starts with a Latin hypercube sampling of the parameter space using 21 cheap and 4 expensive simulations. After this initial mapping, the cheap simulations are used to map the landscape of the transmission over the entire parameter space, while the expensive simulations are used to target the optimum. The total global optimization in 5 dimensions uses 238 cheap simulations (75 minutes) and only 12 expensive simulations (94 minutes) and yields a splitter with a transmission > 87% over the entire wavelength range.

This demonstrates that the combination of simulation techniques with different fidelity and efficient adaptive sampling algorithms can dramatically improve the optimization cycle of high-contrast photonic components.

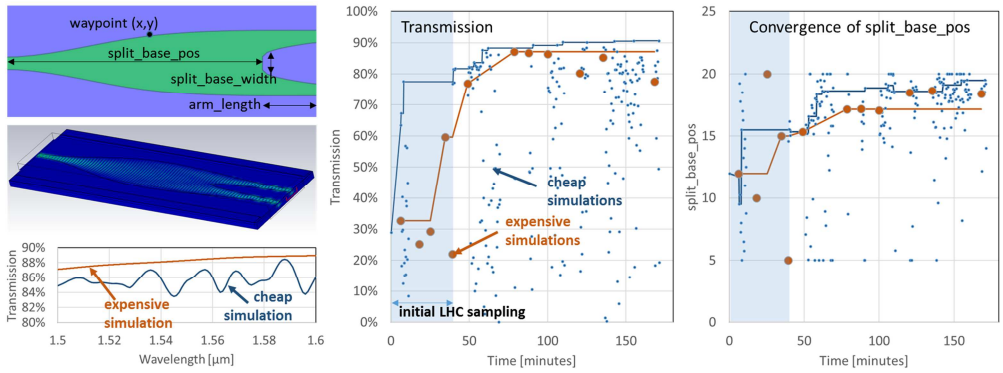

Fig. 3. Optimization of a 1×2 splitter. Left: splitter geometry and simulation of the optimum result. Middle: Evolution of transmission in cheap and expensive simulations. Right. Sampling of one parameter during simulations.

References

[1] W. Bogaerts, M. Fiers, P. Dumon, *Design Challenges in Silicon Photonics,* J. Sel. Top. Quantum Electron. 20(4), pp. 1-8, 2014

[2] M.C. Kennedy, A. O'Hagan,. *Predicting the output from a complex computer code when fast approximations are available.* Biometrika 87, pp.1-13, 2000

[3] M. Fiers, E. Lambert, S. Pathak, P. Dumon, B. Maes, P. Bienstman, W. Bogaerts, *Improving the design cycle for nanophotonic components,* J. Comp. Sci., 4(5), pp. 313-324, 2013

[4] I. Couckuyt, T. Dhaene, P. Demeester, *ooDACE Toolbox: A Flexible Object-Oriented Kriging Implementation*, J. Machine Learning Res. 15, pp. 3183-3186, 2014

[5] *D. Gorissen, K. Crombecq, I. Couckuyt, P. Demeester, T. Dhaene. A Surrogate Modeling and Adaptive Sampling Toolbox for Computer Based Design. J. Machine Learning Res., 11, 2051-2055 (2010)*

OWTNM 2016 | 24TH INTERNATIONAL WORKSHOP ON OPTICAL WAVE & WAVEGUIDE THEORY AND NUMERICAL MODELLING

Feedback-Insensitive Integrated Laser

Perry van SCHAIJK*, Daan LENSTRA, Erwin BENTE
University of Technology, P.O.Box 513, 5600MB Eindhoven, The Netherlands
*p.v.schaijk@tue.nl

It is well known that semiconductor lasers are highly susceptible to external optical feedback (EOF)[1] which is detrimental to laser performance in many applications. EOF is normally prevented using optical isolators, but these cannot be integrated. Therefore we propose to fabricate an integrated feedback-insensitive laser. Simulations show that such a device can be realized as a ring laser in which the clockwise (cw) and counterclockwise (ccw) modes are not optically coupled. We have studied in detail two configurations of integrated ring lasers that show such characteristics. The theoretical analysis for both configurations is based on rate equations backed up by results from simulation packages.

The first ring laser configuration studied is a so called S-ring laser and is sketched in figure 1a. Here, A and B are 2x1 couplers and O is a 2x2 coupler. The field in the ccw mode splits in A and B and joins the cw mode in B and A, respectively. This creates a different behaviour in the cw and ccw directions which favors the cw over the ccw mode such that the ccw mode will be suppressed. Ref. [2] has implemented such a laser and suppression of the cw mode by 35 dB was observed, but EOF sensitivity was not addressed. Back reflections reaching the out coupler port of the ccw mode will end up

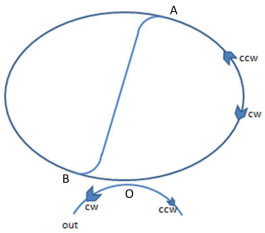

Fig 1a: schematic layout of S-ring laser.

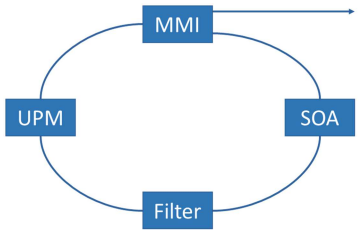

Fig 1b: schematic layout of ring laser with UPM.

in the cw mode and hence are expected to be suppressed as well.

A rate equation analysis for this laser shows that without EOF the cw mode will contain more power than the ccw mode, but the damping of the latter is typically weak, i.e. not exponential but proportional to $1/t^2$, where t is time. Since the ccw mode is at threshold, it is most susceptible for external feedback from the cw mode. Our theory predicts as high as ~10dB cw-ccw power ratio at ~1% EOF. Simulations also show the laser spectrum to be highly sensitive to the feedback. From this we predict that the robustness of such a laser is insufficient for practical applications.

The second laser studied consists of a ring laser and a built-in unidirectional phase modulator (UPM) as shown in figure 2a. Apart from the semiconductor optical amplifier (SOA) and the multi-mode interferometer (MMI) for out coupling, the ring contains a UPM and an appropriate spectral filter. The UPM is explained and demonstrated in [3];

ideally it has unit transmission in one direction (the cw direction in this case) and redistributes power in the other direction over various frequencies as shown in figure 2b. Thus, assuming ideal components total isolation is achieved at the designed operation frequency when this component is combined with a spectral filter.

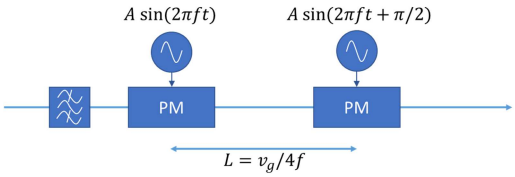

Fig 2a: schematic layout of UPM.

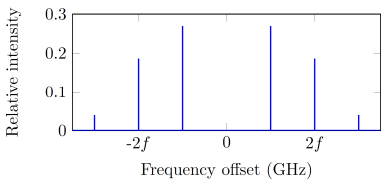

Fig 2b: transmission of UPM in reverse direction.

Analysis shows suppression of ccw mode with respect to cw mode of ~30dB for ~1% EOF (power). Figures 3 show the simulated dependence of the RIN and linewidth on the fraction R of output power that is returned to the laser for three transmission values of the single-pass transmission T_{UPM} of the UPM and filter combination at the operation wavelength. These figures show negligible influence on the RIN and linewidth of the cw output when T_{UPM} is sufficiently small. We therefore conclude that this proposed laser will be highly insensitive to EOF. We have fabricated a photonic integrated circuit with a ring laser with UPM which is currently being characterized. Its design and initial experimental results will be presented.

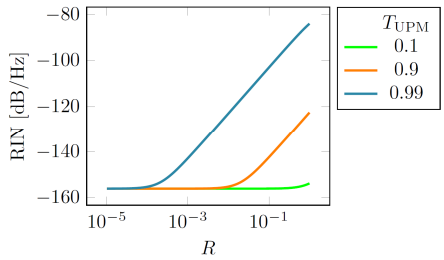

Fig 3a: RIN vs EOF and UPM transmission.

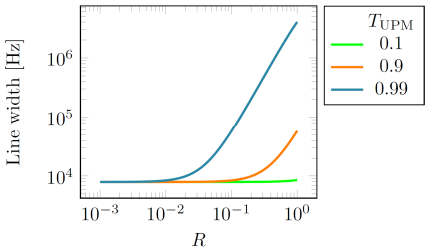

Fig 3b: line width vs EOF and UPM transmission.

References

[1] R. Tkach and A. Chraplyvy, Journal of Lightwave Technology, 4(11):1655–1661, 1986.
[2] Hongjun Cao, Hui Deng, Hai Ling, Chiyu Liu, Vladimir A. Smagley, Robert B. Caldwell, Gennady A. Smolyakov, Allen L. Gray, Luke F. Lester, Petr G. Eliseev and Marek Osinski, Applied Physics Letters 86, 203117 (2005); doi: 10.1063/1.1931044
[3] Christopher R. Doerr, Nicolas Dupuis, and Liming Zhang, Optics Letters, 36(21):4293, November 2011.

The work presented is supported by the Technology Foundation STW under project 13540 as part of the Memphis II program and by the research centre for integrated nanophotonics of the NWO gravitation program.

OWTNM 2016 | 24TH INTERNATIONAL WORKSHOP ON OPTICAL WAVE & WAVEGUIDE THEORY AND NUMERICAL MODELLING

Design of an Optical Nanoantenna with Focusing Sub-wavelength Grating Couplers and Metallic Reflector

A.J. MILLAN-MEJIA*, Y. JIAO, J.J.G.M. VAN DER TOL, M.K. SMIT
Photonic Integration Group (PhI), Dept. of Electrical Engineering, Technische Universiteit Eindhoven, De Rondom 70, 5612AP, Eindhoven, The Netherlands
* a.millan.mejia@tue.nl

In the development of integrated large-scale optical phase array, compact optical nanoantennas are needed. For high resolution arrays, the nanoantenna footprint and the separation between them should be as small as possible to reduce the number of interference orders in the far field [1]. In the development of this nanoantennas in our InP membrane on Silicon (IMOS) platform [2], we use deeply etch focusing grating to reduce the size [3]. In order to increase the optical power emitting up, we add a metal reflector of Silver underneath the semiconductor with a small buffer of 50 nm of SiO_2. This metal layer will also works as a thermal heater, which will change the optical properties of the semiconductor changing the direction of the upcoming light. The last element to be add is a subwavelength ridge which reduces the unwanted Fresnel reflections by reducing the refractive index contrast [3].

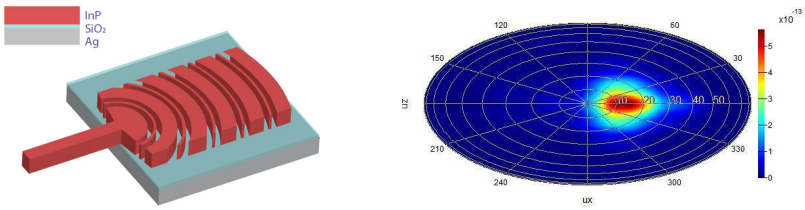

Fig. 4. (a) A schematic of the optical nanoantena, (b) The far-field emission profile.

We simulated the nanoantenna using the 3D-FDTD model. In this case, the commonly 2D-FDTD approximation used in grating simulations is not valid anymore due to the high lateral confinement in the structure. In our 300 nm thick InP membrane, the best grating we got has 5 periods with a pitch of $\Lambda = 880nm$ with a filling factor of 0.52. The subwavelength ridge is 100 nm. Figure 1a illustrated the grating design. We add a buffer layer between the InP and the metal to reduce mode mismatch and therefor, reflections due to the metal. The efficiency obtained at $1.55\mu m$ is 59% of upcoming light and 8% reflections. The far-field emission is centred about 13° from the zenith (Fig 1b). We predict that further optimization could improve this performance. This work was supported by the ERC Project NOLIMITS

References

[1] J. Sun *et al*. *Large-Scale Silicon Photonic Circuits for Optical Phased Arrays*, IEEE journal of selected topics in quantum electronics, vol. 20, no. 4, 2014
[2] J. van der Tol *et al*, *Photonic integration in indium-phosphide membranes on silicon (IMOS)*, Integrated Optics: Devices, Materials, and Technologies XVIII, pp. 89880M-89880M-17, 2014
[3] F. van Laere *et al*. *Compact Focusing Grating Couplers for Silicon-on-Insulator Integrated Circuits*, IEEE photonics technology letters, vol. 19, no. 23, pp 1919-1921, 2007
[4] Y. Wang *et al*. *Focusing sub-wavelength grating couplers with low back reflections for rapid prototyping of silicon photonic circuits*, Optics express, vol. 22, no. 17, pp 20652-20662, 2014

OWTNM 2016 | 24TH INTERNATIONAL WORKSHOP ON OPTICAL WAVE & WAVEGUIDE THEORY AND NUMERICAL MODELLING

Effect of Dielectric Nanoparticles on Efficiency of Organic Solar Cell

Vidhi MANN[1*], Vipul RASTOGI[1]
[1]Indian Institute of Technology Roorkee, Roorkee, 247667, India
[*] vidhimann@gmail.com

Organic solar cells (OSCs) have been of great interest due to their strong potential to reduce the cost of photovoltaics. However, OSCs still have low efficiency up to 5-6% due to the small thickness of the active layer [1]. One of the ways to increase efficiency is to enhance solar absorption in the active layer. Several approaches have been reported to enhance the absorption: metallic nanoparticles, photonic crystals and gratings.

In this article, we propose to incorporate the dielectric nanoparticles layer between anode (ITO) and hole transport layer (PEDOT:PSS) to increase the efficiency of OSCs. The nanoparticles scatter light into the active layer and thereby increase the absorption. We have calculated the scattering efficiency of dielectric nanoparticles embedded in the OSC by using the Mie theory [2] and efficiency of solar cell by finite difference time domain (FDTD) method [3]. The proposed structure consists of glass substrate/ ITO (150nm)/nanoparticles layer/ PEDOT:PSS (60nm)/ P3HT:PCBM (100nm)/ Aluminium (80nm). The diameter and interparticle spacing of nanoparticles are chosen as 50nm and 100nm respectively. The scattering efficiency of different nanoparticles (ZrO_2 and SiC) has been analysed by using Mie theory [2], which is shown in Fig. 1(a). The J-V characteristics of OSC with and without nanoparticles are shown in Fig. 1(b). Incorporation of ZrO_2 nanoparticles increases the J_{sc} by 5.3% and efficiency by 6.7%. SiC nanoparticles increases the J_{sc} by 12.9% and efficiency by 14.9%. The study would be useful in the development of high efficiency OSCs.

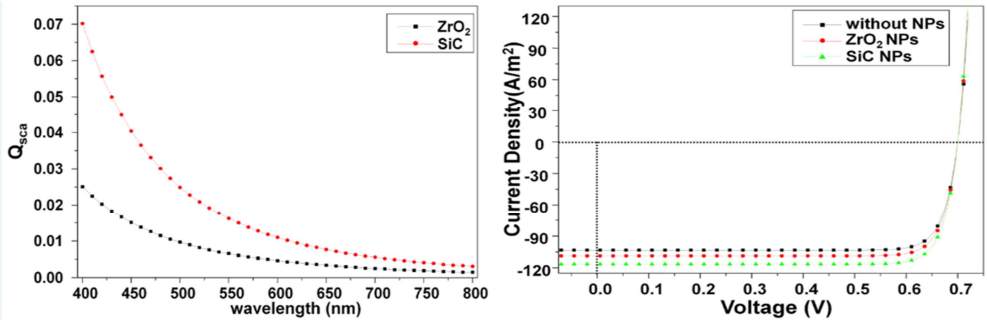

Fig. 5. (a) Scattering efficiencies of ZrO_2 and SiC nanoparticles (b) J-V characteristics of OSC with and without nanoparticles

References

[1] S.H. Park et al., *Bulk heterojunction solar cells with internal Quantum Efficiency approaching 100%*, Nat. Photonics, vol. 3, pp. 297-302, 2009
[2] C. F. Bohren and D.R. Huffman, *Absorption and Scattering of Light by Small Particles*, Wiley, New York, 1983
[3] RSoft RCAD, Fullwave Manual

OWTNM 2016 | 24TH INTERNATIONAL WORKSHOP ON OPTICAL WAVE & WAVEGUIDE THEORY AND NUMERICAL MODELLING

Band Structure Analysis of a 1D Photonic Crystal with a Sawtooth Refractive Index

G. V. MOROZOV[1*], S. CAFFREY[1], D. W. L. SPRUNG[2], J. MARTORELL[3]
[1]Scottish Universities Physics Alliance (SUPA), Institute of Thin Films, Sensors and Imaging, University of the West of Scotland, Paisley PA1 2BE, UK
[2]Dept. of Physics and Astronomy, McMaster University, Hamilton, Ontario L8S 4M1, Canada
[3]Dept. d'Estructura i Constituents de la Materia, Facultat Fisica, University of Barcelona, Barcelona E-08028, Spain
[*]gregory.morozov@uws.ac.uk

In recent paper we analysed reflection/transmission properties of sawtooth crystals, i.e. 1D photonic crystals constructed of layers with linearly increasing refractive index *n(z)* in each period, see Fig. 1. The results were obtained in the exact analytical form in terms of Bessel functions.

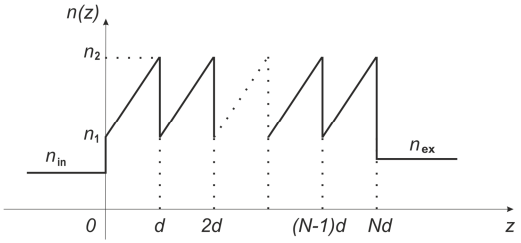

Figure 1: 1D photonic crystal with a sawtooth refractive index.

In this paper, for a sawtooth crystal we construct the Floquet-Bloch fundamental system of solutions, and then obtain and analyse its band structure. For simplicity we restrict our attention to normal propagation. Then, the band structure is defined by two parameters only: the wavenumber of incident light and the ratio of maximum (n_2) and minimum (n_1) refractive indices. The typical behaviour of Floquet-Bloch solutions in the allowed bands, in the bandgaps, and at the bandedges are illustrated. Special attention is given to periodic solutions.
Overall, the results add to a better understanding of the behaviour of light within photonic crystals with linearly graded refractive index layers.

References

[1] G. V. Morozov, D. W. L. Sprung, J. Martorell, *One-dimensional photonic crystals with a sawtooth refractive index: another exactly solvable potential*, New Journal of Physics, vol. 15, 103009, 2013
[2] G. V. Morozov, D. W. L. Sprung, *Floquet-Bloch waves in one-dimensional photonic crystals*, EPL, vol. 96, 54005, 2011
[3] G. V. Morozov, D. W. L. Sprung, *Band structure analysis of an analytically solvable Hill equation with continuous potential*, J. Opt., vol. 17, 035607, 2015

24TH INTERNATIONAL WORKSHOP ON OPTICAL WAVE & WAVEGUIDE THEORY AND NUMERICAL MODELLING

OWTNM2016

20–21 MAY | WARSAW | POLAND

FRIDAY 20TH MAY 2016

14:30-16:00

OWTNM SESSION #1

OPTICAL ARRAYS, GRATINGS AND VIAS

CHAIR: **GREGORY MOROZOV,**
UNIVERSITY OF THE WEST OF SCOTLAND, UK

The University of Nottingham
UNITED KINGDOM · CHINA · MALAYSIA

SUPPORTED BY CZIiTT Centre for Innovation and Technology Transfer Management WUT · SKKP POLISH CONFERENCE & CONGRESS ASSOCIATION · CEZAMAT · EPIC European Photonics Industry Consortium

OWTNM 2016 | 24TH INTERNATIONAL WORKSHOP ON OPTICAL WAVE & WAVEGUIDE THEORY AND NUMERICAL MODELLING

Local Parity-Time-Symmetry Grating Devices for Integrated Optics

Anatole LUPU[1*], Henri BENISTY[2], Andrei V LAVRIENKO[3]
[1]IEF, CNRS, Univ Paris Sud, Université Paris-Saclay, 91405 Orsay, France
[2]Laboratoire Charles Fabry, Institut d'Optique Graduate School, CNRS, Univ Paris Sud, Université Paris-Saclay, 2 Avenue Augustin Fresnel, 91127 Palaiseau, France
[3]DTU Fotonik – Department of Photonics Engineering, Technical University of Denmark, Oersteds Plads 343, DK-2800 Kgs. Lyngby, Denmark
[*] anatole.lupu@u-psud.fr

The aim of the current work is to explore the functionalities of nonuniform Parity-Time -symmetric structures with engineered complex-index-modulation profiles. The use of nonuniform coupling or gain-loss modulation profiles brings a number of advantages as compared to the uniform PT-symmetric structures. The intention of the undertaken approach is to show that many conventional techniques previously developed for passive-type grating-assisted or coupled-waveguide devices for integrated optics can be transposed and adapted to a PT-symmetric case, fostering thus a new generation of active photonic devices.

In our recent work [1] we considered few examples of nonuniform PT-symmetric Bragg gratings with a complex index profile modulated by a slowly varying envelope function, with the aim of combining the apodization techniques of classical Bragg gratings with the advantages of PT-symmetry such as unidirectionality. We demonstrated the possibility to achieve an efficient apodization of the PT-symmetric Bragg grating spectral response with a standard Hamming window function. To ease implementation of the apodization in a real structure with the local binary nature of the real and imaginary index modulations, this approach was extended to the duty-cycle modulated periodic or deterministic aperiodic binary PT-symmetric gratings. We demonstrated how the conventional technique previously developed for passive type Bragg gratings or related devices can be expanded to a PT-symmetric case, provided the constraints of real and imaginary part modulation are properly combined.

In the present contribution we shall further extend this concept to explore the functionalities that can be achieved in the case of four-ports Bragg-grating-assisted directional couplers [2-4] with nonuniform complex PT-symmetric profiles.

References

[1] A. Lupu, H. Benisty, A.V. Lavrinenko, *Tayloring spectral properties of binary PT-symmetric gratings by duty-cycle methods*, accepted JSTQE Special Issue on Parity Time Photonics, 2016
[2] A. Lupu, H. Benisty, and A. Degiron, *Using optical PT-symmetry for switching applications*, Photonics Nanostruct. Fundam. Appl. 12, 305-311, 2014.
[3] A. Lupu, K. Muhieddine, E. Cassan, J-M. Lourtioz, *Dual transmission band Bragg grating assisted asymmetric directional couplers*, Opt. Express 19, 1246-1259, 2011.
[4] K. Muhieddine, A. Lupu, E. Cassan, J-M. Lourtioz, *Proposal and analysis of narrow band transmission asymmetric directional couplers with Bragg grating induced phase matching*, Opt. Express 18, 23183-23195, 2010.

OWTNM 2016 | 24TH INTERNATIONAL WORKSHOP ON OPTICAL WAVE & WAVEGUIDE THEORY AND NUMERICAL MODELLING

Time-Modulated Gain and Loss Parity-Time Symmetric Resonators

Sendy PHANG[1]*, Ana VUKOVIC[2], Stephen C. CREAGH[1], Gabriele GRADONI[1], Phillip SEWELL[2], Trevor M. BENSON[2]

[1]School of Mathematical Sciences, University of Nottingham, Nottingham, NG7 2RD, UK
[2]George Green Institute for Electromagnetics Research, University of Nottingham, NG7 2RD, UK
* sendy.phang@nottingham.ac.uk

Loss has, without a doubt, been one of the key issues in optical communication. On the other hand, the applications of gain have been primarily studied in laser technologies. It has recently been shown that, under a judicious combination of both gain and loss, a new novel system, namely the Parity-Time (PT) symmetric structures, is constructed. In our recent works [1,2], we have developed a semi-analytical method based on the Boundary Integral Equation (BIE) method to study the spectral characteristics of resonator structures with balanced and unbalanced gain/loss in a system which takes the form of coupled resonators and finite chain structures. In particular, we show the impact of dispersion on the spectral behaviour such that PT-symmetry can only be achieved at a single frequency and is sensitive to mismatching conditions.

In this contribution, we explore the time-dynamics of coupled resonators structures, see Fig. 1. For this purpose, a two-dimensional time-domain Transmission-Line Modelling (2DTLM) method equipped with a dispersive gain/loss model is developed. The 2DTLM method is well-suited to model the temporal dynamic of a PT-symmetric coupled structure under time-modulated gain and loss conditions. Figure 1 further shows that, by switching on/off the gain/loss alternatively at a rate described by a switching time parameter, flexible optical spatial switching can be achieved.

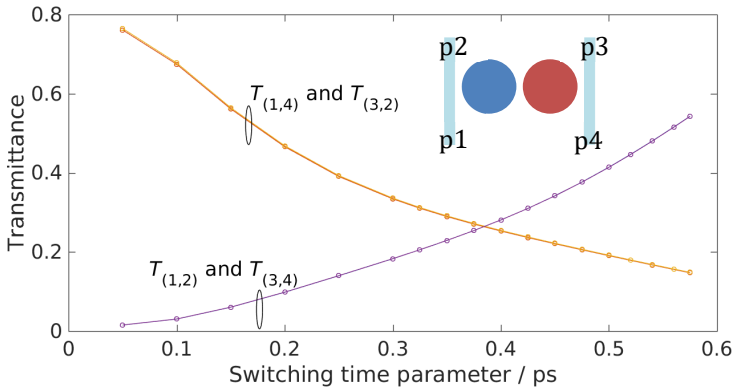

Fig. 6. Transmittance between ports as a function of switching-time parameter.

References

[1] S. Phang, A. Vukovic, S. C. Creagh, T. M. Benson, P. D. Sewell, G. Gradoni, *Parity-time symmetric coupled microresonators with a dispersive gain/loss*, Optics Express, vol. 23, no. 9, 2015

[2] S. Phang, A. Vukovic, S. C. Creagh, G. Gradoni, P. D. Sewell, T. M. Benson, *Localized Single Frequency Lasing States in a Finite Parity-Time Symmetric Resonator Chain*, Scientific Reports, vol. 6, 2016

OWTNM 2016 | 24TH INTERNATIONAL WORKSHOP ON OPTICAL WAVE & WAVEGUIDE THEORY AND NUMERICAL MODELLING

Plane Wave Diffraction by Periodic Arrays of Nonlinear Cylinders

Lijun YUAN[1], Ya Yan LU[2*]
[1]Chongqing Technology and Business University, Chongqng, China
[2]City University of Hong Kong, Hong Kong
[*] mayylu@cityu.edu.hk

In [1, 2], we analyzed linear and nonlinear standing waves on a periodic array of parallel and infinitely long dielectric circular cylinders surrounded by air. The standing waves are special guided modes above the lightline (in the radiation continuum) with a zero Bloch wavenumber. The linear standing waves only exist at a discrete set of frequencies, but the nonlinear standing waves (for cylinders with a Kerr nonlinearity) exist continuously with respect to the frequency.

In this paper, we study the diffraction of plane incident waves by an array of nonlinear circular cylinders. Our study indicates that incident plane waves can couple to the nonlinear standing waves leading to the symmetry-breaking phenomenon. Like optical bistability, symmetry-breaking gives rise to multiple solutions to the nonlinear diffraction problem. In existing studies, these nonlinear phenomena only appear when the incident wave has a sufficiently high intensity. This is true even when the nonlinear effects are enhanced by microcavities. In our case, it seems that plane incident waves with arbitrarily low intensity can couple to the nonlinear standing waves. Therefore, multiple solutions exist even for incident waves of arbitrarily low intensity. In the figure below, we show the transmission coefficients of three solutions associated with

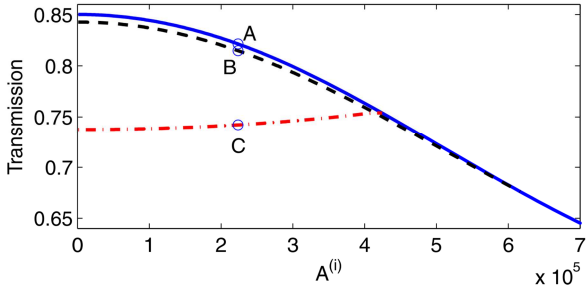

the same plane incident wave for an array with period L at the normalized frequency $\omega L/(2\pi c) = 0.53$. We assume the cylinders have a radius $a = 0.3L$, a refractive index $n_1 = 2.5$ and a nonlinear coefficient $\gamma_1 = 2 \times 10^{-12}\text{m}^2/\text{V}^2$. The horizontal axis is the amplitude $A^{(i)}$ of the incident plane wave. The solid line represents the symmetric solution that does not couple to the nonlinear standing waves. The dashed and dash-dot curves correspond to two asymmetric solutions that couple to the first nonlinear standing wave, and they seem to exist as $A^{(i)} \to 0$.

References

[1] Z. Hu, Y. Y. Lu, *Standing waves on two-dimensional periodic dielectric waveguides,* Journal of Optics, vol. 17, no. 6, 065601, 2015.
[2] L. Yuan, Y. Y. Lu, *Nonlinear standing waves on a periodic array of circular cylinders*, Opt. Express, vol. 23, no. 16, 20636-20646, 2015.

OWTNM 2016 | 24TH INTERNATIONAL WORKSHOP ON OPTICAL WAVE & WAVEGUIDE THEORY AND NUMERICAL MODELLING

On the Thin Spectral Width of Cavity-Resonator-Integrated Grating Filters

Nadège RASSEM*, Anne-Laure FEHREMBACH and Evgueni POPOV

Aix Marseille Université, CNRS, Centrale Marseille,
Institut Fresnel UMR 7249, 13013 Marseille, France
*nadege.rassem@fresnel.fr

Guided Mode Resonance Filter (GMRF) is a reflective narrowband filter that consists of a simple sub-wavelength grating etched on the top of a thin stack layers [1]. That structure combines structural simplicity with high efficiency, rejection rate and quality factor. Their major limitation lies in their weak angular acceptance. To achieve a better angular tolerance, it has been proposed to surround the GMRF with two Distributed Bragg Reflectors (DBR) as represented on Figure 1, forming the so-called Cavity Resonator Integrated Grating Filter (CRIGF) [2, 3]. One phase shift section is inserted between each DBR and the GMRF.

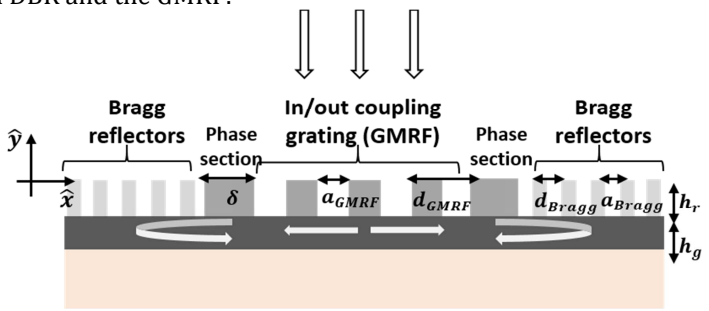

Fig.1. Schematic view of the CRIGF studied with the definition of the parameters: period of the GMRF d_{GMRF}, period of the Bragg grating $d_{Bragg}=d_{GMRF}/2$, width of the grooves $a_{GMRF}=a_{Bragg}$, deep grooves h_r is the silica grating thickness, h_g is the silicon nitride thickness, the phase section length is $\delta=d_{GMRF}$.

In this work, we are interested in the performances of the CRIGF, especially its spectral width, when the size of the GMRF section increases. From numerical calculations, we observe, as expected, that the performances of the CRIGF tends to those of the infinite GMRF with the same parameters and illuminated with the same beam. However the spectral width of the peak obtained with the CRIGF is always smaller than that of the infinite grating.

From numerical calculations, we show that the mode excited in a CRIGF behaves as a lossy Fabry-Pérot cavity mode. This simple approach allows us to explain why the CRIGF resonance is thiner than the infinite grating one.

References

[1] S. S. Wang and R. Magnusson, *Theory and applications of guided-mode resonance filters*, Appl. Opt. 32, pp. 2606-2613, 1993

[2] K. Kintaka, T. Majima, K. Hatanaka, J. Inoue and S. Ura, *Polarization-independent guided-mode resonance filter with cross-integrated waveguide resonators*, Opt. Lett., 37, pp. 3264-3266, 2012

[3] N. Rassem, A.-L. Fehrembach, E. Popov, *Waveguide mode in the box with an extraordinary flat dispersion curve,* J. Opt. Soc. Am. A 32, pp. 420-430, 2015

OWTNM 2016 | 24TH INTERNATIONAL WORKSHOP ON OPTICAL WAVE & WAVEGUIDE THEORY AND NUMERICAL MODELLING

Design of an Optical Via for Large Scale Monolithic Multilayer PICs

Ripalta STABILE*, Jon Ø. KJELLMAN and Kevin A. WILLIAMS
Eindhoven University of Technology, COBRA research institute, P.O. Box 513, 5600 MB Eindhoven, The Netherlands
*R.Stabile@tue.nl

Large-scale integrated optical switch matrices require a complex mesh interconnection which is not well supported by single layer waveguides [1]. A number of dual-layer waveguide methodologies have been proposed to enable 2.5D and 3D photonic integration. Dual waveguide techniques have primarily been used to create new types of devices and functions rather than to improve interconnection. We present a dual width waveguides concept which can allow light routing up and down a monolithic multi-layer InP stack.

The monolithical multi-layer InP integration concept using dual width waveguides to allow light routing up and down the layer stack is presented (Fig. 1). This concept includes two vertically-stacked guiding layers. The top guide layer is multimode to push the excited modes close to the spacer layer. Vertical confinement for the two waveguiding layers is defined by InP cladding layers around an upper and a lower core. A transition between the lower and higher guiding cores is implemented with the cross-section in Fig. 1b: This is the cross-section for the optical via. The waveguide widths defined at the optical via enable phase matching conditions between the two optical cores. A maximum transmitted power of 98.9% is calculated for a coupling length of 190µm after the optical power is coupled back into the bottom waveguiding layer. Methods to isolate the waveguide planes from each other are also proposed for reduced interlayer crosstalk.

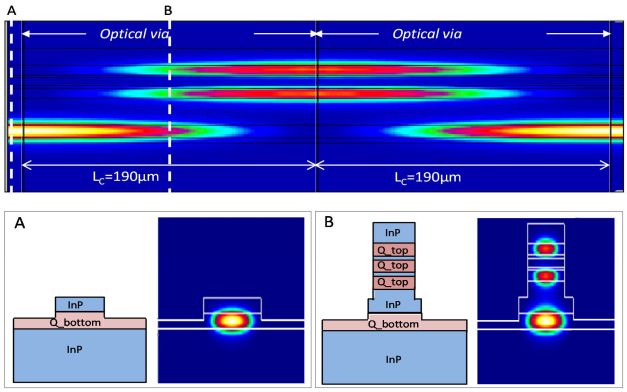

Fig. 7. Lateral view of two optical vias to couple light up and back down (top). On the bottom left, the intensity mode profile in the lower guide, and in the bottom right, the mode intensity profile at the optical via.

References

[1] R. Stabile, A. Albores Mejia, K.A. Williams, *Optics Letters*, vol. 37, pp. 173225-173228, 2012

24TH INTERNATIONAL WORKSHOP ON OPTICAL WAVE & WAVEGUIDE THEORY AND NUMERICAL MODELLING

OWTNM2016

20–21 MAY | WARSAW | POLAND

FRIDAY 20TH MAY 2016

16:00 – 16:45

OWTNM POSTER SESSION

The University of Nottingham
UNITED KINGDOM · CHINA · MALAYSIA

SUPPORTED BY

CZIiTT Centre for Innovation and Technology Transfer Management WUT

SKKP POLISH CONFERENCE & CONGRESS ASSOCIATION

CEZAMAT

EPIC European Photonics Industry Consortium

OWTNM 2016 | 24TH INTERNATIONAL WORKSHOP ON OPTICAL WAVE & WAVEGUIDE THEORY AND NUMERICAL MODELLING

Strain Detection in Two- and Three-Dimensional Periodic Structures with the Low Index Contrast by Monitoring Their Optical Response

Anna K. PIOTROWSKA[1,2*], Daniele ZONTA[1,2], Maurizio FERRARI[2], Marian MARCINIAK[3]

[1]Department of Civil, Environmental and Mechanical Engineering, University of Trento, via Mesiano, 77, Trento, 38123 Italy

[2]Institute for Photonics and Nanotechnology, Via alla Cascata, 56/C, Povo-Trento, 38123 Italy

[3]National Institute of Telecommunications, Szachowa Str. 1, Warsaw, 04-894 Poland

[*] anna.k.piotrowska@gmail.com

Novel complex materials like photonic crystals possess repeatable arrangement of at least two components with different refractive index. The periodic distribution of refractive index provides an important and intensively exploited feature i.e. wavelength and/or polarisation selective interaction with light. Photonic crystals exhibit a photonic stop band that is an optical analogue of electronic stop band in semiconductor crystals [1,2]. Consequently, the incident wavelength equal to the periodicity constant is reflected, while the others are transmitted through the structure. This effect is well defined by the modified Bragg's law and it has been investigated regarding the mechanochromic properties of three-dimensional photonic crystals [3]. In case of three-dimensional structure, the optical response is easily tuneable by mechanically stimulated structural changes. The structural changes cause the change of reflected light spectrum (the blue-shift in case of elongation).
In case of two-dimensional structure, the optical response for mechanical distortion is not so obvious and depends on a fabrication method, components etc.

In this paper we present the results of experimental investigation on transmitting properties of two-dimensional periodic structure of hemi-spherical voids arranged hexagonally in PDMS layer. The results of elongation the sample are visible with the naked eye in the diffraction pattern displayed on the screen behind the sample.

References

[1] J.D. Joannopoulos, S.G. Johnson, J.N. Winn, R.D. Meade, *Photonic Crystals Molding the Flow of Light,* Princeton University Press, New Jersey, 2008

[2] Editors: C. Sibilia, T.M. Benson, M. Marciniak, T. Szoplik, *Photonic Crystals: Physics and Technology*, Springer-Verlag, Milan 2008

[3] D. Zonta, A.Chiappini, A.Chiasera, M.Ferrari, M.Pozzi, L.Battisti and M.Benedetti, *Photonic crystals for monitoring fatigue phenomena in steel structure*, Proc. of SPIE 7292:729215-1 – 729215-10, 2009

OWTNM 2016 | 24TH INTERNATIONAL WORKSHOP ON OPTICAL WAVE & WAVEGUIDE THEORY AND NUMERICAL MODELLING

Electromagnetic Modelling of Large Subwavelength-Patterned Highly Resonant Structures

Anne-Laure FEHREMBACH[1*], Patrick C. CHAUMET[1], Guillaume DEMESY[1], Olivier GAUTHIER-LAFAYE[2,3], Anne SENTENAC[1], Evgeny POPOV[1]

[1]Aix-Marseille Université, CNRS, Ecole Centrale Marseille,
Institut Fresnel UMR7249, 13013 Marseille, France
[2]CNRS, LAAS, 7 av. Du Colonel Roche, F-31400 Toulouse, France
[3]Université de Toulouse, LAAS, F-31400 Toulouse, France
[*] anne-laure.fehrembach@fresnel.fr

Recent advances in nanotechnology of optical components allows for manufacturing of aperiodical structures patterned at a subwavelength scale that have macroscopic dimension of several hundreds or thousands wavelengths. A typical example is the so-called Cavity resonator integrated grating filter (CRIGF) that uses a resonant excitation of a waveguide mode by a dielectric grating, which is put in a box consisting of two Bragg guided wave mirrors, in order to obtain a narrow-band spectral filtering that is characterized by extraordinary large angular tolerances [1]. These filters present a true challenge to computational electromagnetism, because of their large dimensions and fine pattering, but also because of their resonant nature.

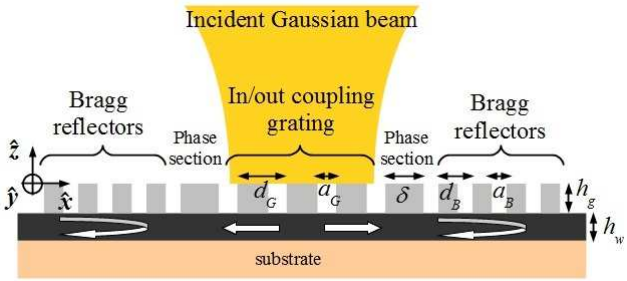

Fig. 8. Representation of a Cavity resonator Integrated Filter.

In this work we compare the performances of the Discrete Dipole Approximation approach to that of the Fourier Modal, the Finite Element and the Finite Difference Time Domain methods, for simulating the spectral behaviour of a CRIGF. When the component is invariant along one axis (two-dimensional configuration), the four techniques yield similar results, despite the modelling difficulty of such a structure. We also demonstrate, for the first time to our knowledge, the rigorous modelling of a three-dimensional CRIGF, with the DDA [2].

References

[1] X. Buet, E. Daran, D. Belharet, F. Lozes-Dupuy, A. Monmayrant, and O. Gauthier-Lafaye, *High angular tolerance and reflectivity with narrow bandwidth cavity-resonator-integrated guided-mode resonance filter*, Opt. Expr. 20, 9322–9327, 2012

[2] P.C. Chaumet, G. Demésy, O. Gauthier-Lafaye, A. Sentenac, E. Popov, and A.-L.Fehrembach, *Electromagnetic modelling of large subwavelength-patterned highly resonant structures*, submitted to Opt. Lett.

OWTNM 2016 | 24TH INTERNATIONAL WORKSHOP ON OPTICAL WAVE & WAVEGUIDE THEORY AND NUMERICAL MODELLING

On the Origin of the Wood's Anomalies in the Extraordinary Transmission Through One-Dimensional Sub-wavelength Periodic Arrays

J. FIALA*, I. RICHTER
Czech Technical University in Prague, Břehová 7, Prague, CZ-11519, Czech Republic
* corresponding author: j.fiala@fjfi.cvut.cz

This contribution is focused on the investigation of the role of surface plasmon-polaritons (SPPs) and the Rayleigh anomalies within the problem of enhanced optical transmission (EOT) through metallic periodic gratings with infinite slits [1,2].

Using the rigorous coupled wave analysis, the total transmitted energy maps of various 1-D arrays of slits are calculated as a function of both the structure geometrical and wave parameters. From these maps, the dispersion curves of the existing modes can be clearly identified together with the cut-off frequencies of the respective modes and the positions of resonances. Apart from the cavity resonances of the fundamental slit-guided mode (cavity mode - CM), playing a significant role, the SPP bound modes and CM-SPP hybrid modes are also identified and analyzed in the case of the studied structures [3].

It is found that the SPPs drastically alter the dispersion relations of the Fabry-Perot conditions of the CMs inside the slit; their mutual interaction subsequently results in the Fano resonances with the pronounced maxima and minima in the spectra – the grating Wood's anomalies. The transmission mechanism, being consequent upon the interaction of mode contributions in the vicinity and inside the slit, is proposed.

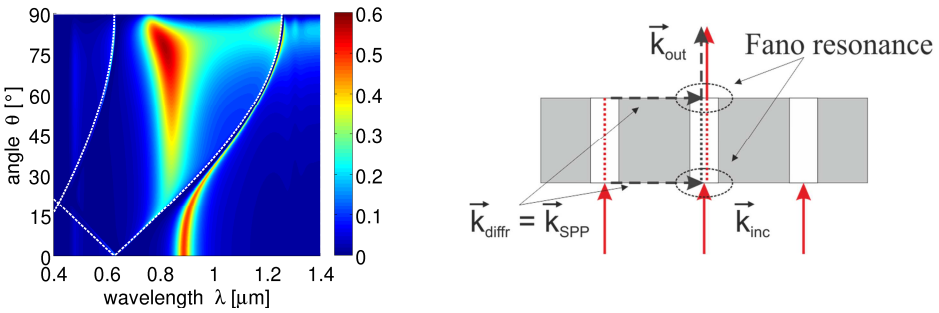

Fig. 9. A transmission map through 1-D array of slits and a proposed transmission mechanism.

References

[1] Q. Cao, P. Lalanne, *Negative role of surface plasmons in the transmission of metallic gratings with very narrow slits*, Phys. Rev. Lett., vol. 88, 057403-1-4, 2002
[2] M. Sarrazin, J.P. Vigneron, J.M. Vigoureux, *Role of Wood anomalies in optical properties of thin metallic films with a bidimensional array of subwavelength holes*, Phys. Rev. B, vol. 67, 085415-1-7, 2003
[3] J. Fiala, I. Richter, *Explanation of extraordinary transmission on 1-D and 2-D metallic gratings*, Proceedings SPIE 9450, 4501T-1-9, 2015

OWTNM 2016 | 24TH INTERNATIONAL WORKSHOP ON OPTICAL WAVE & WAVEGUIDE THEORY AND NUMERICAL MODELLING

Resonances Excited by an Airy Pulse in a Dielectric Layer

Olga KURYZHEVA[1], Alexander NERUKH[1*], Trevor M. BENSON[2]

[1]Kharkov National University of Radio Electronics, 14 Lenin Ave., Kharkov, 61166, Ukraine

[2]George Green Institute for Electromagnetics Research, University of Nottingham, University Park, Nottingham, NG7 2RD, UK

[*] nerukh@gmail.com

Intensive theoretical and experimental investigations of accelerated Airy beams motivated by their unusual features [1] gave rise to numerous investigations with very interesting results. However, such pulses are useful not only because of these features but also by their unusual shape which consists of a high intensity main lobe pulse followed by a train of weaker sub-pulses of decreasing intensities [2].

Interaction of a non-paraxial temporal Airy pulse with a dielectric layer is considered here by using the Volterra integral equation method and behaviour of the initial Airy pulse is studied in detail. It is proposed that the initial pulse $E_0(t,x) = \mathrm{Ai}(-t/T + (x-x_0)/vT)$ is falling onto a dielectric layer of the width a such that it begins to interact with the layer only after zero moment of time t. Here, $\mathrm{Ai}(t)$ is the Airy function, v is a wave velocity outside the layer, x_0 is a source point location and T is a scale coefficient. The field at any point inside or outside the layer is described by the integral equation [3]

$$E = E_0 + \frac{v_1^2 - v^2}{2vv_1^2}\frac{\partial^2}{\partial t^2}\int_0^\infty dt' \int_0^a dx' \theta\left(t - t' - \frac{|x-x'|}{v}\right) E_0(t',x'), \qquad (1)$$

where v_1 is a wave velocity inside the layer and $\theta(x)$ is the Heaviside unit function. The solution of this equation obtained by the resolvent method [3] gives the inner field that allows to calculate the field outside the layer. The results are presented in Fig. 1 where oscillations of the inner field (red) in comparison with the initial wave (blue) are shown.

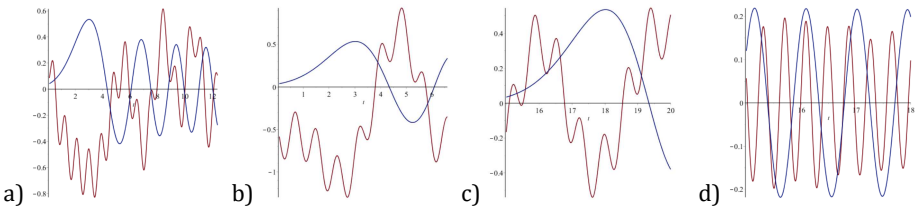

Fig. 1. Oscillated pulses (red) inside the layer excited by the initial Airy pulse (blue): near the illuminated boundary of the layer a) $v/v_1 = 0.8$ and b) $v/v_1 = 1.5$; and at the layer middle c) $v/v_1 = 0.8$ and d) $v/v_1 = 1.5$.

References

[1] G. A. Siviloglou and D. N. Christodoulides, *Accelerating finite energy Airy beams*, Optics Letters 32, pp. 979-981, 2007

[2] T. Winkler et al, *Probing spatial properties of electronic excitation in water after interaction with temporally shaped femtosecond laser pulses*, Applied Surface Science 11, pp. 182, 2015

[3] Nerukh, N. Sakhnenko, T. Benson, P. Sewell, *Non-stationary electromagnetics*, Pan Stanford Publishing, Singapore, pp. 597, 2013

OWTNM 2016 | 24TH INTERNATIONAL WORKSHOP ON OPTICAL WAVE & WAVEGUIDE THEORY AND NUMERICAL MODELLING

Transient Plasmons Dynamics in Metallic Structures

Nadiia P. STOGNII[1,2*], Nataliya K. SAKHNENKO[1]
[1]Department of Higher Mathematics, Kharkiv National University of Radio Electronics, 14 Lenin Ave., Kharkiv, 61166, Ukraine
[2]Laboratory of Micro and Nano Optics, Institute of Radio Physics and Electronics NASU, 12 Ak. Proskury Str., Kharkiv, 61085, Ukraine
* nstognii@gmail.com

Recently, surface plasmon polaritons (SPPs) have attracted great amount of attention due to their potential use for the subwavelength field enhancement and localisation that are explored in single molecule detection, transmission through a subwavelength aperture, subwavelength imaging, and improvement in the performance of conventional photonics components such as modulators and switches and others [1].

We consider the excitation of SPPs on a metal cylinder and shell by a transient pulsed beam. The external beam is modelled by a pulsed complex source point [2] with complex coordinates. To find the excited fields we use a rigorous mathematical tool that allows analysing problems both in the frequency and in the time domains. By applying the Laplace transformation directly to a wave equation we derive an analytical solution in the frequency domain; the time dynamics of the electromagnetic field is recovered by the inverse Laplace transformation. In this way we evaluate the residues at singular points associated with the eigenvalues of the structure and the integral along the branch-cuts in the complex plane. This approach guarantees the calculation with controllable accuracy and allows us to extract and to interpret physical phenomena [3].

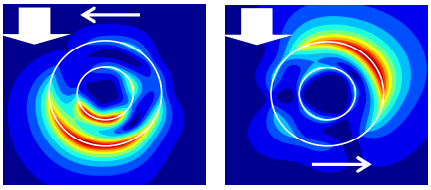

Fig. 10. Snapshots of the dynamic SPP propagation along the metal shell. From the left to the right: $T = 100\pi$, $T = 140\pi$ (T is the normalized time, $T = tc/a$, where t is real time, a is radius of cylinder, c is velocity of light in vacuum).

Figure 1 represents snapshots of the absolute value of the magnetic field of the transient SPP travelling around the metal shell excited by the external transient beam with the eigenfrequency ω_0=0.83. We see that beating of the simultaneously excited SPPs gives rise to asymmetric running field pattern.

References

[1] N. I. Zheludev, *The road ahead for Metamaterials*, Science, vol. 328, pp. 582-583, 2010
[2] A.V. Boriskin and A.I. Nosich, *Whispering-gallery and Luneburg-lens effects in a beam-fed circularly layered dielectric cylinder*, IEEE Trans. Antennas Propag., vol. 50, no. 9, pp. 1245-1249, 2002
[3] N. Sakhnenko, A. Nerukh, T. Benson, and P. Sewell, *Whispering Gallery Mode transformation in a switched microcavity with concentric ring geometry*, Opt. Quantum Electron., vol. 40, no. 11-12, pp. 818-82, 2008

OWTNM 2016 | 24TH INTERNATIONAL WORKSHOP ON OPTICAL WAVE & WAVEGUIDE THEORY AND NUMERICAL MODELLING

Dispersion and Loss Managed Soliton Communication System with Use of New Type of Step-Index Optical Fiber

Tomek KACZMAREK
Kielce University of Technology, Aleja Tysiaclecia Państwa Polskiego 7, Kielce, 25-314, Poland
tkaczmar@tu.kielce.pl

Abstract: Dispersion and loss managed soliton transmission line is presented. Bit rate in return to zero soliton communication system is estimated. 71.4-Gb/s soliton communication system is designed with 20-km amplifier spacing and with T_0 = 1ps initial pulse width. Increasing the width of the initial impulse to T_0 = 2ps allows lengthening the distance between amplifiers to about 80 km at the expense of reducing the bit rate to 35.7-Gb/s.

Introduction: A new type of step-index fiber [1] characterizes by the possibility of flattening of dispersion characteristics for the fundamental mode in the vifinity of third transmission window. Producing such a fiber may be associated with difficulties resulting from the presence of dip in core index profile. Studies on the effect of dip on the properties of propagation are optimistic [2], and they suggest that it is possible to prepare such a fiber using the MCVD method. The main drawback of step-index fiber in accordance with [1] and [2] lies in the fact that the dispersion length of communications link made from such a fiber is equal only few kilometers. Therefore, the distance between amplifiers in communication line built from this fiber will count from one to several kilometers, which makes such implementation impractical. This paper proposes a method for extending the distance between amplifiers, while minimizing attenuation occurring by combining (splicing) the fibers forming the optic link.

Method: In order to extend the distance between amplifiers in the transmission path, it is proposed the use of dispersion management [3]. In order to adapt the transmission link to solitonic requirements dense [4,5] and symmetric [6,7] map was selected. Dense map minimizes changes in pulse amplitude associated with the propagation and thus reduces the so-called dispersion tail, which adversely affect an adjacent pulse. Symmetric map is used in order to minimize jitter and so-called residual dispersion. Minimizing the link attenuation resulting from the joining of optical fibers forming the map is that a change in the nature of the dispersion curve of the fundamental mode is obtained by changing the doping of the core at a constant core radius. Immutable value of the radius of the core ensures minimize attenuation resulting from the splicing of adjacent sections of optical fibers forming the dispersion map. Numerical modeling of propagation a pair of soliton pulses in the proposed link was made using split-step Fourier method [8].

References

[1] T. Kaczmarek, *Dostosowywanie światłowodu skokowego dla propagacji solitonów jasnych (Customizing step index fiber to bright soliton propagation)*, Prz. Telekomun. i Wiad. Telekomun. (Telecommun. Rev. and Telecommun. News) 8-9, pp. 1062-1067, 2011

[2] T. Kaczmarek, *Influence of dip on propagation properties of step index fiber dedicated to bright solitons transmission*, Opt. and Quantum Electron. 47, pp. 107-116, 2015

[3] S. K. Turitsyn, V. K. Mezentsev and E. G. Shapiro, *Dispersion-Managed Solitons and Optimization of the Dispersion Management*, Opt. Fiber Technol. 4, pp. 384-452, 1998

[4] J. Fatome, S. Pitois, P. Tchofo-Dinda, D. Erasme, G. Millot, *Comparison of conventional and dense dispersion managed systems for 160 Gb/s transmissions*, Opt. Commun. 260, pp. 548–553, 2006

[5] A. B. Moubissi, K. Nakkeeran, P. Tchofo Dinda, and S. Wabnitz, *Average Dispersion Decreasing Densely Dispersion-Managed Fiber Transmission Systems*, IEEE Photon. Technol. Lett. 14, pp. 1279, 2002

[6] A. Mecozzi, C. B. Clausen, M. Shtaif, Sang-Gyu Park, and A. H. Gnauck, *Cancellation of Timing and Amplitude Jitter in Symmetric Links Using Highly Dispersed Pulses*, IEEE Photon. Technol. Lett. 13, pp. 445, 2001

[7] A. G. Striegler and B. Schmauss, *Compensation of Intrachannel Effects in Symmetric Dispersion-Managed Transmission Systems*, J. Lightwave Technol. 22, pp. 1877, 2004

[8] G. P. Agrawal, *Nonlinear Fiber Optics*, Academic Press, 5th Ed. 2013

OWTNM 2016 | 24TH INTERNATIONAL WORKSHOP ON OPTICAL WAVE & WAVEGUIDE THEORY AND NUMERICAL MODELLING

Third Order Nonlinear Optical Properties of DCM

Beata DERKOWSKA-ZIELINSKA
Institute of Physics, Faculty of Physics, Astronomy and Informatics,
Nicolaus Copernicus University, Grudziadzka 5, 87-100 Torun, Poland
beata@fizyka.umk.pl

Nonlinear optical properties of 4-dicyanomethylene-2-methyl-6-(p-dimenthyaminostyryl)-4H-pyran (DCM) solution were investigated by standard backward degenerate four wave mixing (DFWM) method at 532 nm [1-8]. Various solvents were used to dissolve DCM powder, which was purchased from Sigma Aldrich Co. It was found that the studied material exhibit large value of third order nonlinear optical susceptibility and this value depends on the polarity of solvent [7].

DCM molecule is well-known as a very efficient laser dye, which is widely used for a tunable light source in a broad spectral region [9]. It is also one of the most commonly used red emitters in color organic light-emitting device (OLED). DCM has a high fluorescence efficiency and is photochemically stable. The photophysical and photochemical properties of the DCM molecule in solution significantly depend on the solvent.

The structure of DCM is characterized by the arylidene moiety with a dimethylamino electron donor group linked to two cyano electron acceptor groups by a conjugated bridge (Fig. 1). Therefore, it has donor–π–acceptor (D–π–A) structures.

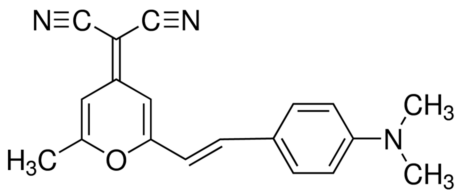

Fig. 11. Molecular structure of DCM.

References

[1] B. Derkowska, K. Jaworowicz, O. Krupka, M. Karpierz, M. Wojdyla, W. Bala, J.G. Grote, F. Kajzar, B. Sahraoui, *Influence of different peripheral substituents on the nonlinear optical properties of cobalt phthalocyanine core*, J. Appl. Phys., vol. 101, pp. 083112, 2007

[2] B. Derkowska, M. Wojdyla, W. Bala, K. Jaworowicz, M. Karpierz, R. Czaplicki, B. Sahraoui, *Dependence of the third order nonlinear optical susceptibility on concentration and peripheral substituent of metallophthalocyanines*, Molecular Crystals and Liquid Crystals, vol. 485, pp. 965-973, 2008

[3] K. Bouchouit, Z. Essaidi, S. Abed, A. Migalska-Zalas, B. Derkowska, N. Benali-cherif, M. Mihaly, A. Meghea, B. Sahraoui, *Experimental and theoretical studies of NLO properties of organic–inorganic materials base on p-nitroaniline*, Chemical Physics Letters, vol. 455, pp. 270-274, 2008

[4] K. Bouchouit, B. Derkowska, A. Migalska-Zalas, S. Abed, N. Benali-cherif, B. Sahraoui, *Nonlinear Optical Properties of Selected Natural Pigments Extracted From Spinach: Carotenoids*, Dyes and Pigments, vol. 86, pp. 161-165, 2010

[5] V. Smokal, B. Derkowska, R. Czaplicki, O. Krupka, A. Kolendo, B. Sahraoui,: *Nonlinear optical properties of thiazolidine derivatives*, Optical Materials, vol. 31, pp. 554-557, 2009

[6] V. Smokal, R. Czaplicki, B. Derkowska, O. Krupka, A. Kolendo, B. Sahraoui, *Synthesis and study of nonlinear optical properties of oxazolone containing polymers*, Synthetic metals, vol. 157, pp. 708-712, 2007

[7] B. Derkowska-Zielinska, *Influence of various solvents on the nonlinear optical properties of metallophthalocyanines (MPcs)*, Proc. SPIE 9652, pp. 965210-1 (1-6), 2015

[8] B. Derkowska, O. Krupka, V. Smokal, B. Sahraoui, *Optical properties of oxazalone derivatives with and without DNA-CTMA*, Optical Materials, vol. 33, 1429-1433, 2011

[9] Chih-Wei Chang, Ya-Ting Kao, Eric Wei-Guang Diau, *Fluorescence lifetime and nonradiative relaxation dynamics of DCM in nonpolar solvent*, Chemical Physics Letters, vol. 374, pp. 110-118, 2003

OWTNM 2016 | 24TH INTERNATIONAL WORKSHOP ON OPTICAL WAVE & WAVEGUIDE THEORY AND NUMERICAL MODELLING

The Numerical Prediction of the Characteristics of Directional Multimodal Couplers for Two-Photon Endoscopy

Hanna STAWSKA[1*], Łukasz PAJEWSKI[1], Adam HEIMRATH[2], Elżbieta BEREŚ- PAWLIK[1]

[1]Telecommunications and Teleinformatics Department, Wroclaw University of Technology, Wybrzeze Wyspianskiego 27, 50-370 Wrocław, Poland

[2]Hologram Industries Polska Spółka z o.o., Plac Solny 16, 50-062 Wrocław, Poland

[*] hanna.stawska@pwr.edu.pl

Multimode fibres have the ability to transmit multiple spatial modes of light simultaneously and can be used to replace the millimetre –thick bundles of fibres with a few hundred micron thick single fibre. The first demonstration of 3D imaging using two-photon excitation through multimode optical fibre (MMF) was in 2015 [1]. The experimental setup depicted in [1] contains a lot of bulk optics which is inconvenient in use due to e.g. calibration problems. Thus, to design an all-fibre setup the proper couplers are needed. In this paper numerical analysis of power distribution transformations in the multimode optical fibre couples is presented. The depicted method is based on the method proposed by Frieden [2]. In our analysis we assume that the intensity distribution within the multimode fibre may be referred to as the joint distribution of a set of random variables. Whatever the light source is, one has to take into account its spatial and angular emission probability density. In the following considerations the energy coefficients assigned to the rays at particular locations and directions will be proportional to the distribution densities of respective random variables. As it is known, the initial ray coordinates can be presented by six random variables: x, y, z –3 spatial variables and α, β, γ -3 angular variables. Then the formal description of the ray image transformation is:

$$(x', y', z', \alpha', \beta', \gamma') = \Im(x, y, z, \alpha, \beta, \gamma) \quad (1)$$

In this paper we present the method of prediction of joint distribution density of these six random variables on the output of the optical medium for given distribution density of input rays and knowledge of $\Im$ transformation. For numerical ray tracing we use the method based on Runge-Kutta integration of differential equations. Next, based on numerical results we prepared several multimode couplers using a grinding and polishing method. We obtained very good accordance between numerical and experimental results.

References

[1] Edgar E. Morales-Delgado, Demetri Psaltis, and Christophe Moser, *Two-photon imaging through a multimode fibre*, Opt. Express 23, 32158-32170, 2015

[2] B.R. Frieden, *The Computer In Optical Research*, Topics in Applied Physics 41, Springer Verlag, 1980

OWTNM 2016 | 24TH INTERNATIONAL WORKSHOP ON OPTICAL WAVE & WAVEGUIDE THEORY AND NUMERICAL MODELLING

Ray Tracing Methods in Numerical Analysis of Double-Clad Microstructured Optical Fibre Coupler

Lukasz PAJEWSKI[1*], Hanna STAWSKA[1], Adam HEIMRATH[2], Elzbieta BERES-PAWLIK[1],

[1]Telecommunications and Teleinformatics Department, Wroclaw University of Technology, Wybrzeze Wyspianskiego 27, 50-370 Wroclaw, Poland

[2]Hologram Industries Polska Spolka z o. o., Plac Solny 16, 50-062 Wroclaw, Poland

[*]lukasz.pajewski@pwr.edu.pl

The microstructured optical fibres (MOF) have found many application in the modern photonic due to their unit properties. MOFs offer large freedom in fibre design. Nowadays many activities are focused on developing high power fibre lasers based on MOFs. In order to obtain a high beam quality and high power laser output the large mode area double-clad (LMA DC) fibres are used. The MOF structures give an opportunity to design a single mode large core fibres due to precise control refractive index between core and cladding. However, the problem still remains as how to achieve the efficient pumping method which does not require bulk optics elements. In LMA DC fibres the pump light should be injected into the inner cladding without access to the fibre ends. In standard fibres side-pumping method is widely used. But this method for MOF laser cavities is still not well developed. Using the side-pumping method, the all-fibre laser cavity can be designed. Side-pumping can be achieved by using side-polish couplers made of active MOF and the multimode pumping fibre. This method was successfully used in standard DC fibre laser cavities [1,2] also the first non-DC MOF coupler was made by side-polishing technique [3].

In order to investigate the parameters of such a coupler the ray tracing method is used. In this article two variants of this method based on [4] and [5] were used and compared. The results obtained from both techniques are consistent. Ray tracing method is relying on the Fermat's principle and it is widely used in lens-systems analysis. However, it was also shown that this method can also be used for analysing fibre optics elements if fibre dimensions are much larger than light wavelength [4]. Based on this analysis, the coupling ratio and insertion losses were obtained. The coupling ratio and insertion losses were optimized by adjusting the bending radius and refraction index between the polished sides blocks. In addition, the modal properties of the MOF have been calculated using a commercial mode solver developed by Lumerical.

References

[1] E. Beres-Pawlik, A. Grobelny, *Construction of a side pumped double-clad fiber using polished couplers,* Optics Communications, vol. 283, pp. 2363-2368, 2010

[2] E. Beres-Pawlik, *High-power laser,* Polish Patent, no. 217027, 2014

[3] H. Kim, J. Kim, U. Paek, B. H. Lee, *Tunable photonic crystal fiber coupler based on aside-polishing technique,* Optics Letters, vol. 29, no. 11, pp. 1194-1196, 2004

[4] A. Heimrath, *A direct method for ray tracing in gradient-index fibres*, Journal of Modern Optics, vol. 35, no. 5, pp. 783-790, 1988

[5] A. Sharma, D. V. Kumar, A. K. Ghatak, *Tracing rays through graded-index media: a new method,* Applied Optics, vol. 21, no. 6, pp. 984-987, 1982

OWTNM 2016 | 24TH INTERNATIONAL WORKSHOP ON OPTICAL WAVE & WAVEGUIDE THEORY AND NUMERICAL MODELLING

Analysis of the Absorption and Refraction Spectra of Photorefractive GaAs - AlGaAs Heterostructures for Dynamic Diffractive Elements

Eliza MIŚKIEWICZ[1*], Marek WICHTOWSKI[1], Andrzej ZIÓŁKOWSKI[1], Ewa WEINERT-RĄCZKA[1]

[1]Telecommunications and Photonics Department, Faculty of Electrical Engineering, West Pomeranian University of Technology in Szczecin, ul. 26 kwietnia 10, Szczecin, 71-126, Poland

[*] eliza.miskiewicz@zut.edu.pl

The photorefractive effect is a nonlinear phenomenon relying on local refraction (and absorption) index changes induced by light of non-uniform spatial intensity. For the typical photorefractive media the nonlinear response occurs for low light intensities and the reaction time varies from miliseconds to several minutes. Long response time limits the use of those media in fast optical information processing applications. The semi-insulating GaAs – AlGaAs multiple quantum wells (SIMQW) overcome this drawback. They use the enhanced electro-optic properties of quantum confined excitons in quantum well structures to produce thin films that can be used in diffractive optical elements, including dynamic holography [1]. They have very high sensitivity and short response time.

One of the most popular systems of operation for the GaAs - AlGaAs multiple quantum well structure is the Franz-Keldysh geometry, with an external electric field applied along the planes of quantum wells [1],[2],[3]. Applying the high external electric field causes ionization of excitons, shortening their life time. Manifestation of this process is the broadening and decreasing of the peaks corresponding to excitonic transitions in the absorption spectrum and is thus called electroabsorption [2].

In this work the analysis of experimentally obtained absorption and refraction spectra of GaAs – $Al_{0.3}Ga_{0.7}As$ SIMQW structures is presented. Examined material consists of a 100-period superlattice of 7 nm GaAs wells and 6 nm AlGaAs barriers. The structure was proton-implanted at 80 keV and 160 keV with the same ion doses for each energy, to ensure the semi-insulating properties. Three series of samples with the proton fluxes of $1x10^{12}$ cm^{-2}, $1,5x10^{12}$ cm^{-2} and $2x10^{12}$ cm^{-2} were prepared and the measurements were conducted for various applied electric fields. The experiment results allow to define the influence of implantation parameters on the electroabsorpion spectra.

References

[1] P. Günter, J. P. Huignard, *Photorefractive Materials and their Applicatioms 1*, Springer, New York 2006.

[2] S. Balasubramanian, I. Lahiri, Y. Ding, M.R. Melloch, D.D. Nolte, *Two-wave-mixing dynamics and nonlinear hot-electron transport in transverse-geometry photorefractive quantum wells studied by moving gratings*, Appl. Phys. B, vol. 68(5), pp. 863-869, 1999

[3] M. Wichtowski, *Wave mixing analysis in photorefractive quantum wells in the Franz–Keldysh geometry under a moving grating,* App. Phys. B, vol. 115(4), pp. 505-516, 2013

OWTNM 2016 | 24TH INTERNATIONAL WORKSHOP ON OPTICAL WAVE & WAVEGUIDE THEORY AND NUMERICAL MODELLING

Model for a Few-Mode Nonlinear Propagation of Optical Pulse in Multimode Optical Fiber

Vladimir A. BURDIN*, Anton V. BOURDINE
Povolzhskiy State University of Telecommunications and Informatics (PSUTI),
Lev Tolstoy str.-23, Samara, 443010, Russia
* burdin@psati.ru

So-called nonlinear Shannon limit led to demand a research for alternative waveguide systems instead standard singlemode optical fibers for new generation high bit rate networks [1]. Therefore both few-mode optical fibers and multimode optical fibers operating in a few-mode regime may be considered. Processes of mode group propagation over multimode optical fibers under taking into account nonlinearity and dispersion are usually described by coupled nonlinear Schrödinger equations (CNLSE) [2-4]. Those equations written for long-haul fiber optic links may be solved by split step method [4]. However known conventional solution schemes for mentioned method realization do not take into account mode parameter and mode coupling dependence on transmitted optical signal characteristics that does not provide correct solution of CNLSE.

This work presents developed modification of CNLSE for modeling and simulation of mode propagation in a few-mode regime under taking into account nonlinearity, dispersion and fiber irregularity that partially lifts noted restrictions. We describe proposed approach and represent an example of simulation of mode set propagation over link with multimode optical fibers operating in a few-mode regime.

References

[1] A.D. Ellis, *The nonlinear Shannon limit and the need for new fibres*. Proc. of SPIE, vol. 8434, 84340H, 2012
[2] I.N. Sisakyan, A.V. Schwarzburg, *Nonlinear dynamics of picosecond pulses in fiber-optic lightguides*, Quantum Electronics, vol. 11, no 9, pp. 1703-1721, 1984
[3] S.M. Shirokov, *Approximate parametrical models of dynamics of self-influence of pulses in nonlinear optical environments with mode dispersion*, Computer Optics, vol. 14-15, no 2, pp. 117 – 124, 1995
[4] G. Agrawal, *Nonlinear fiber optics*, Academic Press, 2001

24TH INTERNATIONAL WORKSHOP ON OPTICAL WAVE & WAVEGUIDE THEORY AND NUMERICAL MODELLING

OWTNM2016

20–21 MAY | WARSAW | POLAND

FRIDAY 20TH MAY 2016

16:45-18:15

OWTNM SESSION #2

PLASMONICS

CHAIR: **MANFRED HAMMER,**
UNIVERSITY OF PADERBORN, GERMANY

The University of Nottingham
UNITED KINGDOM · CHINA · MALAYSIA

SUPPORTED BY

CZIiTT Centre for Innovation and Technology Transfer Management WUT

SKKP POLISH CONFERENCE & CONGRESS ASSOCIATION

CEZAMAT

EPIC European Photonics Industry Consortium

OWTNM 2016 | 24TH INTERNATIONAL WORKSHOP ON OPTICAL WAVE & WAVEGUIDE THEORY AND NUMERICAL MODELLING

Simulations of Sensing Capabilities of Propagating Modes Supported by a Sparse Array of Metal Nanoparticles

Pavel KWIECIEN[1*], Ivan RICHTER[1], Barbora ŠPAČKOVÁ[2], Jiří HOMOLA[2]
[1]Czech Technical University in Prague, Faculty of Nuclear Sciences and Physical Engineering, Department of Physical Electronics, Břehová 7, 115 19 Prague 1, Czech Republic
[2]Institute of Photonics and Electronics AS CR, v.v.i., Chaberská 57, Prague 8, Czech Republic
* pavel.kwiecien@fjfi.cvut.cz

In this contribution, results of numerical modeling of sensing capabilities of guided modes within plasmonic sensors composed of a sparse array of metal nanoparticles obtained with our in-house two-dimensional RCWA tool will be presented.

Here we demonstate the biosensing capabilities of a plasmonic sensor which is based on propagating modes supported with localized surface plasmons within an array of gold cylinders [1]. The sensing structure consist of a two-dimensional rectangular array of gold cylinders (see Fig. 1.) of a diameter 30 nm and height h (typically h = 90 nm) and period Λ (typically Λ = 150 nm) as a parameter. Two different cases were assumed, concerning the excitation scheme: 1) via prism (Structure 1 in Fig. 1), 2) prism + layer of a cytop material (Structure 2 in Fig. 1). To model optical responses of such sensor structures, our in-house RCWA tool [2] has been used. Further, sensing capabilities of the structures are expressed in terms of the figure of merit related to sensitivities and surface refractive index changes. In our modeling tool, we have included and applied several efficiency-improving approaches (e. g. normal vector field, proper field calculation). In this presentation, we will also discuss several numerical issues, concerning EM field profiles of guided sensing modes, convergences and FOM optimization strategies.

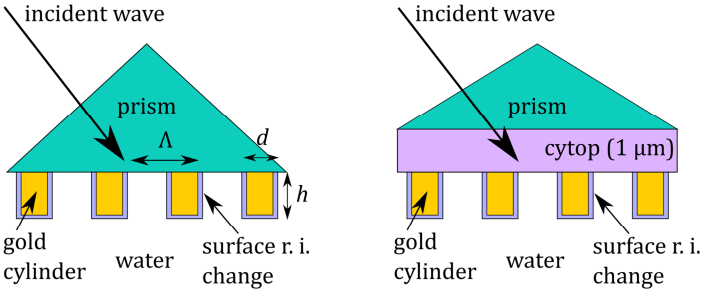

Fig. 12. Designs of optical biosensors.

References

[1] Špačková et al., *Consideration of photonic and mass-transfer aspects on the performance of a biosensor based on localized surface plasmons on an array of gold cylinders*, Sensors, 2012 IEEE, p. 1, 2012
[2] http://rcwa-2d.sourceforge.net

OWTNM 2016 | 24TH INTERNATIONAL WORKSHOP ON OPTICAL WAVE & WAVEGUIDE THEORY AND NUMERICAL MODELLING

Doping and Connecting Graphene Dimers for a Tunable Absorption Spectrum

Gilles ROSOLEN*, Bjorn MAES
Micro- and Nanophotonic Materials Group, University of Mons,
Place du Parc, 20, 7000, Mons, Belgium
* gilles.rosolen@umons.ac.be

Although Mie described resonances of metallic nanoparticules in 1908, their resonant properties are still under strong investigation nowadays. These particles show an important interaction with light, promising a wide range of applications such as biosensing [1], nonlinear optics [2], nanocircuits [3], optoelectronics [4] and transparent displays [5]. In the meantime, graphene enjoys a tremendous interest for its plasmon resonance tunability [6].

In this communication, we demonstrate the facile tunability of the optical response of graphene nanodisks. Via simulations, a graphene dimer absorption is investigated and new modes appear: higher order dark modes, normally bright for single disks become bright. Furthermore, an enhanced and narrower resonance is obtained connecting the dimer with a graphene ribbon bridge: the charge transfer plasmon. All these excitations are tunable with graphene doping, paving the way for new optoelectronic devices.

Graphene single disk resonances have already been investigated [7], but here we extend the study to higher order modes, and to coupled and uncoupled dimers. Although various resonances are dark under normal incidence (they do not couple with the incident field), we show that they become bright (they resonate) when we consider graphene nanodisk dimers [8]. The simulations are performed with a three-dimensional Comsol scattered field study and the graphene disk modes are obtained with an Eigenfrequency analysis, corroborated with an analytical model. Fig. 1a shows the considered dimer of 60 nm diameter graphene disks separated by a 5 nm distance. One of the disk is 0.4 eV doped and the second one has a doping varying from 0 to 1 eV. Their absorption efficiency under normal incidence (electric field in the x-direction) is represented in the logarithmic scale in Fig. 1b.

We observe two main patterns: one curved (with stronger absorption for the curved line at the top) and one vertical. The straight vertical resonances are from the fixed 0.4 eV doped graphene disk with the first dipolar mode resonating at 6.3 μm and the higher order modes appearing at smaller wavelengths. On the other hand, the curved pattern comes from the disk with varying doping. The continuous (dashed) black lines represent the theoretical 6 first modes of the varying (0.4 eV) doping graphene disk.

When the resonance patterns (curved and straight) interact, the modes hybridize and give rise to two anti-crossing resonances. This is observed in points 1 and 2 or in points 3 and 4 in Fig. 1b. The corresponding enhanced electric fields are represented on the right and show that the dipolar mode hybridization leads to a dark mode (point 1) and a bright mode (point 2). Higher order modes are indeed excited in points 3 and 4, where the quadrupolar mode is appearing on the 0.4 eV doped disk, thanks to the dipolar mode of the 0.65 eV doped disk.

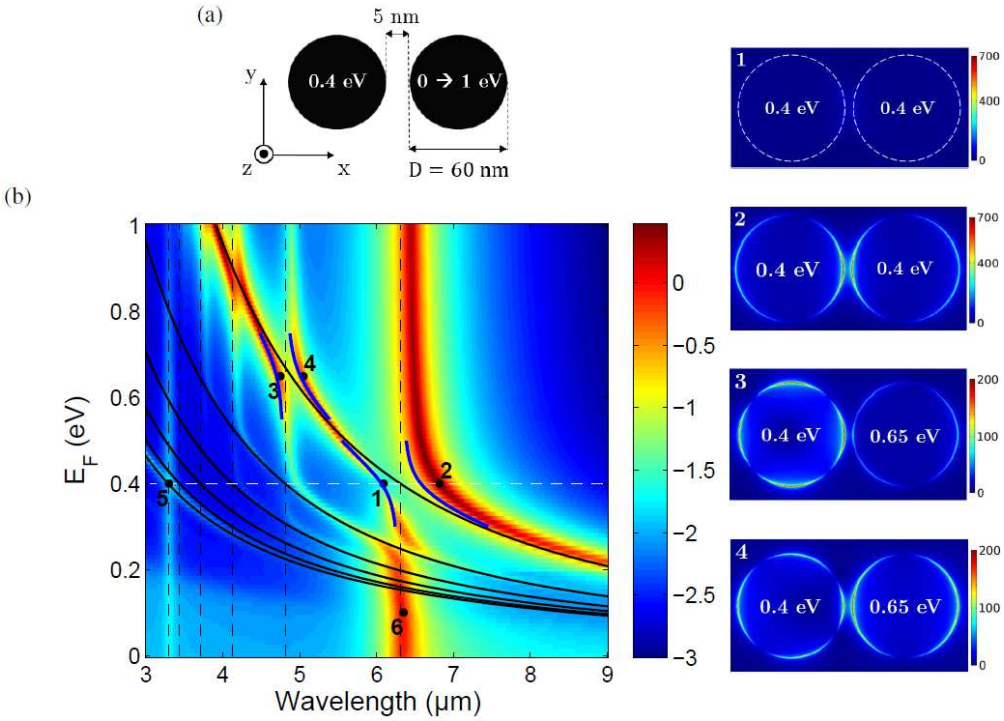

Fig. 13. (a) Graphene dimer with one disk of 0.4 eV doping and the other of varying doping. Normal incidence along z-direction. (b) Logarithm of the absorption efficiency of a graphene dimer with a fixed 0.4 eV disk and a varyingly doped disk (from 0 to 1 eV) as a function of the wavelength for x-polarization. Continuous black lines represent the first six modes with varying doping, the vertical dashed lines for 0.4 eV. (1-4) Enhancement of the electric field (total electric field over incident electric field) for particular points of Fig.1b.

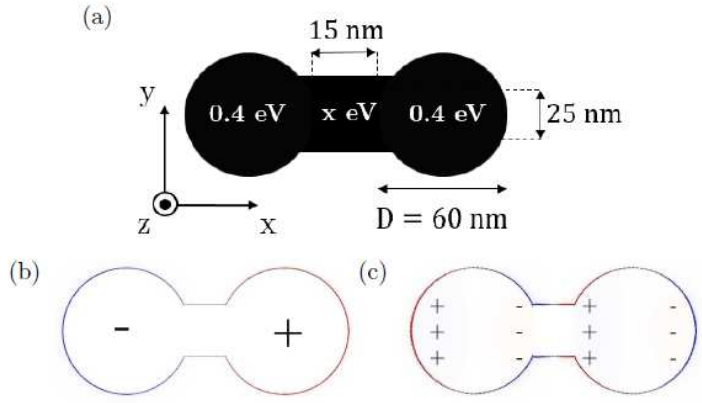

Fig. 2. (a) Scheme of the studied structure. (b) Charge densities of the charge transfer plasmon resonance and (c) the screened bonding dipolar plasmon.

Finally, we introduce a graphene ribbon to connect the two disks to allow electric charges to oscillate from one disk to the other: the charge tranfer plasmon. It is

represented in Fig. 2.a. We examine two graphene disks (diameter D = 60 nm) separated by a distance of 15 nm and identically doped (0.4 eV). The charge transfer junction is 25 nm wide.

The resonance is tuned via the doping of the junction, varying from 0.4 to 1 eV. Under normal incidence, with x-polarized electric field, the absorption efficiency spectrum is characterized by two resonances, as seen in Fig. 3. The first is smaller and blue shifted from the non-bridged dimer resonance. That resonance is called the screened bonding dipolar plasmon: the non-bridged dipolar-dipolar resonance stems from capacitive coupling, which is screened when a conductive bridge is connecting the zones of charge accumulation. The charge distrubution is represented in Fig. 2c.

The other, second resonance is red-shifted, stronger and narrower than the non-bridged dimer resonance. The particular oscillation of the electrons between the disks is presented on Fig. 2b: one disk is a positive pole and the other is a negative one. With the junction, the dimer acts as a continuous particle of larger length, which consequently induces a redshift. Finally, it is worth noticing the strong junction doping dependence on the resonant wavelength, going from 12 to 14 µm for a 0.4 eV to 1.0 eV junction.

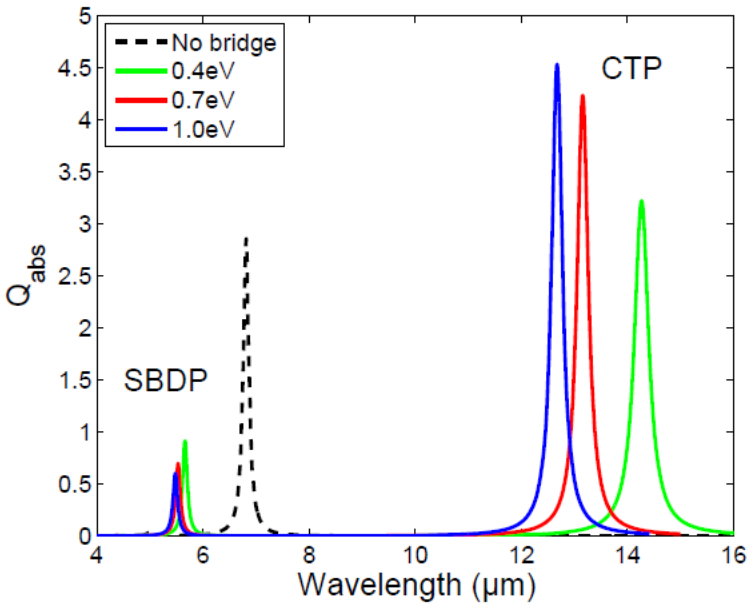

Fig. 3. Absorption efficiency of a graphene charge transfer dimer with varying bridge doping. The non-bridged dipolar-dipolar resonance is plotted in black dashed line for comparison.

In conclusion, we simulate the infrared response of asymmetric graphene dimers, induced by different doping levels, leading to a complex and tunable absorption spectrum. We demonstrate mode hybridization with dark modes becoming bright, and vice versa. Furthermore, strong and tunable absorption efficiencies with charge

transfer plasmon resonances are observed when the graphene disks are coupled via a bridge of varying doping. Finally, graphene shows its interest for the ease of tunability: with conventional metals the optical properties are only adjusted when the metal is exchanged or if the particle or the junction size is changed. Our findings could lead to molecular junction conduction measurements or to tunable sensors.

References

[1] J.N. Anker et al. *Biosensing with plasmonic nanosensors*. Nature Materials, vol. 7, no. 6, pp. 442-453, 2008

[2] Monique A. van der Veen et al. *Nonlinear optical enhancement caused by a higher order multipole mode of metallic triangles*. Journal of Materials Chemistry C, vol. 3, pp. 1576-1581, 2015

[3] N. Engheta. *Circuits with light at nanoscales: Optical nanocircuits inspired by metamaterials*, Science, vol. 317, no. 5845, pp. 1698-1702, 2007

[4] F. Bonaccorso et al. *Graphene photonics and optoelectronics*. Nature Photonics, vol. 4, pp. 611-622, 2010

[5] C. W. Hsu et al. *Transparent displays enabled by resonant nanoparticle scattering*. Nature Communications, vol. 5, 2014

[6] M. Jablan et al. *Plasmonics in graphene at infrared frequencies*. Physical Review B, vol. 80, no. 24, 245435, 2009

[7] F. G. de Abajo. *Graphene plasmonic: Challenge and opportunities.* ACS Photonics, vol. 1, pp. 135-152, 2014

[8] G. Rosolen et al. *Asymmetric and connected graphene dimers for a tunable plasmonic response*, Physical Review B, vol. 92, no. 20, 205405, 2015

OWTNM 2016 | 24TH INTERNATIONAL WORKSHOP ON OPTICAL WAVE & WAVEGUIDE THEORY AND NUMERICAL MODELLING

Optical Bistability and Self-Pulsation with Long-Range Hybrid Plasmonic Disk Resonators

Thomas CHRISTOPOULOS[1*], Odysseas TSILIPAKOS[2], Emmanouil E. KRIEZIS[1]
[1]Department of Electrical & Computer Engineering, AUTH, 54124 Thessaloniki, Greece
[2]Institute of Electronic Structure and Laser, FORTH, 71110 Heraklion, Crete, Greece
[*] cthomasa@ece.auth.gr

Optical bistability and self-pulsation with disk resonators based on the Long-Range Hybrid Plasmonic Waveguide (LRHPW) are studied using a theoretical framework combining perturbation theory, Coupled Mode Theory (CMT) and the Finite Element Method (FEM). The physical system is designed for Kerr bistability with minimum power threshold and high Extinction Ratio (ER). It is moreover shown to support spontaneous oscillations with high Modulation Depths (MD).

Nonlinear phenomena in resonant systems are known to lead in bistable behaviour due to positive feedback [1]. Importantly, the intensity build-up in the resonator lowers the power needed for nonlinearity manifestation. The nonlinear response can be studied by means of a CMT framework [2] taking into account all relevant phenomena: Kerr, two photon absorption and free carrier effects. By properly tuning the carrier lifetime τ_c by means of carrier sweeping we can demonstrate both Kerr-induced bistability for memory/switching operations and self-pulsation for tunable optical clock applications.

Figure 1(a) depicts a travelling-wave resonator, side-coupled to a bus waveguide. The physical implementation is based on the LRHPW with the gaps occupied by a highly nonlinear $\chi^{(3)}$ polymer (DDMEBT). Through rigorous 3D FEM simulations we find that R = 1.158 μm and g = 400 nm lead to Kerr bistability at minimum power levels and maximum ER [2]. Specifically, by reducing τ_c to 8 ps we demonstrate bistable action with an input power of 40 mW and an ER of 22 dB [Fig. 1(b)]. The system can switch between states in less than 50 ps, and is thus suitable for ultrafast memory applications. On the other hand, when τ_c lies around 45 ps we observe self-pulsation [Fig. 1(c)] with high modulation depth (> 0.8) and an oscillation frequency which can vary between 7.15-9 GHz when tuning the input power in the range of 25-45 mW.

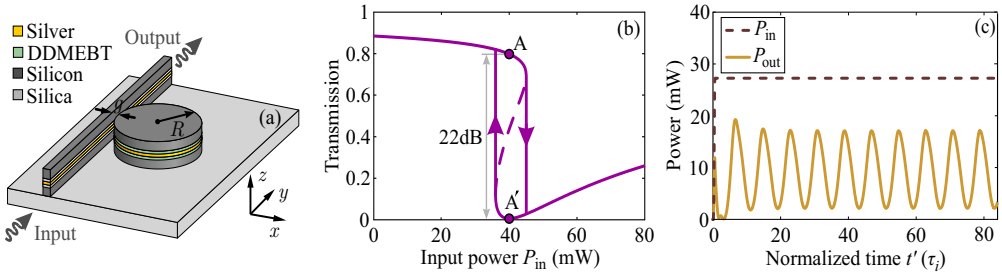

Fig. 1. (a) LRHPW-based disk resonator, side-coupled with a bus waveguide. (b) Bistability curve leading to bistable states at $P_{in} = 40$ mW with ER = 22 dB after suppressing free carriers ($\tau_c = 8$ ps). (c) Self-pulsing behaviour at $P_{in} = 27$ mW ($\tau_c = 45$ ps), with $f = 7.5$ GHz and MD = 0.8.

References

[1] M. Soljacic et al., *Phys. Rev. E.* **66**(5), 055601(R), 2002
[2] O. Tsilipakos , T. Christopoulos and E. E. Kriezis, *J. Lightw. Technol.,* **34**(4), 1333-1343, 2016

OWTNM 2016 | 24TH INTERNATIONAL WORKSHOP ON OPTICAL WAVE & WAVEGUIDE THEORY AND NUMERICAL MODELLING

Improved Nonlinear Plasmonic Waveguides: Modal Spatial Transitions and Loss Reduction

Mahmoud M. R. ELSAWY, Gilles RENVERSEZ*
Aix Marseille Université, CNRS, Centrale Marseille, Institut Fresnel UMR 7249,
13013 Marseille, France
* gilles.renversez@fresnel.fr

Nonlinear plasmonic slot waveguides (NPSWs) have been a flourishing discipline, at least since 2007 [1], due to the strong light confinement and due to the possible control of the solutions by the power unlike the linear case [1,2]. Nevertheless, the loss is still a fundamental issue which seriously limits the propagation length and consequently possible applications. In our work, we present a complete study of a NPSW improved by the inclusion of supplementary dielectric buffer layers between the nonlinear core of focusing Kerr type and the semi-infinite metal regions. We use the fixed power algorithm in the Finite Element Method to compute the linear and nonlinear stationary solutions. For the TM polarization, the added buffer layers have two main consequences. First, they reduce the overall losses and allow us to obtain low loss solutions at high powers. Second, they modify the types of solutions that propagate in the NPSWs for both linear and nonlinear cases. In the linear case, in addition to the symmetric linear plasmonic profile obtained in the simple plasmonic structure with linear core such that its effective index is above the linear core refractive index, we obtained a new field profile, in which the mode follows the cosine type profile in the core with plasmonic tails at the interfaces. In the nonlinear case, if the effective index of the symmetric linear mode is above the core linear refractive index, the mode field profiles now exhibit a spatial transition from a plasmonic type profile to a solitonic type one. We provide full phase diagrams of the TM operating regimes of these improved NPSWs as a function of the buffer layer thicknesses, core thickness and the total power. These phase diagrams describe the existence and the type of modes that can be found in our improved NPSW. Our structure also provides longer propagation length due to the decrease of the losses compared to the simple NPSWs. The stability of the main nonlinear TM modes is also investigated numerically using the FDTD. Then, we also demonstrate the existence of TE waves for both linear and nonlinear cases for some configurations. This improved NPSWs could be fabricated and characterized experimentally due to the realistic parameters we used to model them.

References

[1] E. Feigenbaum and M. Orenstein, Plasmon-soliton, Opt. Lett, vol. 32, pp. 674-676, 2007.
[2] W. Walasik and G. Renversez, Plasmon-soliton waves in planar slot waveguides, I. Modeling, Phys. Rev. A, vol. 93, 013825, 2016.
[3] M. M. R. Elsawy and G. Renversez, Improved nonlinear slot waveguides using dielectric buffer layers: properties of TM waves, Opt. Lett, vol. 41, no. 6, 2016.

OWTNM 2016 | 24TH INTERNATIONAL WORKSHOP ON OPTICAL WAVE & WAVEGUIDE THEORY AND NUMERICAL MODELLING

Leaky and Bound Modes on Stripe Plasmonic Waveguide Related Structures

Hsuan S. LIU[1], Hung-chun CHANG[1,2,3*]
[1]Graduate Institute of Photonics and Optoelectronics,
[2]Department of Electrical Engineering,
[3]Graduate Institute of Communication Engineering,
National Taiwan University, Taipei 10617, Taiwan
* hungchun@ntu.edu.tw

The stripe plasmonic waveguide, which has the simple structure with a metal stripe fabricated on top of a substrate, as depicted in Fig. 1(a), is one of the earlier investigated surface plasmon polariton (SPP) waveguides. Zia et al. [1] conducted finite-difference numerical calculations to obtain leaky and bound modes of the stripe waveguide for different gold stripe widths and showed that the leaky mode can possess longer propagation distance. We recently used an in-house developed full-vector finite-element imaginary-distance beam propagation method (FV-FE-IDBPM) to perform high-resolution analysis for the same structure and obtained peculiar modal characteristics [2], such as non-monotonic effective index versus the stripe width curves. High spatial resolution in the analysis also reveals the details of the leaky fields in the substrate, as seen in Fig. 1(b) for the Re[E_y] profile of the TM_1 leaky mode. This major field component is distributed mainly above the air-metal interface, while that of the bound mode is below the stripe in the substrate. Such behavior can be easily understood from the counterpart modes of a corresponding planar waveguide by extending the gold stripe width to infinity, for which the leaky-mode field is mainly located in the air side with field leakage in the substrate. Our study has been extended to the structure with the gold stripe replaced by a circular silver nanowire. The corresponding bound and leaky modes are obtained. Fig. 1(c) and (d) shows an example of the Re[E_x] and Re[E_y] profiles of the air-metal leaky mode. Detailed discussions of these modes and related applications will be given in the presentation.

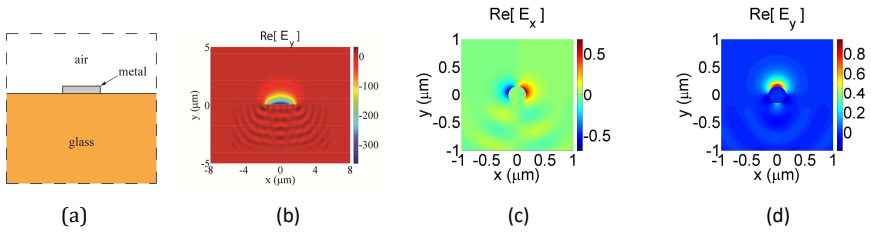

Fig. 14. (a) Cross-section of the stripe plasmonic waveguide. (b) Re[E_y] profile of the TM_1 leaky mode on the structure of (a) with gold stripe width of 3.7 μm at λ = 800 nm. (c) (d) Re[E_x] and Re[E_y] profiles of the air-metal mode on the structure of (a) when the stripe is replaced by a circular silver nanowire with radius of 160 nm at λ = 500 nm.

References

[1] R. Zia, M. D. Selker, M. L. Brongersma, *Leaky and bound modes of surface plasmon waveguides*, Phys. Rev. B, vol. 71, 165431, 2005

[2] H. H. Liu, H. C. Chang, *High-resolution analysis of leaky modes in surface plasmon stripe waveguides*, J. Lightwave Technol., 2016, in revision

OWTNM 2016 | 24TH INTERNATIONAL WORKSHOP ON OPTICAL WAVE & WAVEGUIDE THEORY AND NUMERICAL MODELLING

Detecting Weak Modes in Plasmonic Systems Using Complex Polarisation Charge

T. V. RAZIMAN, Olivier J. F. MARTIN*
Nanophotonics and Metrology Laboratory (NAM),
Swiss Federal Institute of Technology Lausanne (EPFL), Lausanne - 1015, Switzerland
* olivier.martin@epfl.ch

When light falls on an object placed in a background of a different dielectric constant, it induces polarisation charge on the object according to classical electromagnetic theory [1]. If all domains in the system have homogeneous dielectric permittivities, the induced charge lies only on the surfaces, which is a good approximation for most plasmonic systems where quantum effects are not significant. This surface charge forms the foundation of plasmonics [2], and have been used to explain various features in plasmonic systems such as scattering, forces, coupling, second harmonic generation and Fano resonances.

Polarisation charge calculated by numerical simulation methods in the frequency domain is represented as a complex quantity. Though complex numbers simplify the mathematics, they are conceptually tricky to deal with. In particular, ignoring the imaginary part of the charge by naively following the maxim that the real part is the physically relevant quantity gives misleading and erroneous results. We explain how the real and imaginary parts of the complex polarisation charge in plasmonic systems can be understood and visualised to retrieve maximum physical information while avoiding pitfalls. We also demonstrate that the complex valuedness of the charge, far from being a nuisance to deal with, in fact helps us to detect weak modes in the system which would otherwise be overshadowed by the stronger modes. By utilising the symmetries in the system along with the complex polarisation charge, we show how much more information can be obtained about the underlying physics. We discuss the effect of various factors that affect the charge such as resonances, polarisation, symmetry and retardation on charge, and introduce phase-correction, polarisation ellipse representation and symmetric decomposition as methods to visualise the complex charge distributions in plasmonic systems.

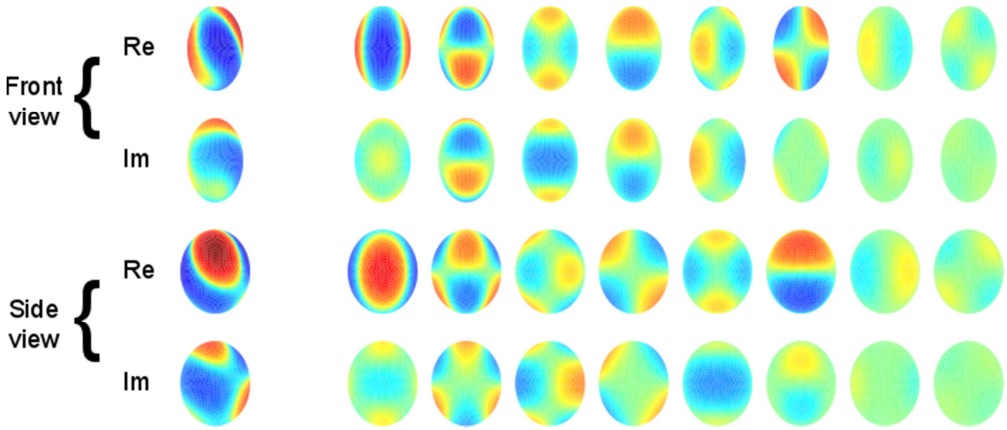

Fig 1. Front and side views of the real and imaginary parts of polarisation charge formed on a 200 nm × 250 nm × 300 nm gold ellipsoid in air upon oblique incidence at 2.55 eV, and the charge decomposed into various odd and even symmetries about the ellipsoid axes.

References

[1] J. D. Jackson, *Classical Electrodynamics* (Wiley, 1998), 3rd ed.
[2] S. A. Maier, *Plasmonics: Fundamentals and Applications* (Springer, 2007).

24TH INTERNATIONAL WORKSHOP ON OPTICAL WAVE & WAVEGUIDE THEORY AND NUMERICAL MODELLING

OWTNM2016

20–21 MAY | WARSAW | POLAND

SATURDAY 21ST MAY 2016

09:00 – 10-30

OWTNM SESSION #3

WAVEGUIDE BASED DESIGN

CHAIR: **ANNE-LAURE FEHREMBACH,**

AIX-MARSEILLE UNIVERSITÉ, CNRS, FRANCE

The University of Nottingham
UNITED KINGDOM · CHINA · MALAYSIA

SUPPORTED BY

CZIiTT Centre for Innovation and Technology Transfer Management WUT

SKKP POLISH CONFERENCE & CONGRESS ASSOCIATION

CEZAMAT

EPIC European Photonics Industry Consortium

OWTNM 2016 | 24TH INTERNATIONAL WORKSHOP ON OPTICAL WAVE & WAVEGUIDE THEORY AND NUMERICAL MODELLING

Hybrid Coupled Mode Modelling in 3-D

Manfred HAMMER*
Theoretical Electrical Engineering, Paderborn University, Paderborn, Germany
*manfred.hammer@uni-paderborn.de

Frequently, the functioning of an integrated-optical circuit can be understood in terms of the interaction of modal fields, the simulation and design of which is well established through numerical eigenproblem-solvers. It then remains to predict the interplay of these modes. We address this task by a ”Hybrid” variant (HCMT) of Coupled Mode Theory. The formalism of Ref. [1] has been extended to spatially three-dimensional configurations, leading to efficient, quantitative, and interpretable models in the frequency domain.

Starting point is a physically plausible expression for the electromagnetic field in a composite circuit. Suitable modes of its constituting elements are computed numerically by means of a commercial finite-element solver [2]. Then the total field is approximated as a superposition of these vectorial profiles, with amplitudes that are functions of their - potentially different - “natural” propagation coordinates. Discretization of these into 1-D finite elements, followed by Galerkin-type projection, leads to small-size systems of linear equations. Their solutions permit to inspect the wave interaction in terms of the variations of the amplitude functions, and to assemble approximations of the overall optical fields.

This contribution outlines the theoretical background, and discusses briefly limitations and implementational details. Beyond a series of consistency checks, our first results include simulations of configurations consisting of straight channels with fairly arbitrary rectangular cross section, position, and orientation. Figure 1 shows an example.

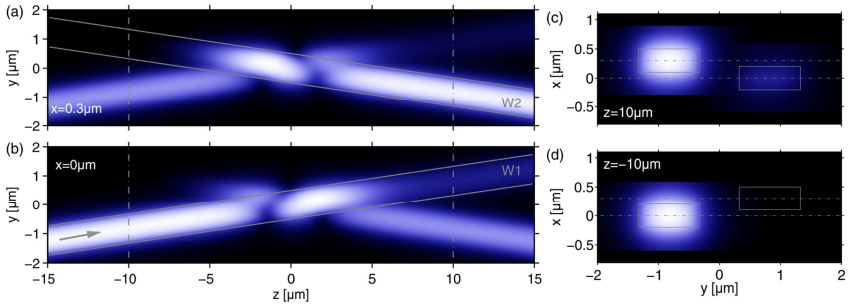

Fig. 1. X-crossing of two partly intersecting straight channels.

Rectangular cores (1.0 µm × 0.4 µm, refractive index 1.99 : 1.45) cross at an angle of 9.44°. The plots show the absolute value |H| of the optical magnetic field, on the horizontal y-z-planes at the center levels x=0.3 µm, x=0 of the upper (a, W2) and lower waveguide (b, W1), and on the vertical planes at z=10 µm (c, output) and at z=−10 µm (d, input), for TE-like excitation (arrow) at a wavelength of 1.55 µm. The HCMT simulation predicts output powers of 1% (W1, TE), 3% (W1, TM), 93% (W2, TE), and 3% (W2, TM) carried by the vectorial, TE- or TM-dominant modes.

References

[1] M. Hammer, *Hybrid analytical / numerical coupled-mode modeling of guided wave devices,* Journal of Lightwave Technology, 25(9), pp. 2287–2298, 2007
[2] JCMwave GmbH, Berlin, Germany; http://www.jcmwave.com

OWTNM 2016 | 24TH INTERNATIONAL WORKSHOP ON OPTICAL WAVE & WAVEGUIDE THEORY AND NUMERICAL MODELLING

Coupled-Mode Theory for Complex-Index, Corrugated Multilayer Stacks

Hannes LÜDER[1,2], Martina GERKEN[1], Jost ADAM[2*]
[1]Institute of Electrical and Information Engineering, Christian-Albrechts-Universität zu Kiel, Kaiserstraße 2, 24143 Kiel, Germany
[2]Mads Clausen Institute, University of Southern Denmark, Alsion 2, 6400 Sønderborg, Denmark
[*] jostadam@mci.sdu

We present a coupled-mode theory (CMT) approach for modelling multilayer thin-film devices with complex material parameters and periodic corrugations. Our method provides fast computation and extended physical insight as compared to standard numerical methods.

Nanostructuring of multilayer thin-film devices, e. g. OLEDs, is a common technique to manipulate the light emission, absorption and/or the field distribution inside the device. Recently, compound binary grating structures have been proposed for tailoring the angular emission spectrum of light emitting thin-film devices [1] and for increasing the sensitivity of refractive index sensors [2]. Here, we show a coupled-mode theory approach for modelling such devices. We first calculate the modes of the unperturbed waveguide (Fig.1), used as basis functions in the coupled-mode formalism. The waveguide corrugation is treated as a perturbation and leads to coupling between the modes. Expanding our previous work [3], we introduce perfectly matched layer (PML) boundary conditions to maintain a discrete, complete set of modes [4], and allow for complex-index materials. These extensions cause the resulting eigenvalue equation to be non-Hermitian, introducing two major consequences. First, the eigenvalues (i. e. the modes' n_{eff}) have to be found in the complex plane (Fig. 2). Second, the classical mode orthogonality is no longer valid. We address both challenges by a combination of three complex-root solving algorithms and by choosing a bi-orthogonal basis, obtained by solving the corresponding adjoint problem. With the modal solutions of the unperturbed waveguide, we calculate the coupling coefficients, which describe the mode coupling caused by the introduced periodic corrugation. The lossy complex waveguide modes do not directly correspond to the classical radiation modes. We therefore analyse the mode-coupling equations using a near-to-far-field transformation.

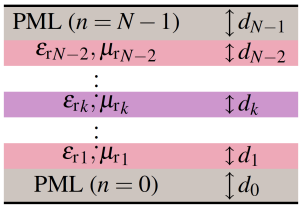

Fig. 1. Multilayer slab waveguide with PMLs and perfectly conducting boundaries.

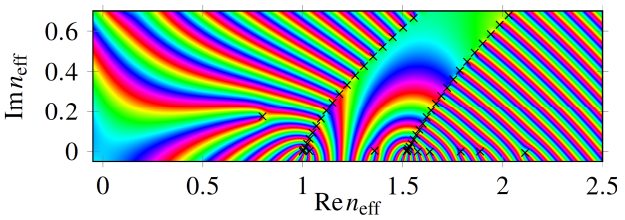

Fig. 2. Phase portrait of a waveguide characteristic function *f*. The complex n_{eff}-plane is colored by translating *phase* $f(n_{\mathrm{eff}})$ into color values. The eigenvalues are marked by "×".

References

[1] C. Kluge et al., Opt. Express 22, A1363-A1371, 2014
[2] L.T. Neustock et al., Journal of Sensors, Article ID 6174527, 2016
[3] J. Adam, H. Lüder, and M. Gerken, OWTNM 2015
[4] W.-P. Huang and J. Mu, Opt. Express 17, 19134-19152, 2009

OWTNM 2016 | 24TH INTERNATIONAL WORKSHOP ON OPTICAL WAVE & WAVEGUIDE THEORY AND NUMERICAL MODELLING

Optical Properties of a Four-Layer Waveguiding Nanocomposite Structure in the Near-IR Regime

I. S. PANYAEV[1], N. N. DADOENKOVA[1,2], Yu. S. DADOENKOVA[1,2,3], I. L. LYUBCHANSKII[2*], M. KRAWCZYK[4], I. A. ROZHLEYS[5], D. G. SANNIKOV[1]

[1]Ulyanovsk State University, Ulyanovsk, 432017, Russian Federation
[2]Donetsk Physical & Technical Institute of the National Academy of Sciences of Ukraine, Donetsk, 83114, Ukraine
[3]Novgorod State University, Veliky Novgorod, 173003, Russian Federation
[4]Adam Mickiewicz University, Poznań, 61-614, Poland
[5]National Research Nuclear University MEPhI, Moscow, 115409, Russian Federation
[*] I.Lyubchanskii@science.ru.nl

In this communication, we investigate analytically and numerically the optical and power characteristics of the four-layered structure composed of a magneto-optical guiding layer (yttrium iron garnet, YIG) on a semi-infinite dielectric substrate (silicon oxide, SiO_2), covered by a planar nanocomposite (NC) guiding layer surrounded by vacuum, as depicted in Fig. 1(a). The system is transparent in the near-infrared regime. The NC consists of alternating nanolayers of gadolinium-gallium-garnet (GGG) and titanium oxide (TiO_2). The dispersion equation is obtained in terms of the effective medium approximation [1] taking into account the bigyrotropic properties of the magneto-optic layer. Such a complex waveguide structure is shown to exhibit useful properties, particularly, a spatial-polarization filtration of TE- and TM-modes depending on the geometric parameters of the guiding layers.

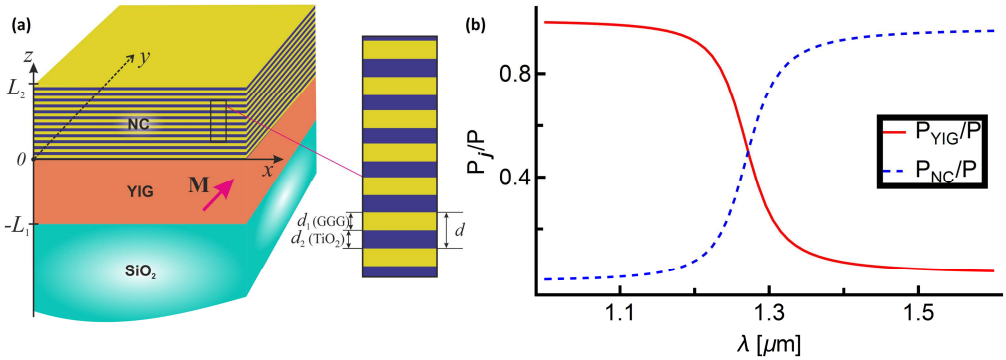

Fig. 15. Topology of the structure (a) and power flux rates (b) in guiding NC and YIG layers.

As an example, the power fluxes are presented in Fig. 1(b) for the TE_0 mode for the structure with the following parameters: $L_1 = L_2 = 7$ μm, $d_1/d_2 = 1$. The Q-factor modulation of the power fluxes reaches the value of about 12 dB in the wavelength range ~100 nm in the waveguide layers. The conditions for the optimal guiding mode switching are obtained.

References

[1] L.M. Brekhovskikh, *Waves in layered media*, Academic Press, New York, 1960

OWTNM 2016 | 24TH INTERNATIONAL WORKSHOP ON OPTICAL WAVE & WAVEGUIDE THEORY AND NUMERICAL MODELLING

Low loss Estimation in Thin Film Configurations by Means of Leaky Wave Resonances

Christoph WÄCHTER[1*], Riccardo RIZZO[1], Francesco MICHELOTTI[2], Peter MUNZERT[1], Norbert DANZ[1]

[1]Fraunhofer Institute for Applied Optics and Precision Engineering,
Albert-Einstein-Straße 7, 07745 Jena, Germany
[2]Dipartimento di Scienze di Base ed Applicate per l'Ingegneria, SAPIENZA
Università di Roma, Via A. Scarpa 16, Roma 00161, Italy
[*] christoph.waechter@iof.fraunhofer.de

High quality optical coatings require the knowledge of the absorption losses of the deposited materials. A precise measurement of low Im(n+ik)≤ 10^{-6} is usually carried out by laser induced deflection or laser calorimetry since the accuracy of spectrophotometry is limited due to losses k>10^{-4}.

Thin film stacks can be considered as resonators with a reflectivity determined by loss rates due to radiation towards the surrounding media as well as due to absorption, [1],

$$R = \frac{\left(\rho_{rad}^{air} - \rho_{rad}^{substrate} + \rho_{abs}\right)^2}{\left(\rho_{rad}^{air} + \rho_{rad}^{substrate} + \rho_{abs}\right)^2} \quad . \tag{1}$$

Above the TIR-angle (with no losses towards air) and with an approximate balance of material and radiation losses the resonant coupling to leaky waves results in distinct dips of the reflectivity, cf. Fig.1, which can be measured simply by goniometry.

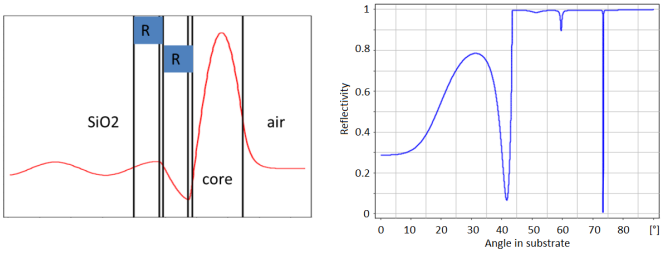

Fig. 16. ARROW field profile (left) and reflectivity in case of critical coupling (right).

To this end appropriate layer stacks exhibiting e.g. ARROW- or Bloch-surface-wave-resonances have to be designed. Finally, an inverse problem is to be solved to relate the reflectivity of a manufactured layer stack to the actual optical constants [2] including the losses and to the thicknesses of the layers. The whole concept from structure design to loss evaluation works actually and results in accuracies down to k~10^{-6}.

References

[1] K. Y. Bliokh, *Unusual Resonators: Plasmonics, metamaterials, and random media*, Rev. Mod. Phys., vol. 80, pp. 1201-1213, 2008

[2] O. Stenzel, et al., *Investigation on the reproducibility of optical constants of TiO_2, SiO_2, and Al_2O_3 films prepared by plasma ion assisted deposition*, Opt. Mat. Express, Vol. 5, No. 9, 002006, 2015

OWTNM 2016 | 24TH INTERNATIONAL WORKSHOP ON OPTICAL WAVE & WAVEGUIDE THEORY AND NUMERICAL MODELLING

Backscatter Model for Nanoscale Silicon Waveguides

Yufei XING[1,2*], Ang LI[1,2], Raphaël VAN LAER[1,2], Roel BAETS[1,2], Wim BOGAERTS[1,2,3]
[1]Photonics Research Group, Ghent University-Imec, Technologiepark 15, Ghent, 9052, Belgium
[2]Center for Nano- and Biophotonics, Ghent University, Belgium
[3]Luceda Photonics, Dendermonde, 9200, Belgium
[*] yufei.xing@ugent.be

Waveguides are the most fundamental building block in photonics, and their behaviour is considered to be well-understood. Usually they are typically considered as simple light guiding channels – with linear phase change and propagation losses. But in high contrast waveguides we have to consider backscattering induced by sidewall roughness, which leads to surprisingly strong fluctuations in the waveguide transmission spectrum. Fig. 1 shows measured transmission spectrum of waveguides of different length. They are ~450 nm x 220 nm air-clad silicon-on-insulator waveguides fabricated by imec's 193 nm deep UV lithography. We observe that fluctuations in the spectrum increase drastically with the waveguide length. The 7-cm-long waveguides produce flucuations above 15 dB.

We attribute the fluctuations to backscattering of light on the rough waveguide sidewalls. This roughness sets up a large number of scattering centers. On each of them, a small portion of light is reflected with a random phase (and amplitude). As shown in Fig. 2, unscattered forward propagating light (solid red line) interferes with many forward contributions that are the result of at least two backscattering/reflection processes (blue lines), and the transmitted light therefore shows sharp interference fringes.

To study the transmission spectrum rigorously, we built a model in the circuit simulator CAPHE, which models waveguides as a series of very short cascaded lumped sections (Fig. 2) of an identical length (50 μm) and a defined loss α. To incorporte backscattering, each section has a defined reflectivity r and a random phase change φ uniformly distributed between 0 and 2π. As shown in Fig. 1, with a reasonable choice of parameters (loss and reflectivity), our model explains and accuractely captures the observed 10 dB fluctuations in 7-cm-long silicon waveguides. This is a first step towards a full understanding and mitigation of such anomalous waveguide behavior.

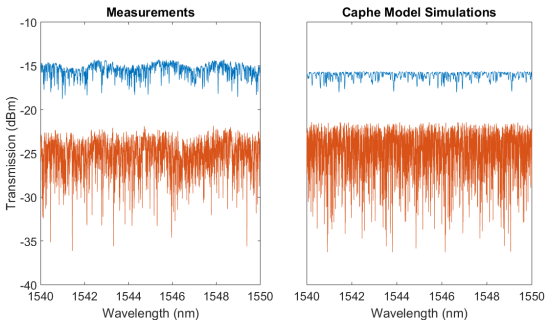

Fig. 1. Measured and simulated transmission spectrum of 1 cm (blue) and 7 cm (orange) SOI strip waveguides.

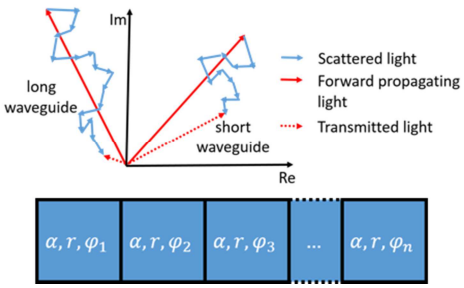

Fig. 2. Upper: Phasor plot of light in waveguides. Lower: Lumped circuit model of waveguides.

OWTNM 2016 | 24TH INTERNATIONAL WORKSHOP ON OPTICAL WAVE & WAVEGUIDE THEORY AND NUMERICAL MODELLING

Design of Dual Layer, Dual Width Waveguides for Giant Group Velocity Dispersion

Jon Øyvind KJELLMAN*, Ripalta STABILE, Kevin A. WILLIAMS
Eindhoven University of Technology, COBRA research institute, P.O. Box 513, 5600 MB Eindhoven, The Netherlands
* J.Kjellman@tue.nl

Existing technology platforms for photonic integration have a number of component designs for light generation, detection, switching, filtering, etc. Although highly sophisticated photonic integrated circuits can be realized using these components, these circuits are mostly applied to processing of signal pulses longer than 10 ps (< 100 GHz.) For processing of ultrafast pulses in the sub-picosecond regime, new components are required. One such component is broad bandwidth dispersive elements.

To enable flexible design of dispersive components we have numerically investigated the dispersion of an asymmetric dual layer, dual width waveguide illustrated in fig. 1(a). This design is based on the principle of resonant giant group velocity dispersion in the super modes of asymmetric, coupled waveguides [1]. Besides a significant increase in the magnitude of the dispersion, this principle allows pulses to be both up and down chirped on the same chip depending on which super mode is excited.

On resonance, this waveguide design has symmetric and asymmetric super modes as illustrated in fig. 1(b). The design allows the dispersion relation of the cores to be tailored individually by changing the upper and lower core widths. Changing the top waveguide width tunes the dispersion resonance over a 100 nm wavelength range as shown in fig. 1(c). At a wavelength of 1.55 µm the magnitude of dispersion is an order of magnitude larger than in comparable III/V waveguides.

The presentation will also discuss geometric constraints, an approach for selective excitation of the super modes, and how wide-bandwidth dispersion can be realized.

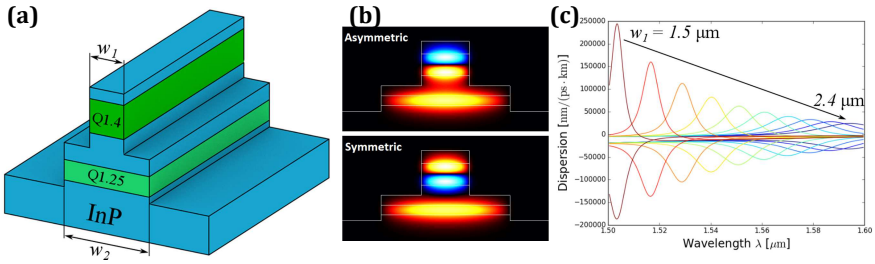

Fig. 17. (a) Dual layer, dual width waveguide design; (b) waveguide super modes at resonance; and (c) dispersion for various top widths with fixed bottom width.

References

[1] U. Peschel, T. Peschel, and F. Lederer, *Appl. Phys. Lett.*, 67(15):2111, 1995

24TH INTERNATIONAL WORKSHOP ON OPTICAL WAVE & WAVEGUIDE THEORY AND NUMERICAL MODELLING

OWTNM2016

20–21 MAY | WARSAW | POLAND

SATURDAY 21TH MAY 2016

11:00-13:00

OWTNM SESSION #4

PHOTONIC DESIGN

CHAIR: **CHRISTOPH WÄCHTER,**
FRAUNHOFER INSTITUTE FOR APPLIED OPTICS AND PRECISION ENGINEERING, JENA, GERMANY

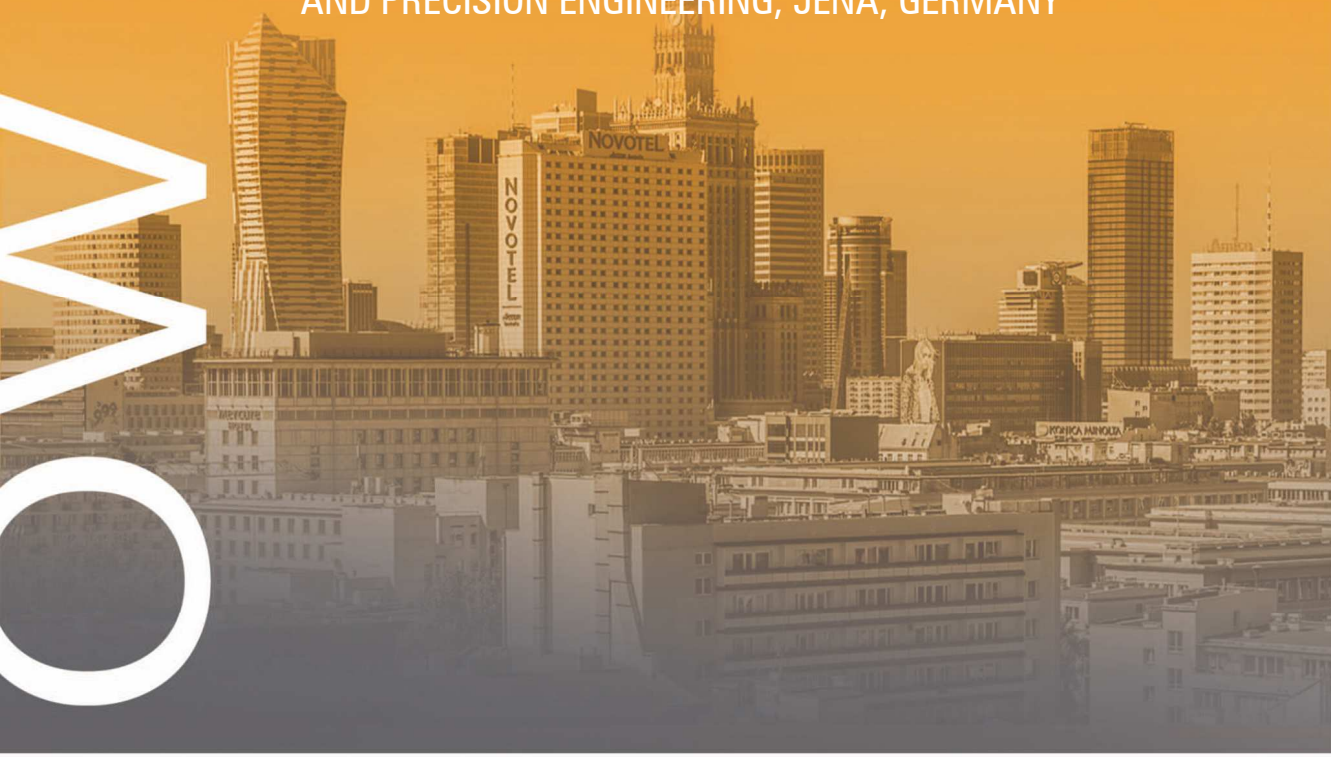

The University of Nottingham
UNITED KINGDOM · CHINA · MALAYSIA

SUPPORTED BY CZIiTT Centre for Innovation and Technology Transfer Management WUT · SKKP POLISH CONFERENCE & CONGRESS ASSOCIATION · CEZAMAT · EPIC European Photonics Industry Consortium

OWTNM 2016 | 24TH INTERNATIONAL WORKSHOP ON OPTICAL WAVE & WAVEGUIDE THEORY AND NUMERICAL MODELLING

Numerical Investigation of Mid-Infrared Laser Action in Pr^{3+} Doped Chalcogenide Fibre Laser

L. SÓJKA[1,2], Z. TANG[1], D. FURNISS[1], H. SAKR[1], E. BEREŚ-PAWLIK[2], A. B. SEDDON[1], T. M. BENSON[1], S. SUJECKI[1*]

[1]George Green Institute for Electromagnetics Research, University of Nottingham, University Park, NG7 2RD Nottingham, UK

[2]Telecommunications and Teleinformatics Department, Wroclaw University of Technology, Wybrzeze Wyspianskiego 27, 50-370 Wroclaw, Poland

[*] slawomir.sujecki@nottingham.ac.uk

High power mid-infrared fibre laser sources with emitting wavelengths covering the range stretching from 4 μm to 5.5 μm offer many applications in remote sensing, medicine and defence [1]. However, in order to access these wavelengths, low phonon host materials are needed. Among the most promising host materials for this wavelength region are chalcogenide glasses [1]. Chalcogenide glasses possess good rare earth ion solubility, high refractive index and can be drawn into fibre. These characteristics make chalcogenide glasses a promising host material for rare-earth ions [1-4]. Recent publications show that there is a particularly large interest in mid-infrared fluorescence from the $({}^3F_2,{}^3H_6) \rightarrow {}^3H_5$ (~3.7-4.2 μm), and ${}^3H_5 \rightarrow {}^3H_4$ (4.3-5.0 μm) transitions of Pr^{3+} doped selenide glass [2-4]. This is because Pr^{3+} in chalcogenide glass has a high pump absorption cross-section, and also because it can be pumped with commercially available laser diodes. In order to achieve the first mid-infrared laser action in chalcogenide glass fibres the population mechanisms need be understood in detail.

Numerical modelling of Pr^{3+} chalcogenide doped fibre laser is presented in this paper. The spectroscopic parameters were extracted from in-house prepared selenide Pr^{3+} doped chalcogenide glass samples and used in modelling. In this contribution particular attention is paid to pumping schemes. The cascade scheme already reported in literature[4] is compared to a resonant pumping scheme. Additionally, the laser performance was tested against pump wavelength, fibre length, signal wavelength, and output coupler reflectivity. The modelling results show that the proposed resonant pumping scheme using a high power QCL pump is a better solution than an indirect pumping using a 2.1 μm laser. The results obtained show also resonant pumping allows for a significant reduction in the laser threshold and an increase in the laser efficiency when compared with cascade lasing.

References

[1] A. Seddon, Z. Tang, D. Furniss, S. Sujecki and T. Benson, *Progress in rare-earth-doped mid-infrared fiber lasers*, Opt. Express 18, pp. 26704-26719, 2010

[2] H. Sakr, D. Furniss, Z. Tang, L. Sojka, N. A. Moneim, E. Barney, S. Sujecki, T. M. Benson and A. B. Seddon, *Superior photoluminescence (PL) of Pr^{3+}-In, compared to Pr^{3+}-Ga, selenide-chalcogenide bulk glasses and PL of optically-clad fiber*, Opt. Express 22, pp. 21236-21252, 2014

[3] L. Sójka, Z. Tang, D. Furniss, H. Sakr, A. Oladeji, E. Bereś-Pawlik, H. Dantanarayana, E. Faber, A. B. Seddon, T. M. Benson and S. Sujecki, *Broadband, mid-infrared emission from Pr3+ doped GeAsGaSe chalcogenide fiber, optically clad*, Opt. Mater. 36(6), pp. 1076-1082, 2014

[4] S. Sujecki, A. Oladeji, A. Phillips, A. B. Seddon, T. M. Benson, H. Sakr, Z. Tang, E. Barney, D. Furniss, Ł. Sójka, E. Bereś-Pawlik, K. Scholle, S. Lamrini and P. Furberg, *Theoretical study of population inversion in active doped MIR chalcogenide glass fibre lasers (invited)*, Opt Quant Electron 47, pp. 1389-1395, 2015

OWTNM 2016 | 24TH INTERNATIONAL WORKSHOP ON OPTICAL WAVE & WAVEGUIDE THEORY AND NUMERICAL MODELLING

Numerical Investigation of All-Optical Switching in Nonlinear Chalcogenide Fibre Bragg Gratings due to Cross-Phase and Self-Phase Modulation

Ľubomír SCHOLTZ*, Libor LADÁNYI, Jarmila MÜLLEROVÁ
Institute of Aurel Stodola, Faculty of Electrical Engineering, University of Žilina,
ul. kpt. J. Nálepku 1390, 03101 Liptovský Mikuláš, Slovak Republic
* scholtz@lm.uniza.sk

All-optical switching in nonlinear chalcogenide fiber Bragg gratings (FBG) can be achieved thanks to the third-order nonlinear optical parameters of chalcogenide glasses. Two principal nonlinear effects with similar power requirements can result in the bistable transmission/reflection of an input optical pulse. In the self-phase modulation (SPM) regime switching is achieved by the intense probe pulse itself. Using cross-phase modulation (XPM) a strong pump alters the FBG refractive index experienced by a weak probe pulse. As a result of this the detuning of the probe pulse from the centre of the photonic band gap occurs. We present the comparison of SPM and XPM switching simulated using the symmetrized optimized split-step method, the time-domain transfer matrix method and the finite difference method.

Further we present the results of numerical investigation of the effect of modulation instability formed in nonlinear FBGs. The modulation instability occurs if the material response time is lower than the transient time of the pulse through the grating. Possibilities of the successful elimination of the output pulse degradation via the modulation instability under different conditions implemented into numerical experiments (different pulse widths, input powers and FBG parameters, e.g. materials, types and lengths) are suggested. In Fig.1 the modulation instability in case of a 3 ns input Gaussian pulse (left) can be observed. If a 30 ps input pulse (right) enters the grating the modulation instability in the reflected pulse disappears under the same FBG parameters.

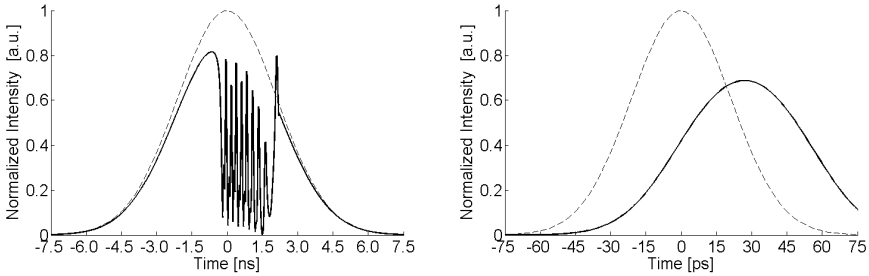

Fig. 18. The temporal response of 3 ns (left) and 30 ps (right) input pulses (dashed line) of 190 MW/cm² peak intensity reflected (solid lines) by a uniform nonlinear FBG (the length of 0.01 m, the modulation depth of 1×10^{-4}).

Acknowledgements: This paper was partly supported by the Slovak Research and Development Agency under the project APVV-0025-12.

OWTNM 2016 | 24TH INTERNATIONAL WORKSHOP ON OPTICAL WAVE & WAVEGUIDE THEORY AND NUMERICAL MODELLING

Analysis of Single-Frequency Radiation from Fiber Laser with Bragg Reflectors: Numerical Simulation by the Method of Single Expression

Hovik BAGHDASARYAN[1*], Tamara KNYAZYAN[1], Tamara HOVHANNISYAN[1], Marian MARCINIAK[2]

[1] National Polytechnic University of Armenia, 105 Terian str.Yerevan 0009, Armenia

[2] National Institute of Telecommunications, 1 Szachowa Street, 04-894 Warsaw, Poland

[2] Kielce University of Technology, al. Tysiaclecia Panstwa Polskiego 7, 25-314 Kielce, Poland

* hovik@seua.am

Single-frequency fiber lasers are specific light sources suitable for optical communication, interferometric sensing, coherent light detection and ranging, laser spectroscopy, etc. [1]. The suitable structures are distributed Bragg reflector (DBR) fiber lasers consisting of two fiber Bragg gratings (FBGs) at the ends of an active fiber [2] (Fig.1).

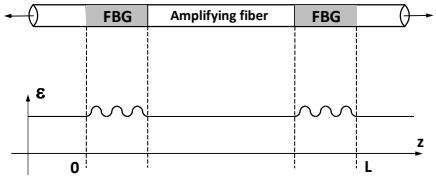

Fig. 1. Schematic of DBR fiber laser.

To reach the single-frequency lasing the length of an active medium (amplifying fiber) should be determined correctly via computer simulation. Since FBG mirrors are modulated structures which are inseparable parts of a lasing structure, then for resonant characteristics of the laser structure correct wavelength-scale numerical simulation is pertinent. For self-consisting numerical simulation the method of single expression is used [3]. In the modelling, initially, at the central wavelength of FBGs, known as Bragg wavelength, transmission spectra of DBR fiber laser have been analysed for different lengths of the fiber between FBGs at the absence of loss or gain. Starting from the minimal length of the fibre, full transmission at the Bragg wavelength is obtained for the row of increasing lengths of the fiber. Inclusion of the specific value of gain in the active fiber of these lengths permitted to obtain radiation along the fiber. At the other wavelengths multiple transparency peaks not corresponding to radiation are observed. An existence of one dominant mode radiation at the Bragg wavelength is explained by the optical field distribution within the resonator. Maximal field amplitude within the active fiber is observed for the resonant Bragg wavelength only. In conclusion, the possibility of single-frequency radiation from DBR fiber laser at the specific lengths of the active fiber has been obtained by the correct wavelength-scale simulation.

References

[1] W. Shi, *Single-frequency fiber lasers using rare-earth-doped silica*, SPIE Newsroom, 2015

[2] Y.O. Barmenkov et al., *Effective length of short Fabry-Perot cavity formed by uniform fiber Bragg gratings,* OPTICS EXPRESS, vol. 14, No. 14, pp. 6394-6399, 2006

[3] H.V. Baghdasaryan, T.M. Knyazyan, *Problem of Plane EM Wave Self-action in Multilayer Structure: an Exact Solution*, Opt. &Quant. Electr., vol. 31, No. 9/10, pp.1059-1072, 1999

OWTNM 2016 | 24TH INTERNATIONAL WORKSHOP ON OPTICAL WAVE & WAVEGUIDE THEORY AND NUMERICAL MODELLING

Design of Silica Few-Mode Optical Fibers with Enlarged Core Diameter

Anton V. BOURDINE*, Vladimir A. BURDIN
Povolzhskiy State University of Telecommunications and Informatics (PSUTI),
Lev Tolstoy str.-23, Samara, 443010, Russia
* bourdine@yandex.ru

Nowadays nonlinear effects occurring in standard silica singlemode optical fibers during propagation of optical signals grouped by DWDM systems with narrow channel spacing are the main issue for a passage to new-generation transport networks providing high bit rates of hundreds Tbps and more [1, 2]. Decreasing of fiber own nonlinearity is obvious effective method for suppression of nonlinear effects in fiber optic link. For conventional silica telecommunication optical fibers this may be performed either by choice of corresponding core special dopant materials or by enhancing of effective area that may be realized also by enlarging of core diameter. Enlarged optical fiber core diameter leads to new higher order modal components occurring and it requires management of differential mode delay (DMD), which is the main linear distortion effect for optical signal propagating over optical fiber under a few-mode regime [3]. This work presents alternative method for design special refractive index profiles of silica few-mode fibers with enlarged core diameter that provides suppression of nonlinear effects due to great effective mode area and decreased DMD over central region of wavelength "C"-band. We represent some results of refractive index profile synthesis for 6-mode silica optical fiber with core diameter 22 μm and effective mode area more 140 μm^2 for low-order guided modes and computed spectral curves of guided mode staff dispersion parameters over "C"-band.

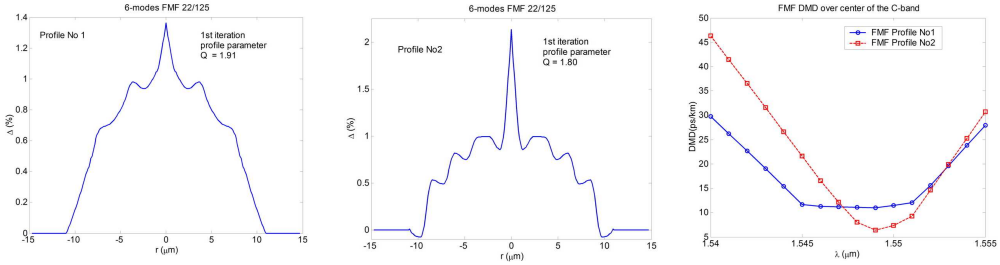

Fig. 1. Results of 6-mode FMF with 22 μm core diameter design: synthesized graded refractive index profiles and DMD curves over C-band central region computed for profile samples.

References

[1] R.-J. Essiambre et al. *Capacity limits of optical fiber networks*, IEEE Journal of Lightwave Technology, vol. 28, no 4, pp. 662 – 701, 2010
[2] A. Mecozzi et al. *Nonlinear Shannon limit in pseudolinear coherent systems*, IEEE Journal of Lightwave Technology, vol. 30, no 12, pp. 2011 – 2024, 2012
[3] S. Bottacchi, *Multi-Gigabit transmission over multimode optical fibre. Theory and design methods for 10GbE systems*, John Wiley & Sons Ltd, West Sussex, 2006

OWTNM 2016 | 24TH INTERNATIONAL WORKSHOP ON OPTICAL WAVE & WAVEGUIDE THEORY AND NUMERICAL MODELLING

Six-Mode-Group Fiber Amplifier for SDM System

Ankita GAUR[1]*, Vipul RASTOGI[1]
Indian Institute of Technology Roorkee, Roorkee, Uttarakhand, 247667, India
* ankitagaur.phy@gmail.com

Space division Multiplexing (SDM) is a breakthrough technology that could enhance data carrying capacity beyond Shannon limits by increasing spatial degree of freedom of fiber [1]. A few mode fiber (FMF) provides parallel and orthogonal channels for signal transmission. To utilize such a fiber in optical communication, it is necessary to develop few-mode erbium-doped fiber amplifier (EDFA) [2].

We propose a segmented-core EDFA with optimum doping profile. The first and third segments are made of Ge-doped silica with refractive index difference Δ of 0.48% and 1%, respectively. The second segment and the cladding are made of silica. Additionally, the first segment is partially doped and the third segment is extra-annulus doped with Er^{+3} ions. The mode profiles and effective indices have been calculated by using transfer matrix method. The fiber supports six mode groups LP_{01}, LP_{02}, LP_{11}, LP_{21}, LP_{31}, and LP_{41} (20 modes including degeneracy and polarization) with effective index separation greater than 4×10^{-4}. Gain modelling of EDFA is according to Ref. [3]. The input signal power used in each signal mode at 1530 nm is 30 μW. The fiber supports 30 pump modes at 980 nm and the input power used in each pump mode is 6 mW. Fig 1(a) shows that differential modal gain (DMG) of five mode groups LP_{01}, LP_{11}, LP_{21}, LP_{31}, and LP_{41} is less than 1 dB due to extra-annulus doping of third segment. Additionally, gains of LP_{02} mode group intersect with the gains of other mode groups due to partial doping of first segment. Therefore, we have achieved less than 1 dB DMG of six mode groups for fiber length lying between 2.4 m and 3.7 m. The results in Fig. 1(b) show that DMG of six mode groups over C-band is less than 2.5 dB with fiber of length 3.6 m. The proposed fiber would be useful for SDM system.

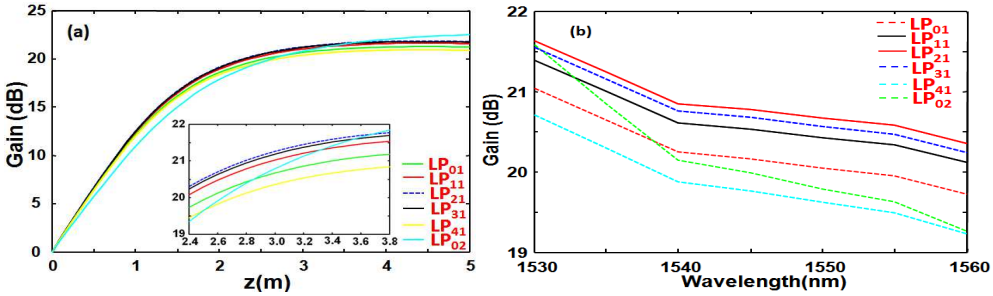

Fig. 19. Variation of gains of signal mode groups (a) with fiber length (b) over C-band.

References

[1] D. J. Richardson et al., *Space-division multiplexing in optical fibers*, Nat. Photonics, vol. 7, no. 5, pp. 354-362, 2013
[2] H. Onos et al., *Improvement of differential modal gain in few-mode fiber amplifier by employing ring core erbium-doped fiber*, Electron. Lett., vol. 51, no. 2, pp. 172-173, 2015
[3] N. Bai et al., *Multimode fiber amplifier with tunable modal gain using a reconfigurable multimode fiber*, Opt. Express, vol. 19, no. 17, pp. 16601-16611, 2011

OWTNM 2016 | 24TH INTERNATIONAL WORKSHOP ON OPTICAL WAVE & WAVEGUIDE THEORY AND NUMERICAL MODELLING

Numerical Simulation of the Dispersion-Managed Soliton Pulse Propagation

Libor LADÁNYI*, Ľubomír SCHOLTZ, Jarmila MÜLLEROVÁ
Institute of Aurel Stodola, Faculty of Electrical Engineering, University of Žilina,
ul.kpt. J.Nálepku 1390, Liptovsky Mikulas, 03101, Slovakia
* ladanyi@lm.uniza.sk

The term soliton refers to any optical field that does not change during propagation because of a delicate balance between nonlinear and linear effects in the medium. This kind of balance can be described by the nonlinear Schrödinger equation. A transmission system using dispersion-managed solitons is an attractive candidate for future high-speed and long-distance optical communications.

The aim of the paper is to demonstrate the ultrashort pulse transmission in amplified fiber link using solitons pulses under the influence of third-order dispersion (TOD). One of the main goals is to numerically obtain the eigensolution under the influence of TOD in a lossless fiber link. In practical systems, the fiber loss cannot be ignored and is compensated periodically by optical amplifiers.

The spectral changes caused in normal and anomalous dispersion regime in case of solitary input wave will be demonstrated. To simulate the spectral changes, it is necessary to use robust numerical method and also to ensure stability of the solutions. In this case we have focused on the numerical method of lines to solve the wave equation governing optical soliton.

As the input power becomes higher, the short pulse region gradually moves into the anomalous dispersion area, since the zero-dispersion transmission becomes degraded by the interaction between fiber nonlinearity and TOD. These interactions will have a huge influence on the final shape of the soliton pulse spectra, which can also lead to an overall degradation of the signal transmitted in the fiber. The Figure on the left side represents the soliton pulse distortion as a result of failure to provide a perfect balance between the dispersion and nonlinear effects.

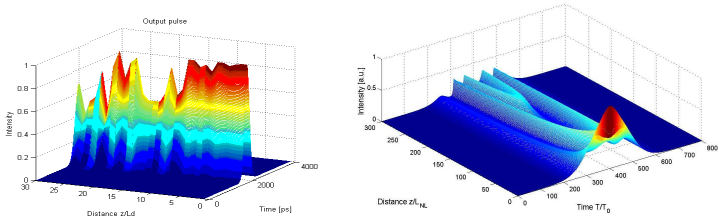

Fig. 20. Time and spectral signal distortion during the propagation in the optical fiber.

Acknowledgment: This work was partly supported by the Slovak Research and Development Agency under the project No. APVV-0025-12.

OWTNM 2016 | 24TH INTERNATIONAL WORKSHOP ON OPTICAL WAVE & WAVEGUIDE THEORY AND NUMERICAL MODELLING

VPImodeDesigner: An Integrated Framework for Modeling Optical Waveguides and Fibers

Sergei F. MINGALEEV[1*], Vladimir A. IRKHIN[1], Nikolay V. KARELIN[1], Igor G. KOLTCHANOV[2], and André RICHTER[2]

[1] VPI Development Center, Filimonova str. 15, Minsk, 220037, Belarus

[2] VPIphotonics GmbH, Carnotstrasse 6, Berlin, 10587, Germany

[*] sergei.mingaleev@vpiphotonics.com

We present VPImodeDesigner [1], a versatile simulation environment for the design and optimization of high-index-contrast and diffused (graded-index) straight and bent optical waveguides and fibers, made of dispersive and lossy, isotropic and anisotropic materials (including non-diagonal and gyrotropic anisotropy). The core of the tool comprises a set of finite-difference mode solvers supporting non-uniform discretization mesh and PML boundary conditions. All optical materials (lossy, dispersive, anisotropic, thermo-optic) are treated through the standardized interface, thus allowing to start prototyping with idealized materials, and later replacing them very easily with fully realistic ones. The physical quantities are handled as objects possessing both, values and units. This allows, in particular, to freely use either frequency or wavelength for describing arbitrary dispersive waveguide or material properties. Elaborated object-oriented interfaces are provided for waveguide cross-section definition and non-uniform mesh customization, treatment of calculated guided modes and all the main mode properties. In particular, the vector mode fields, as well as their scalar field components, support all standard mathematical operations as objects. Consequently, the Poynting vector or energy density can be calculated in a single line of code; plotting or integrating them in the desired area requires only one additional command. Built-in sweeps by frequency/wavelength, temperature, and bend radius, with embedded least-square fitting and interpolation of the calculated mode properties (including group index and dispersion) support the very fast and productive design workflow. All this functionality is provided as a scriptable Python-based simulation environment that can be conveniently accessed through the IPython Notebooks. It supports an easy integration with circuit-level simulation tools and can be also combined with the SciPy ecosystem providing open-source software for mathematics, science, and engineering.

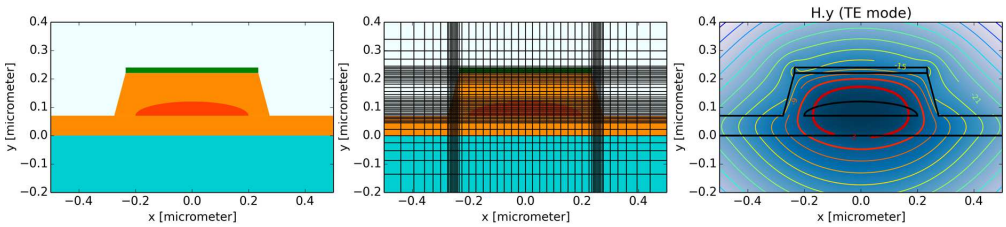

Fig. 21. Illustration of modeling a high-index-contrast active optoelectronic device: cross-section (left), its non-uniform discretization (center), and calculated mode profile (right).

References

[1] See http://vpiphotonics.com/Tools/ModeDesigner/

OWTNM 2016 | 24TH INTERNATIONAL WORKSHOP ON OPTICAL WAVE & WAVEGUIDE THEORY AND NUMERICAL MODELLING

Design Space Exploration of Functional Blocks for On-chip Mode Division Multiplexing

Alberto PARINI[1*], Yann G. BOUCHER[1,2], Patrice FÉRON[1], Christophe PEUCHERET[1]
[1]FOTON Laboratory, CNRS UMR 6082, University of Rennes 1, ENSSAT, 22305 Lannion, France
[2]ENIB, Technopôle Brest-Iroise, CS 73862, 29238 Brest, France
[*] alberto.parini@univ-rennes1.fr

Most of the optical networks-on-chip (ONOCs) architectures proposed so far in the literature rely for their operation on wavelength division multiplexing (WDM) [1]. A limitation to the WDM approach for on-chip communications stems from the difficulty of integrating light sources on a silicon CMOS compatible platform. Therefore, to optimise the use of the available lasers, a further dimension inherent to optical communications can be leveraged to implement on-chip networking, namely the spatial (modal) one. In mode-division multiplexing (MDM) techniques [2], distinct communication channels are allocated, on the same common wavelength, to the various modes of a multi-mode waveguide.

While for on-chip WDM networks the awareness on the requirements of functional building blocks is well established, for on-chip MDM systems, on the contrary, the design constraints at both device and system levels are still an open issue of investigation. The aim of this contribution is to explore, by means of analytical (scattering matrix formalism) and numerical (FDTD) tools, the design space of different MDM building blocks. A selection of MDM devices is depicted in Figure 1. Panel (a) shows an asymmetric directional couplers implementing TE_0 to TE_1 multiplexing via a phase matching condition. Panel (b) shows an orthogonal crossing between two bi-mode waveguides; here, the optical response must be assessed in both TE_0 and TE_1 operating modes. Microrings can also be exploited for routing in the multimode domain, as presented in Panel (c).

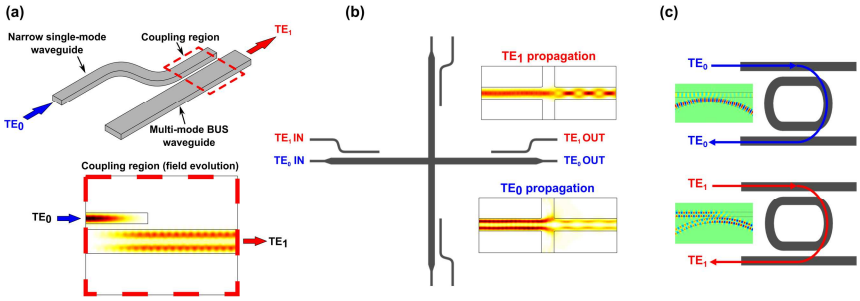

Fig. 22. Building blocks for on-chip MDM. (a) Asymmetric coupler for TE_0 to TE_1 multiplexing. (b) Multimode orthogonal crossing. (c) Multimode ring resonator.

This work is supported by the Labex CominLabs (ANR-10-LABX-07-01), "3D-Optical-ManyCores" project: http://www.3d-opt-many-cores.cominlabs.ueb.eu/

References

[1] A. Parini et al., *BER Evaluation of a Passive SOI WDM Router*, IEEE Photonics Technology Letters, Vol. 25, No. 23, December 1, 2013

[2] C. Peucheret et al., *Signal Processing for On-Chip Space Division Multiplexing*, Advanced Photonics OSA Technical Digest, SpT2E.3, 2015

24TH INTERNATIONAL WORKSHOP ON OPTICAL WAVE & WAVEGUIDE THEORY AND NUMERICAL MODELLING

OWTNM2016

20–21 MAY | WARSAW | POLAND

SATURDAY 21ST MAY 2016

14:00-15:30

OWTNM SESSION #5

ANALYSIS, THEORY AND MODELLING

CHAIR: **MARIAN MARCINIAK,**
NATIONAL INSTITUTE OF TELECOMMUNICATIONS, POLAND

The University of Nottingham
UNITED KINGDOM · CHINA · MALAYSIA

SUPPORTED BY CZIiTT Centre for Innovation and Technology Transfer Management WUT · SKKP POLISH CONFERENCE & CONGRESS ASSOCIATION · CEZAMAT · EPIC European Photonics Industry Consortium

OWTNM 2016 | 24TH INTERNATIONAL WORKSHOP ON OPTICAL WAVE & WAVEGUIDE THEORY AND NUMERICAL MODELLING

Polarisation Singularities in Disordered Photonic Crystals for On-Chip Spin-Photon Entanglement

Daryl M. BEGGS*, Ben LANG, Andrew B. YOUNG, Ruth OULTON
Centre for Quantum Photonics, University of Bristol, HH Wills Physics Laboratory, Tyndall Avenue, Bristol, BS8 1TL, UK
* daryl.beggs@bristol.ac.uk

A polarisation singularity occurs at a position in the electromagnetic field where one of the parameters describing the local polarisation ellipse becomes singular or undefined. For example, C-points occur where the orientation of the local polarisation ellipse is singular. Photonic crystal waveguides are known to support C-points, thanks to the large longitudinal component of the electric field in the waveguide mode. C-points occur at positions where this longitudinal component is equal to the transverse one, but with a quarter-wave phase slip; hence it has local circular polarisation.

These C-points allow a photonic crystal waveguide to display local chirality, even though the global chirality is zero. Such local chirality has particular consequences for quantum emitters, which tend to be point-like dipole emitters and often possess their own chirality. For example, electron transitions in quantum dots impart angular momentum on the photons they emit. If such a quantum dot is placed at a C-point, this angular momentum interacts with the local chirality to give a unidirectional emission dependent on the spin of the electron. Such spin-dependent unidirectional emission is a very attractive property for quantum information applications, as it allows for deterministic entanglement of spin and photon path information [1]. Here, we will show how this can be used to build a spin-photon interface that can convert quantum information stored in static qubits into flying qubits.

We also study the effects of disorder in the photonic crystal waveguide on the polarisation singularities. We find that C-points are remarkably robust to the introduction of disorder, persisting far beyond expected levels of disorder in real waveguides [2].

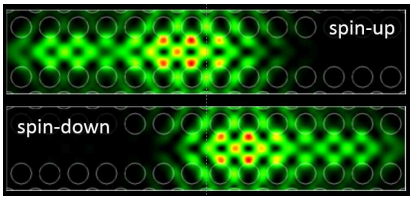

Fig. 23. FDTD simulation of a quantum dot placed at a C-point in the photonic crystal waveguide. We find a correlation of >99% between spin of the electron and emission direction into the waveguide.

References

[1] A. B Young, A. C. T. Thijssen, D. M. Beggs, P. Androvitsaneas, L. Kuipers, J. G Rarity, S. Hughes, R. Oulton, *Polarization engineering in photonic crystal waveguides for spin-photon entanglers*, Phys. Rev. Lett., vol. 115, 153901, 2015

[2] B. Lang, D. M. Beggs, A. B. Young, J. G. Rarity, R. Oulton, *Stability of polarization singularities in disordered photonic crystal waveguides*, Phys. Rev. A, vol. 92, 063819, 2015

OWTNM 2016 | 24TH INTERNATIONAL WORKSHOP ON OPTICAL WAVE & WAVEGUIDE THEORY AND NUMERICAL MODELLING

Two-Mode Waveguide with Nonlinear Ring Resonator

Yann G. BOUCHER[1,2*], Alberto PARINI[2], Patrice FÉRON[2]
[1]ENIB, Technopôle Brest-Iroise, CS 73862, 29238 Brest cedex, France
[2]CNRS, UMR 6082 FOTON, ENSSAT/Université Rennes 1, CS 80518, F-22305 Lannion cedex
* yann.boucher@enib.fr

We investigate theoretically and numerically the properties of a system made of a two-mode waveguide (WG) coupled to a single-mode nonlinear (Kerr) ring resonator (RR) of total length L [Fig. 1]. Time dependence is taken as $\exp(+i\,\omega t)$.

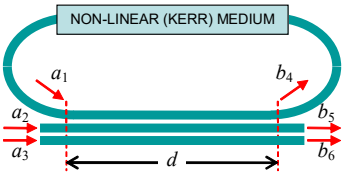

Fig. 24. Schematic representation of the system in terms of scattering parameters, with the two-mode waveguide formally described as two coupled single-mode waveguides.

The two-mode lower WG being formally equivalent to two coupled single-mode WGs [1], the coupling zone of length d is well described by a (3×3) matrix of the form:

$$\begin{pmatrix} b_4 \\ b_5 \\ b_6 \end{pmatrix} = \begin{pmatrix} \rho & -i\,\kappa & X \\ -i\,\kappa & \tau & -i\,\kappa' \\ X & -i\,\kappa' & \rho' \end{pmatrix} \begin{pmatrix} a_1 \\ a_2 \\ a_3 \end{pmatrix}, \tag{1}$$

with scattering parameters easily derived from coupled-mode theory [2]. Closing the loop with $a_1 = b_4\, \mathrm{e}^{-i\,\beta\,(L-d)}$ (where β is the propagation constant), then reversing to the even (e) and odd (o) supermode basis, we obtain not only the (2×2) Jones-like matrix of the system, but also the internal fields in the RR. For instance, b_4 reads:

$$b_4 = a_e\,\frac{\sqrt{2}}{2}\left(\frac{X - i\,\kappa}{1 - R\,\mathrm{e}^{-i\,\phi}}\right) + a_o\,\frac{\sqrt{2}}{2}\left(\frac{X + i\,\kappa}{1 - R\,\mathrm{e}^{-i\,\phi}}\right), \tag{2}$$

where $R\,\mathrm{e}^{-i\,\phi} = \rho\,\mathrm{e}^{-i\,\beta\,(L-d)}$, and a_e (resp. a_o) denotes the amplitude of the *even* (resp. *odd*) input mode. Both modes are equally coupled into the RR and contribute to the nonlinear effect. With $\phi = \phi_{lin} + 2\,\pi\,(|b_4|^2/P_K)$ the total phase, where P_K is the Kerr power of reference, a self-consistent calculation enables one to determine the internal state, thus the bistability domain. Moreover, the system can work as a nonlinear mode mixer.

This work is supported by Labex CominLabs (ANR-10-LABX-07-01), "3D-Optical-ManyCores" project: http://www.3d-opt-many-cores.cominlabs.ueb.eu/

References

[1] Y.G. Boucher, *Analytical model for the coupling constant of a directional coupler in terms of slab waveguides*, Opt. Eng., vol. 53 (7), 071810, 2014
[2] A. Yariv, P. Yeh, *Optical Waves in Crystals*, Wiley, New York, 1984

OWTNM 2016 | 24TH INTERNATIONAL WORKSHOP ON OPTICAL WAVE & WAVEGUIDE THEORY AND NUMERICAL MODELLING

Simulation Methods for Multiperiodic and Aperiodic Nanostructured Dielectric Waveguides

Moritz PAULSEN[1], Lars Thorben NEUSTOCK[1,2], Sabrina JAHNS[1], Jost ADAM[3], Martina GERKEN[1*]

[1]Institute of Electrical and Information Engineering, Christian-Albrechts-Universität zu Kiel, Kaiserstraße 2, 24143 Kiel, Germany

[2]Electrical Engineering, Stanford University, 350 Serra Mall, Stanford, CA 94305-9505, USA

[3]Mads Clausen Institute, University of Southern Denmark, Alsion 2, 6400 Sønderborg, Denmark

[*] mge@tf.uni-kiel.de

Nanostructured dielectric waveguides are of high interest for biosensing applications, light emitting devices as well as solar cells. Multiperiodic and aperiodic nanostructures allow for custom-designed spectral properties as well as near-field characteristics with localized modes [1-4]. Here, a comparison of experimental results and simulation results obtained with different simulation methods is presented. We fabricated and characterized multiperiodic nanostructured dielectric waveguides with two, three, and four compound grating periods as well as aperiodic nanostructured waveguides based on Rudin-Shapiro, Fibonacci, and Thue-Morse binary sequences. The near-field and far-field properties are calculated employing the finite-element method (FEM), the finite-difference time-domain (FDTD) method as well as a rigorous coupled wave algorithm (RCWA). Exemplary, Fig. 1 shows results for a Thue-Morse nanostructured waveguide.

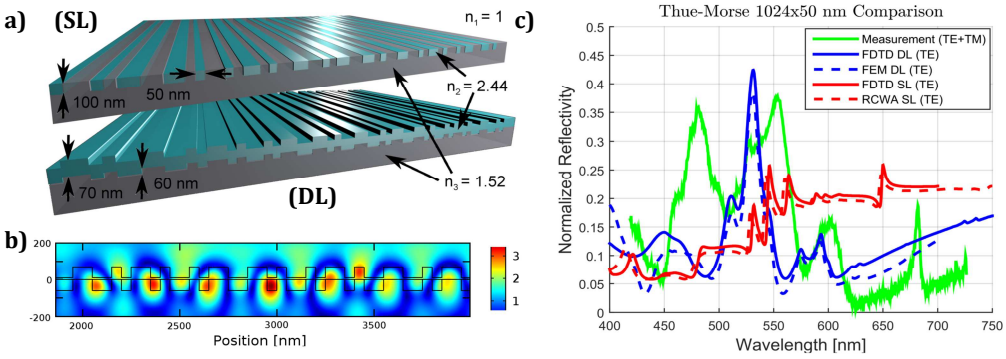

Fig. 25. a) Waveguides with Thue-Morse nanostructure in single-layer (SL) and double-layer (DL) configuration. b) Near-field image at 530 nm resonance calculated with FEM in [V/m]. c) Experimental reflectivity results and results of different simulation methods.

References

[1] S. V. Boriskina, A. Gopinath, L. Dal Negro, *Optical gap formation and localization properties of optical modes in deterministic aperiodic photonic structures*, Opt. Express 16, 18813, 2008

[2] E. Maciá, *Exploiting aperiodic designs in nanophotonic devices*, Rep Prog Phys 75, 036502, 2012

[3] C. Kluge, J. Adam, N. Barié, P. J. Jakobs, M. Guttmann, M. Gerken, *Multiperiodic nanostructures for photon control*, Opt. Express 22, A1363-A1371, 2014

[4] L. T. Neustock, S. Jahns, J. Adam, M. Gerken, *Optical waveguides with compound multiperiodic grating nanostructures for refractive index sensing*, J. of Sensors, 6174527, 2016

OWTNM 2016 | 24TH INTERNATIONAL WORKSHOP ON OPTICAL WAVE & WAVEGUIDE THEORY AND NUMERICAL MODELLING

High-Order Split-Step Time-Domain Modelling of Optoelectronic Devices with Distributed Feedback

Sergei F. MINGALEEV[1*], Igor G. KOLTCHANOV[2], Eugene S. SOKOLOV[1], Stanislau G. SAVITSKI[1], André RICHTER[2]

[1]VPI Development Center, Filimonova str. 15, Minsk, 220037, Belarus

[2]VPIphotonics GmbH, Carnotstrasse 6, Berlin, 10587, Germany

[*] sergei.mingaleev@vpiphotonics.com

We present a versatile model for designing optoelectronic devices. It significantly extends the established transmission-line laser model (TLLM), which was used during the last two decades as universal method for simulating distributed active devices [1]. Our model implements a fourth-order split-step computational scheme [2] with highly accurate description of DFB and DBR gratings, including apodized, chirped, non-reciprocal and sampled Bragg gratings. It supports non-uniform step sizes and embeds several dynamically tunable infinite-impulse response (IIR) digital filters for accurate modelling of fractional group delays and multi-Lorentzian fitting of arbitrary carrier-dependent measured gain and electro-absorption spectra. All major physical effects, such as free-carrier absorption and free-carrier dispersion, two-photon absorption and Kerr nonlinearity, Pockels and Franz-Keldysh or Stark effects, are supported as well. Together with the built-in support of multi-section electrical contacts and lumped reflectors, this allows highly realistic modelling of Fabry-Perot and more complex DFB/DBR lasers, semiconductor optical amplifiers, electro-absorption modulators, and almost any other types of distributed optoelectronic devices with either distributed or lumped feedback. The described model is integral part of the professional simulation environment VPIcomponentMaker Photonic Circuits [3].

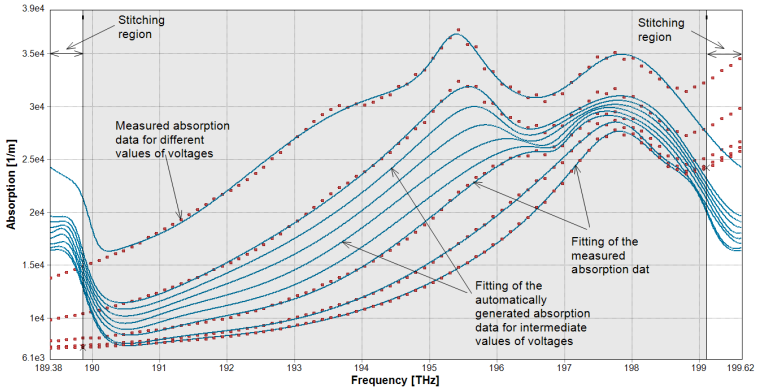

Fig. 26. Automated multi-Lorentzian fitting of measured electro-absorption spectra.

References

[1] A.J. Lowery, *Transmission-line modelling of semiconductor lasers: the transmission-line laser model*, Int. J. Numerical Modeling, vol. 2, no. 2, pp. 249-265, 1989

[2] Y.-P. Xi, W.-P. Huang, and X. Li, *High-order split-step schemes for time-dependent coupled-wave equations*, IEEE J. Quantum Electron., vol. 43, no. 5, pp. 419-425, 2007

[3] See http://vpiphotonics.com/Tools/PhotonicCircuits/

OWTNM 2016 | 24TH INTERNATIONAL WORKSHOP ON OPTICAL WAVE & WAVEGUIDE THEORY AND NUMERICAL MODELLING

An Assessment of Polynomial Approximations for the Time-Domain Beam Propagator

Hendrik KLEENE*, Dirk SCHULZ
TU Dortmund, Friedrich-Wöhler-Weg 4, Dortmund, 44227, Germany
* hendrik.kleene@tu-dortmund.de

The application of explicit time domain methods for the simulation of electromagnetic fields in photonic devices is limited by the choice of small time steps. Explicit approaches based on different polynomial expansions of the time propagator are discussed for the feasibility to apply large time steps.

Introduction: For conventional explicit methods, the required time step depends on the spatial discretization because of stability concerns. A dense spatial discretization results in a very small time step leading to large computation times. To increase the time step, implicit approaches [1] are reasonable, but also lead to high computations times due to the required solution of matrix-vector equations. Algorithms are needed allowing explicit formulations and large time steps.

Summary: The mentioned assessment is based on a discretized scalar Helmholtz-equation. The time propagation algorithm can be derived and written as

$$\vec{\Psi}(t+\Delta t) = H([A]) \cdot \vec{\Psi}(t) - \vec{\Psi}(t-\Delta t) = 2 \cdot \cos\left(\sqrt{[A]} \cdot \Delta t\right) \cdot \vec{\Psi}(t) - \vec{\Psi}(t-\Delta t). \quad (1)$$

$\vec{\Psi}(t)$ denotes the discretised field distribution in time and the operator $H([A])$ depends on a spatial discretization matrix $[A]$. The time step is chosen to be $\Delta t = n \cdot \Delta t_c$, where Δt_c is the time step arising from Courant's stability condition defined by $\Delta t_c \cdot \sqrt{\lambda_{max} = 1}. \lambda_{max}$ is the maximum eigenvalue of matrix $[A]$. The coefficients a_i of polynomial approximation of the operator are determined in the eigenvalue domain for the corresponding operator

$$H(\lambda) = 2 \cdot \cos\left(\sqrt{\lambda} \cdot \frac{n}{\sqrt{\lambda_{max}}}\right) = 2 \cdot \cos\left(n \cdot \frac{n}{\sqrt{\lambda_{max}}}\right) = \sum_{i=0}^{N} a_i \cdot P_i(\lambda). \quad (2)$$

The square root term varies between 0 and 1, so the operator can be easily approximated by means of Chebychev or Bernstein polynomials represented by the functions $P_i(\lambda)$. These polynomial expansions are investigated.

Conclusion: In contrast to implicit approaches the solution of linear matrix-vector equations can be omitted. The Chebychev and Bernstein polynomials of higher orders can be calculated using recurrence relations allowing an efficient explicit method.

References

[1] K. Q. Le., T. Benson, P. Bienstman, *Application of modified Pade approximant operators to time-domain beam propagation methods*, J. Opt. Soc. Am. B, vol. 26, no. 12, pp. 2285-2289, 2009

MAIN SPONSOR

CONFERENCE SPONSORS

EXHIBITORS

www.ecio2016.com

ISBN: 978-83-64102-11-0

Editor
Warsaw University of Technology
Institute of Microelectronic and Optoelectronics
Warsaw, Poland
email: ecio@imio.pw.edu.pl
phone: +48 22 234 5047
fax: +48 22 234 6063